

Behind the image: first EHT results

Oliver Porth

Anton Pannekoek Institute, Amsterdam



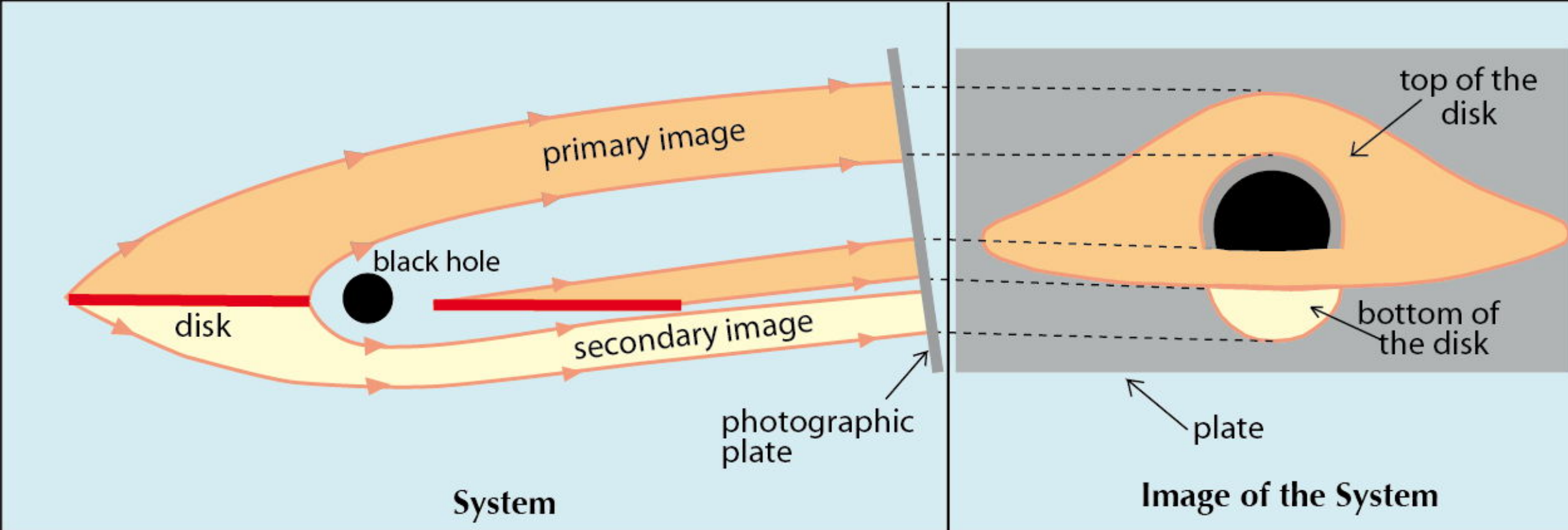
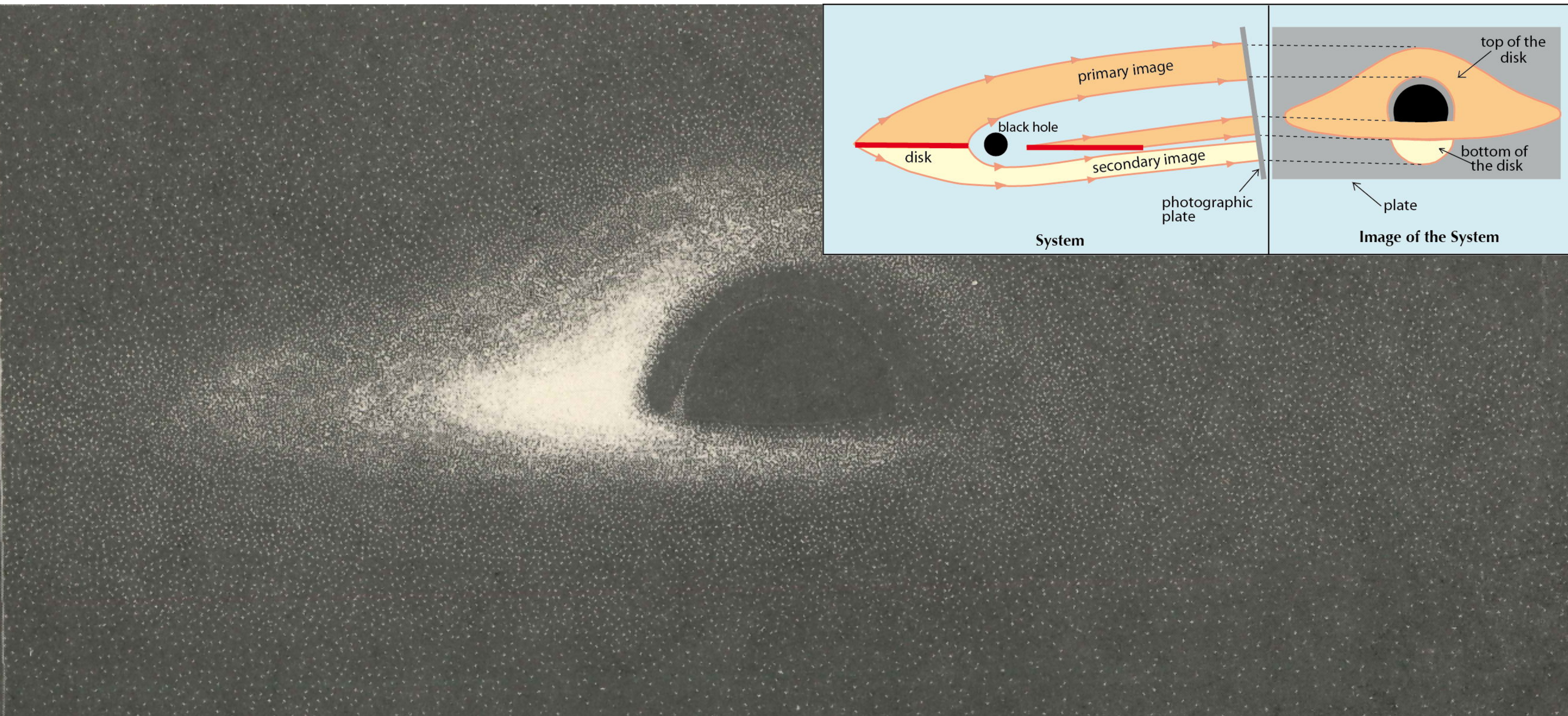
Event Horizon Telescope



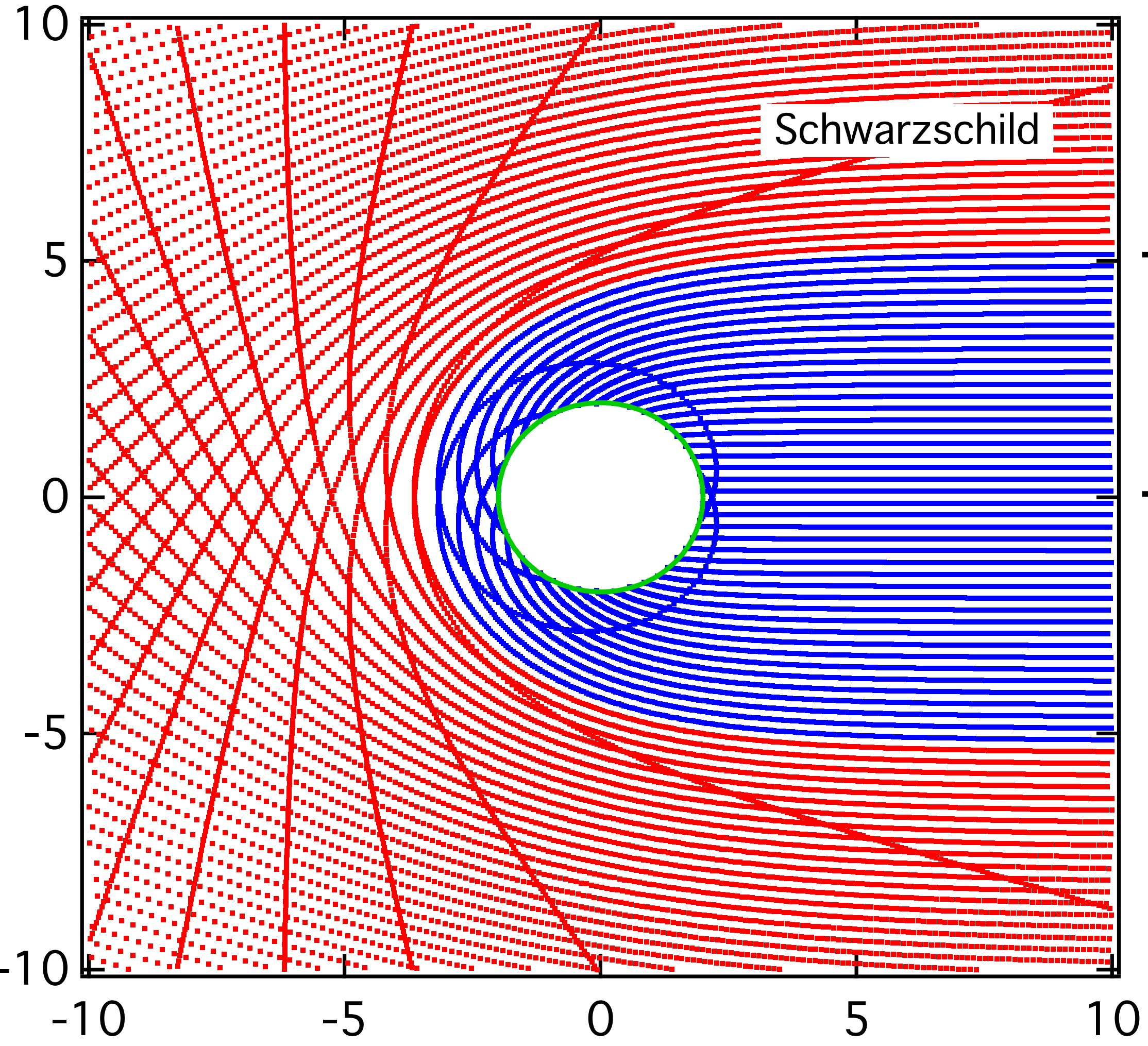
- ▶ Measuring the black hole shadow:
 - ▶ Unique and **repeatable**, strong field test of gravity
 - ▶ Event horizon signature, unique **testbed** for theories of gravity, space and time
- ▶ **Resolve** driver of the most energetic events in the universe
 - ▶ Probe **supermassive** black holes over 10^3 scales
 - ▶ **Plasma physics** in extreme environments

- ▶ Measuring the black hole shadow:
 - ▶ Unique and **repeatable**, strong field test of gravity
 - ▶ Event horizon signature, unique **testbed** for theories of gravity, space and time
- ▶ **Resolve** driver of the most energetic events in the universe
 - ▶ Probe **supermassive** black holes over 10^3 scales
 - ▶ **Plasma physics** in extreme environments

The black hole shadow



The black hole shadow



$$\theta_g = \frac{GM}{c^2 D}$$

$D = 16.8 \text{ Mpc}$
 $M = 6.5 \times 10^9 M_\odot$

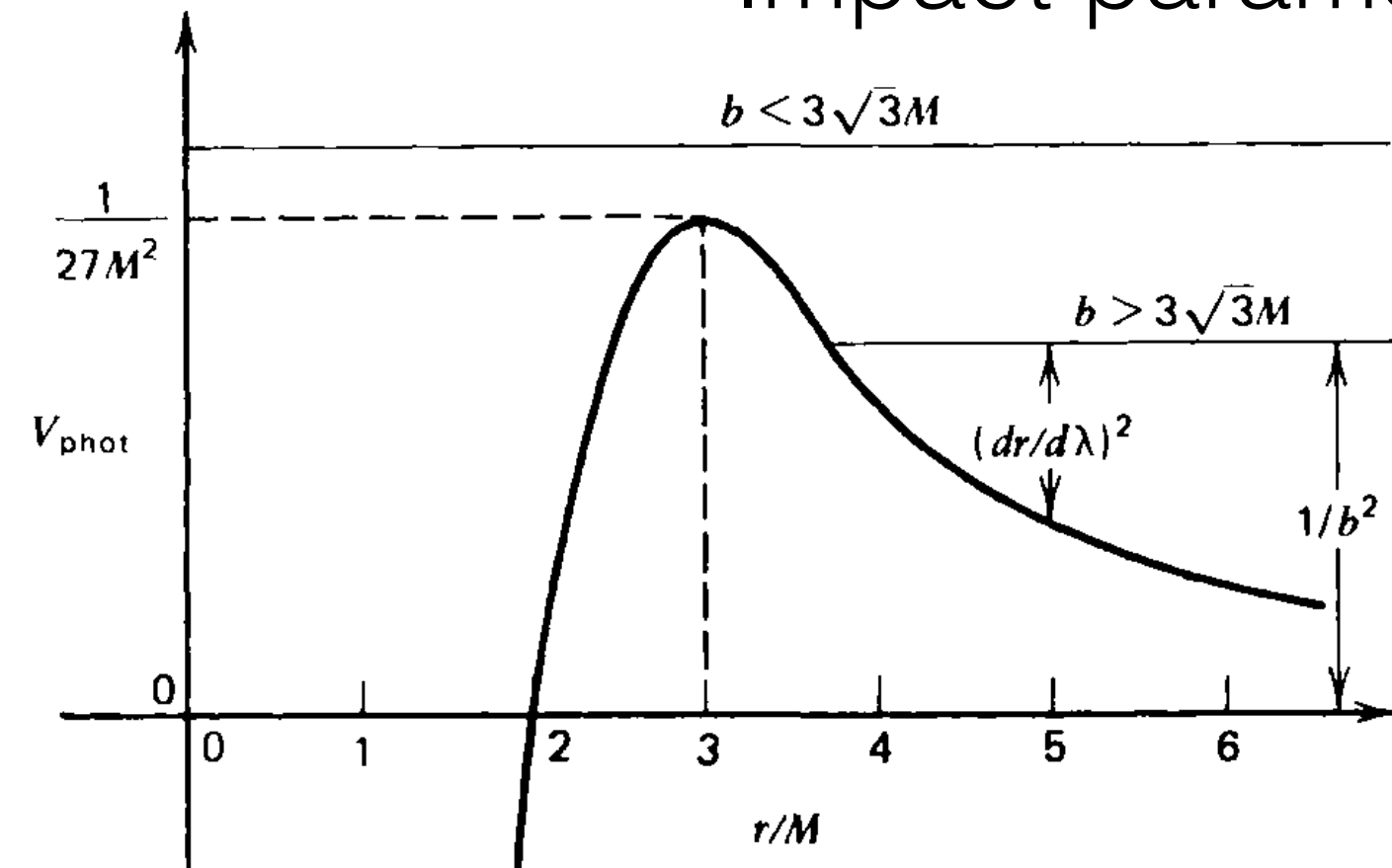
$$\Rightarrow \theta_g = 4 \mu\text{as}$$

Schwarzschild Horizon: $2\theta_g$

Marginally stable Photon orbit: $3\theta_g$

Impact parameter Photon capture: $27^{1/2}\theta_g$

$\sqrt{27}$



Shapiro & Teukolsky (Wiley VCH)

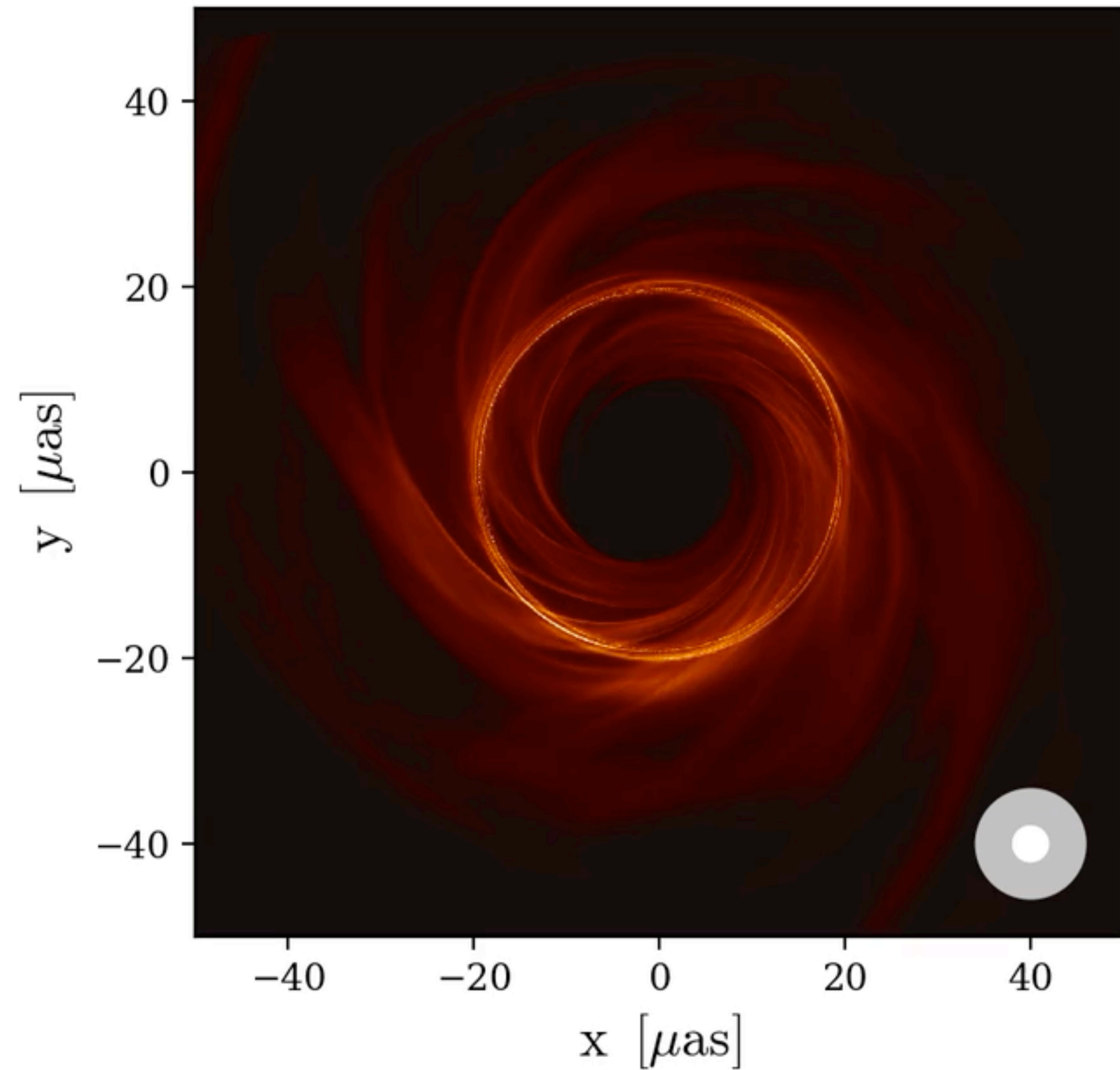
$$V_{\text{phot}}(r) = \frac{1}{r^2} \left(1 - \frac{2M}{r} \right)$$

$$\left(\frac{dr}{d\lambda} \right)^2 = \frac{1}{b^2} - V_{\text{phot}}(r)$$

Observed Shadow: $\hat{d} = 2 \times \sqrt{27}\theta_g \simeq 40 \mu\text{as}$



The black hole shadow



- ▶ Kerr: shadow depends on
 - ▶ Inclination
 - ▶ Spin
 - ▶ cross-section changes only by $\sim 4\%$

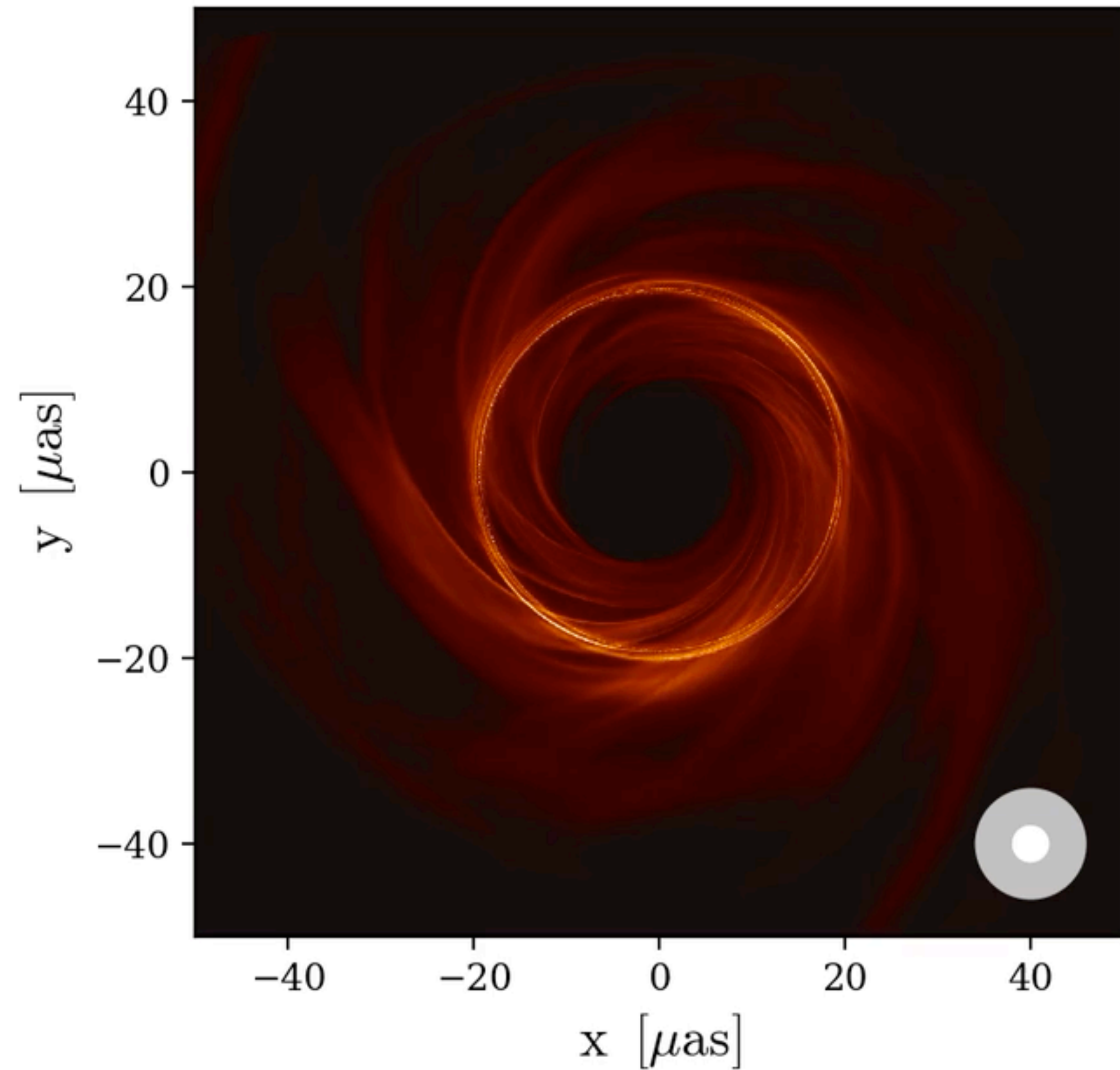
Measuring the shadow size is a robust null-test of GR

G. Wong, B. Prather, C. Gammie (Illinois)



Event Horizon Telescope

The black hole shadow



- ▶ Kerr: shadow depends on
 - ▶ Inclination
 - ▶ Spin
 - ▶ cross-section changes only by $\sim 4\%$

Measuring the shadow size is a robust null-test of GR

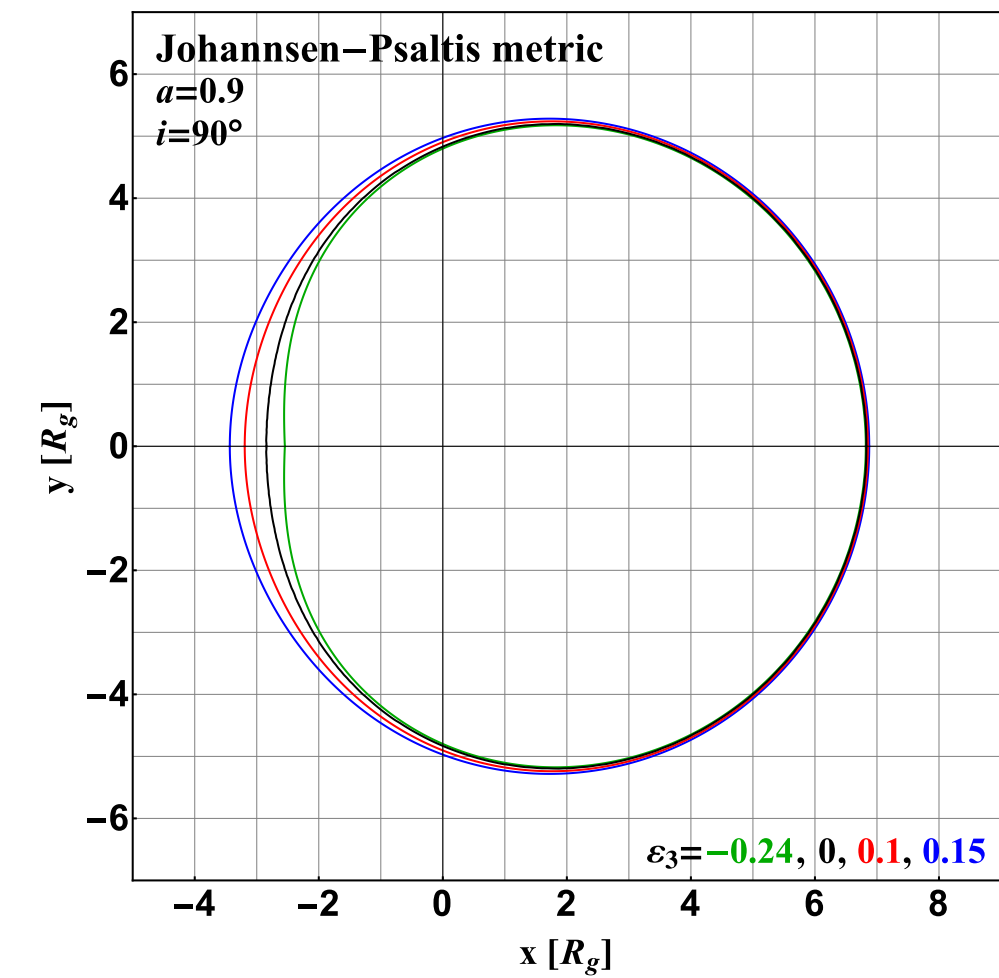
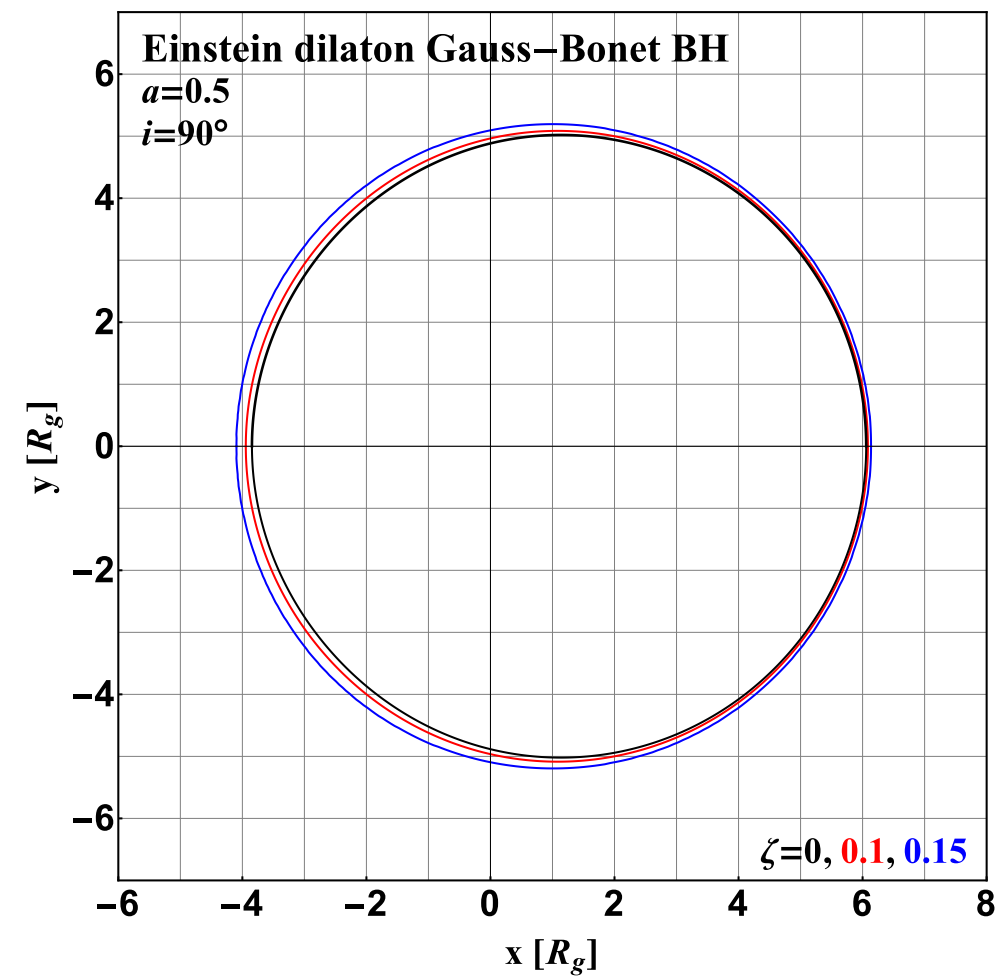
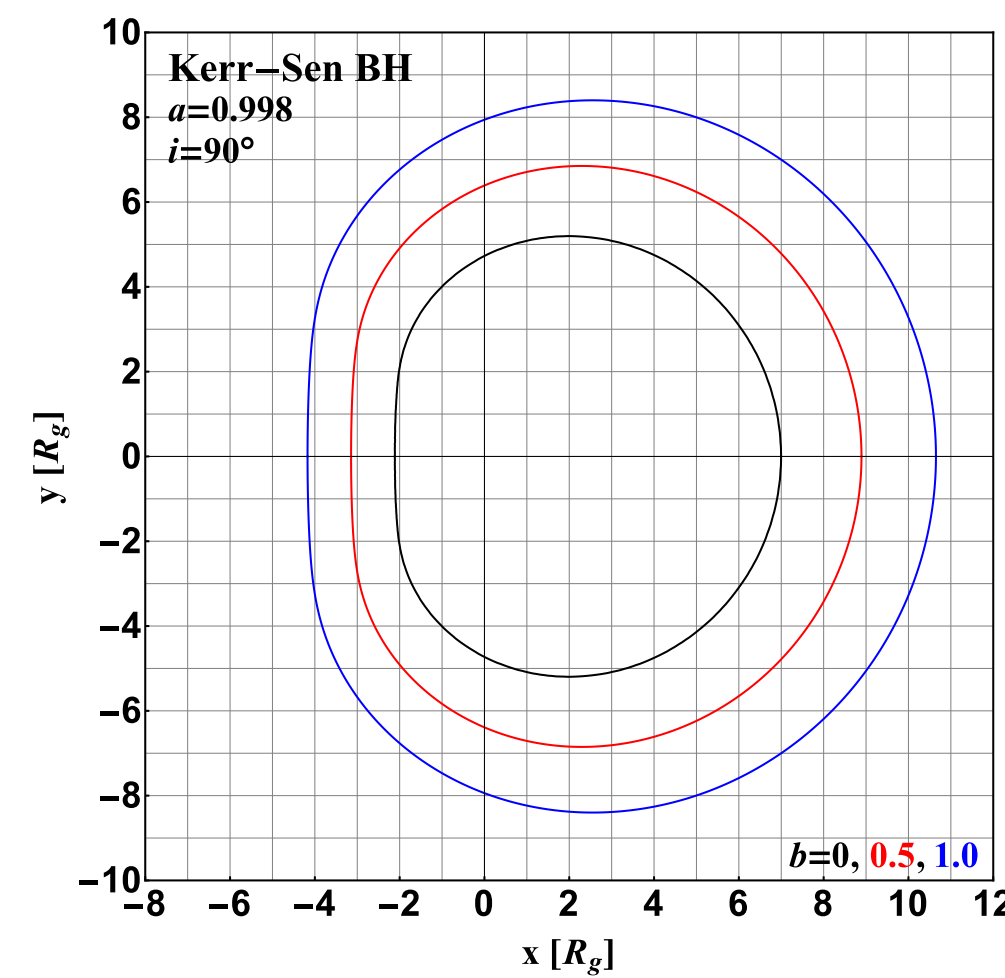
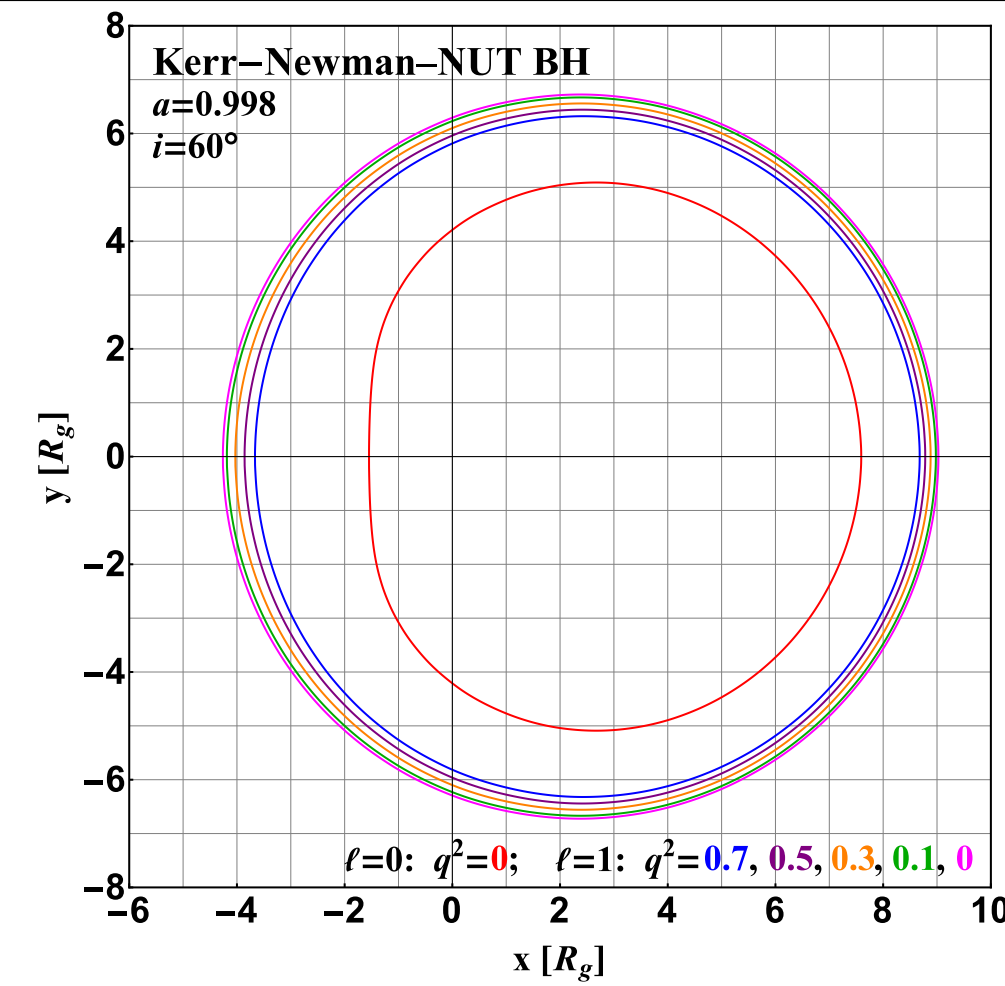
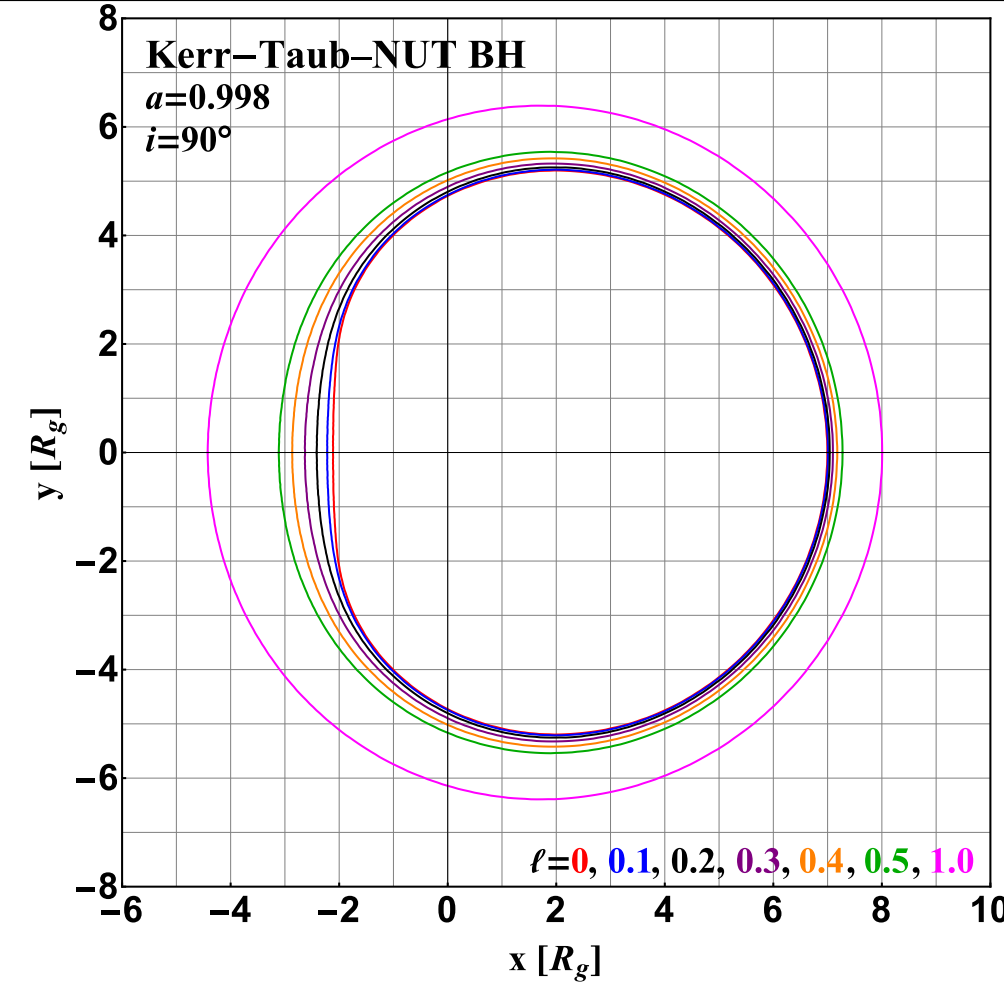
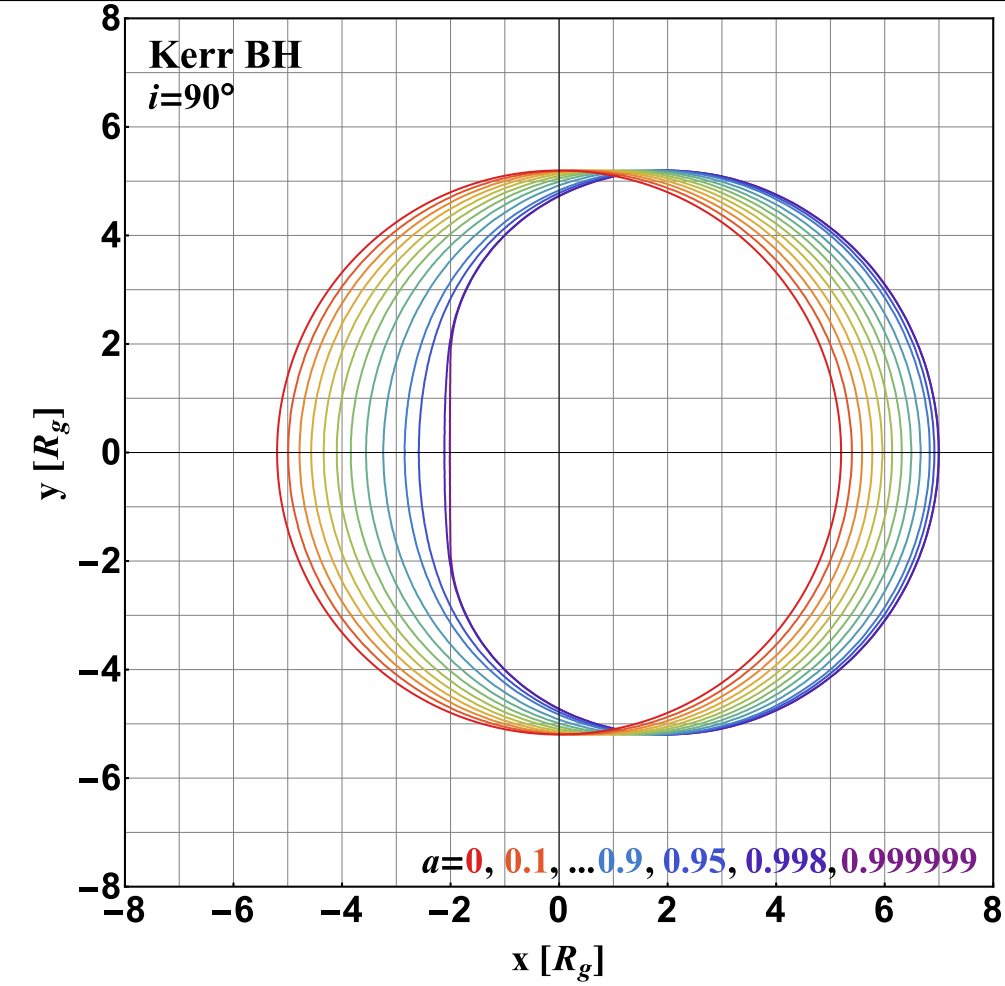
G. Wong, B. Prather, C. Gammie (Illinois)



Event Horizon Telescope

The black hole shadow

“Shadow Industry” from Goddi et al. (2017)



Mapping out the photon ring will allow to test different theories of gravity

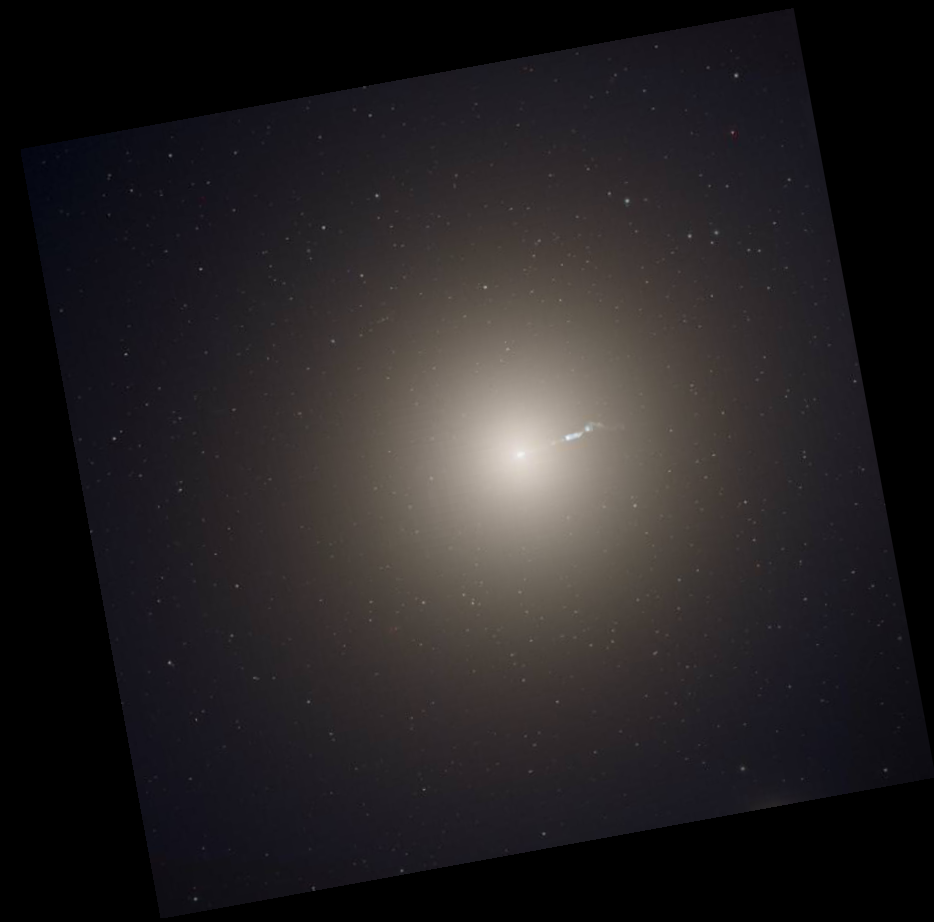


Event Horizon Telescope

The radio jet in M87 (Virgo A)

Elliptical galaxy in center of Virgo cluster 50 Million lightyears away

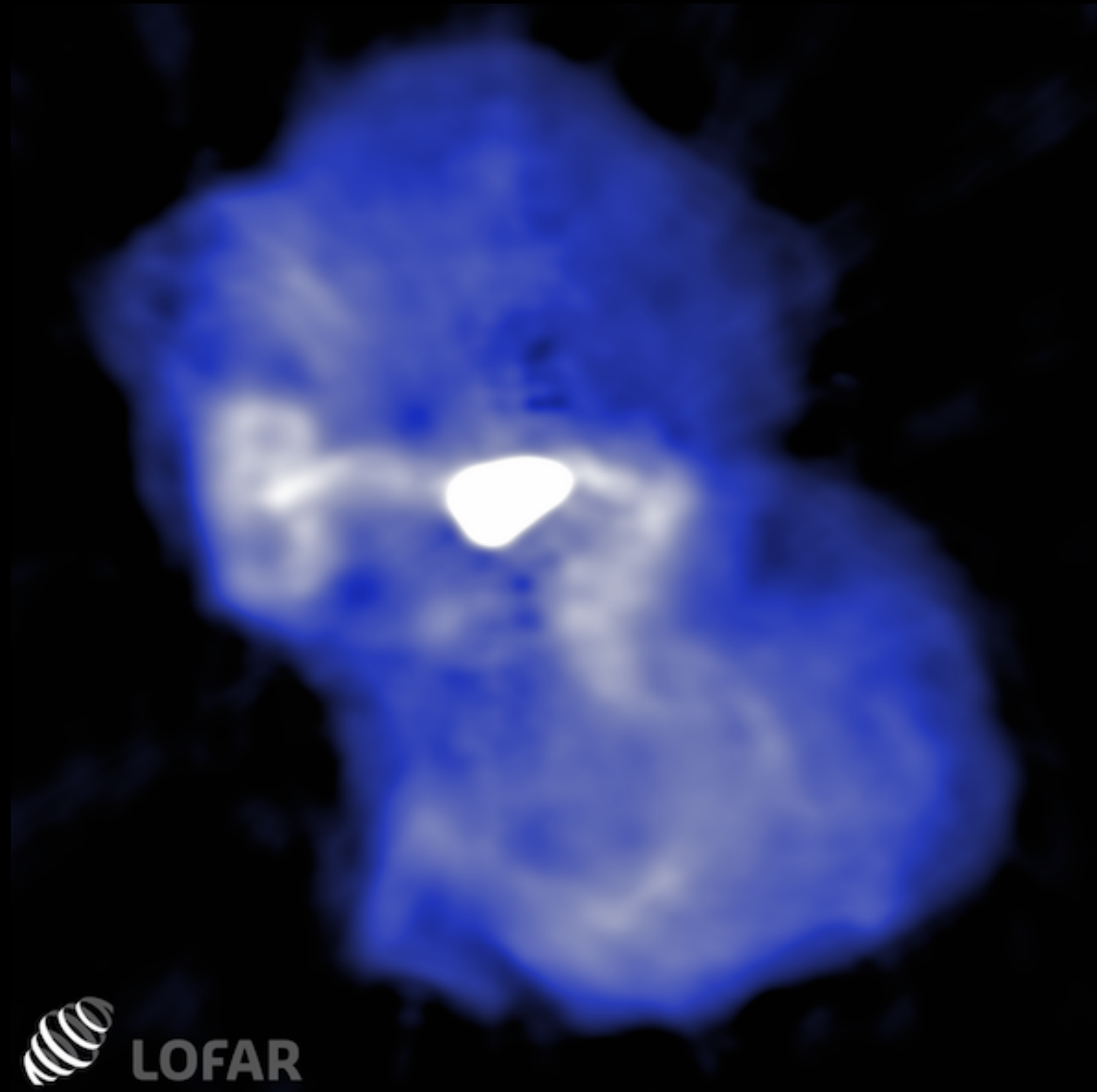
There is evidence for a central dark mass of $3-6 \times 10^9 M_{\text{sun}}$



The radio jet in M87 (Virgo A)

Elliptical galaxy in center of Virgo cluster 50 Million lightyears away

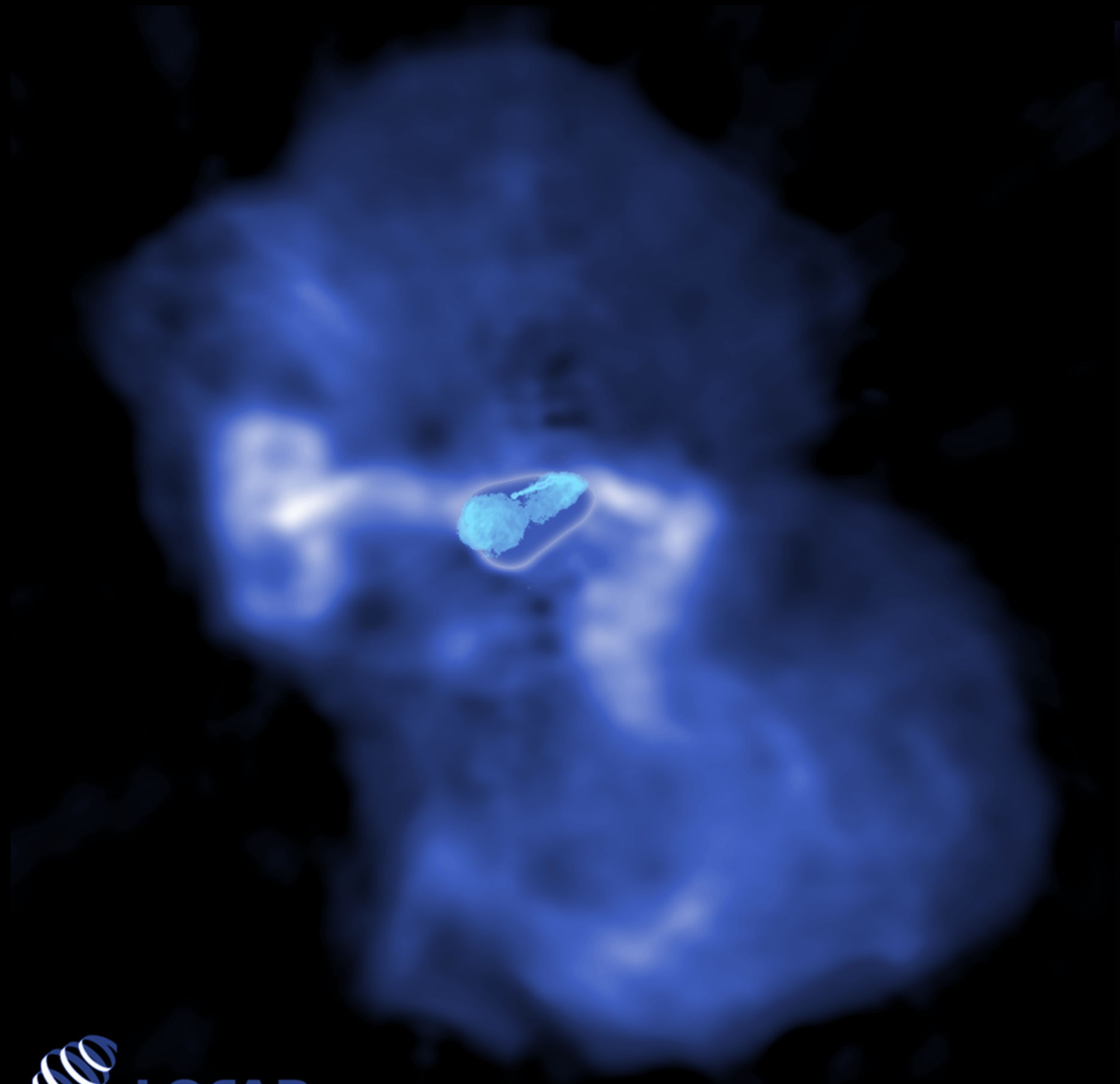
There is evidence for a central dark mass of $3-6 \times 10^9 M_{\text{sun}}$



The radio jet in M87 (Virgo A)

Elliptical galaxy in center of Virgo cluster 50 Million lightyears away

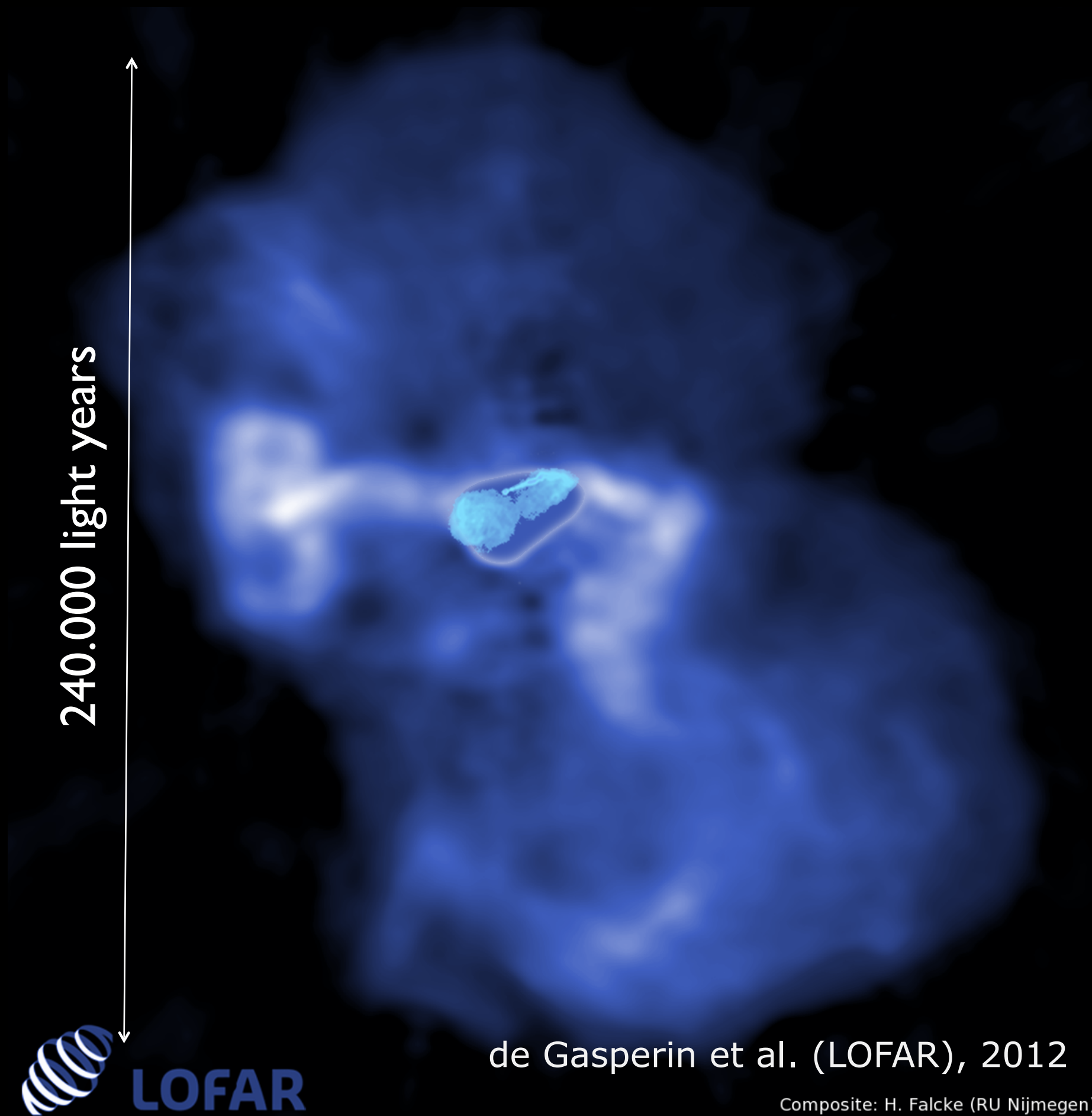
There is evidence for a central dark mass of $3-6 \times 10^9 M_{\text{sun}}$



The radio jet in M87 (Virgo A)

Elliptical galaxy in center of Virgo cluster 50 Million lightyears away

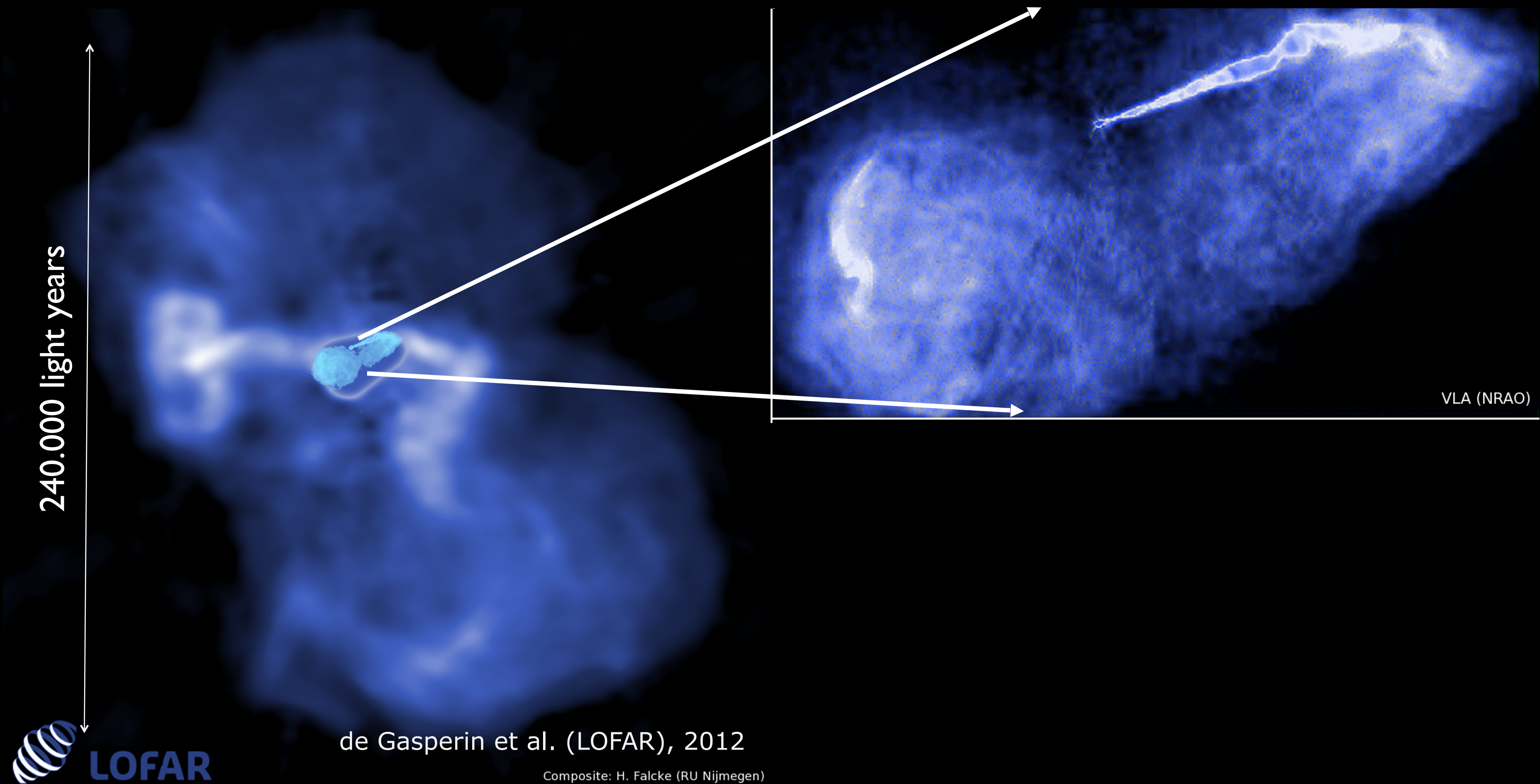
There is evidence for a central dark mass of $3-6 \times 10^9 M_{\text{sun}}$



The radio jet in M87 (Virgo A)

Elliptical galaxy in center of Virgo cluster 50 Million lightyears away

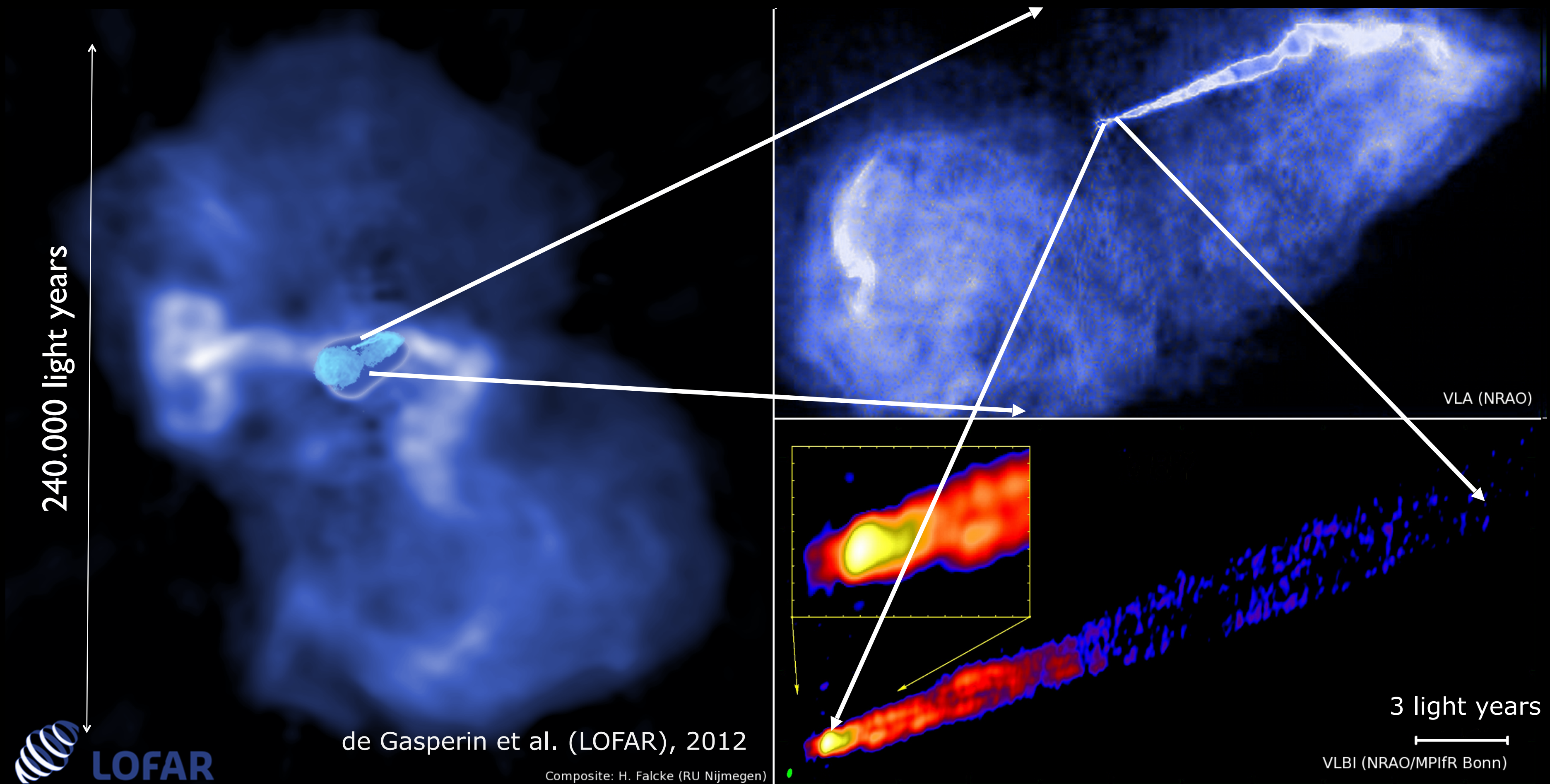
There is evidence for a central dark mass of $3-6 \times 10^9 M_{\text{sun}}$



The radio jet in M87 (Virgo A)

Elliptical galaxy in center of Virgo cluster 50 Million lightyears away

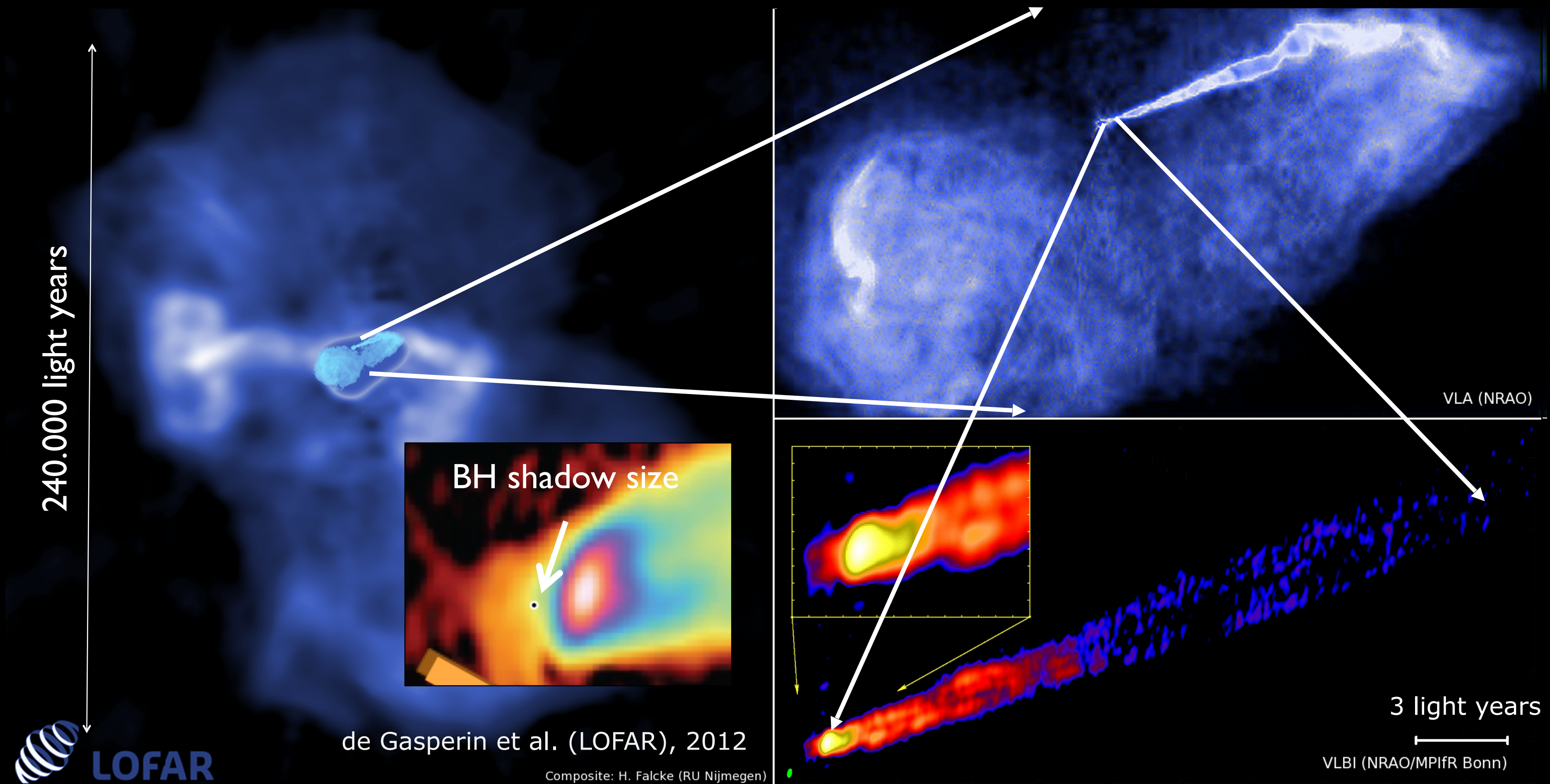
There is evidence for a central dark mass of $3-6 \times 10^9 M_{\text{sun}}$



The radio jet in M87 (Virgo A)

Elliptical galaxy in center of Virgo cluster 50 Million lightyears away

There is evidence for a central dark mass of $3-6 \times 10^9 M_{\text{sun}}$



Global Structure of M87

- **Parabolic** ($z \propto r^{1.7}$) over $10^5 r_s$
- Above bondi sale: **conical** streamlines
 $z \propto r$
- Stationary feature HST-1 due to jet recollimation?

Jet power¹:

10^{42} erg/s – 10^{45} erg/s

BH-mass:

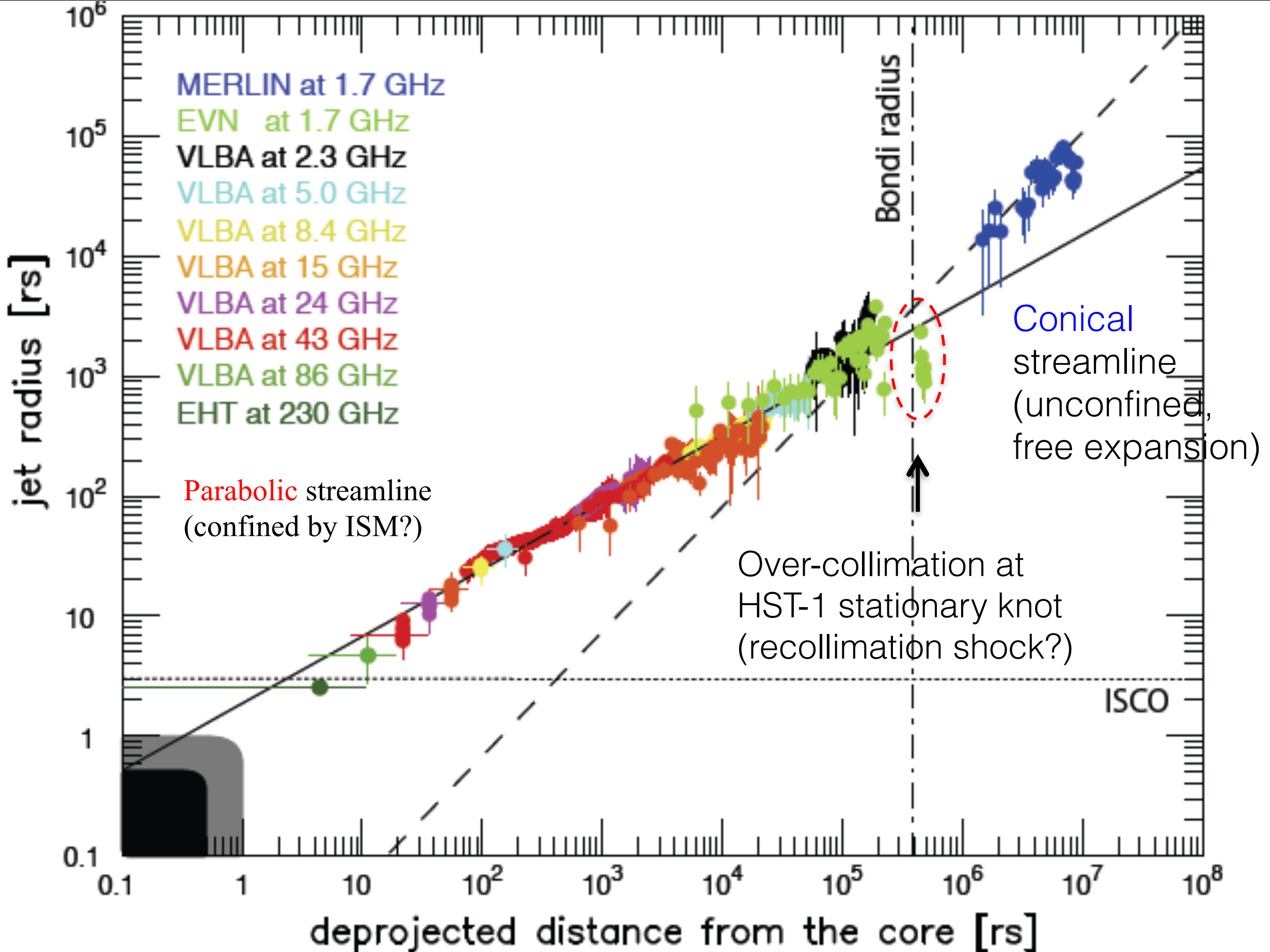
$3.45 \cdot 10^9 M_{\text{sun}}$ (Walsh et al., 2013)

$6.14 \cdot 10^9 M_{\text{sun}}$ (Gebhard et al. 2011)

Distance:

16.8 Mpc (Bird+, 2010, Blakeslee+ 2009, Cantiello 2018)

Asada & Nakamura (2012),
Hada et al. (2013)



¹Reynolds et al. (1996), Li et al. (2009), de Gasperin et al. (2012), Broderick et al. (2015), Prieto et al. (2016)



Event Horizon Telescope

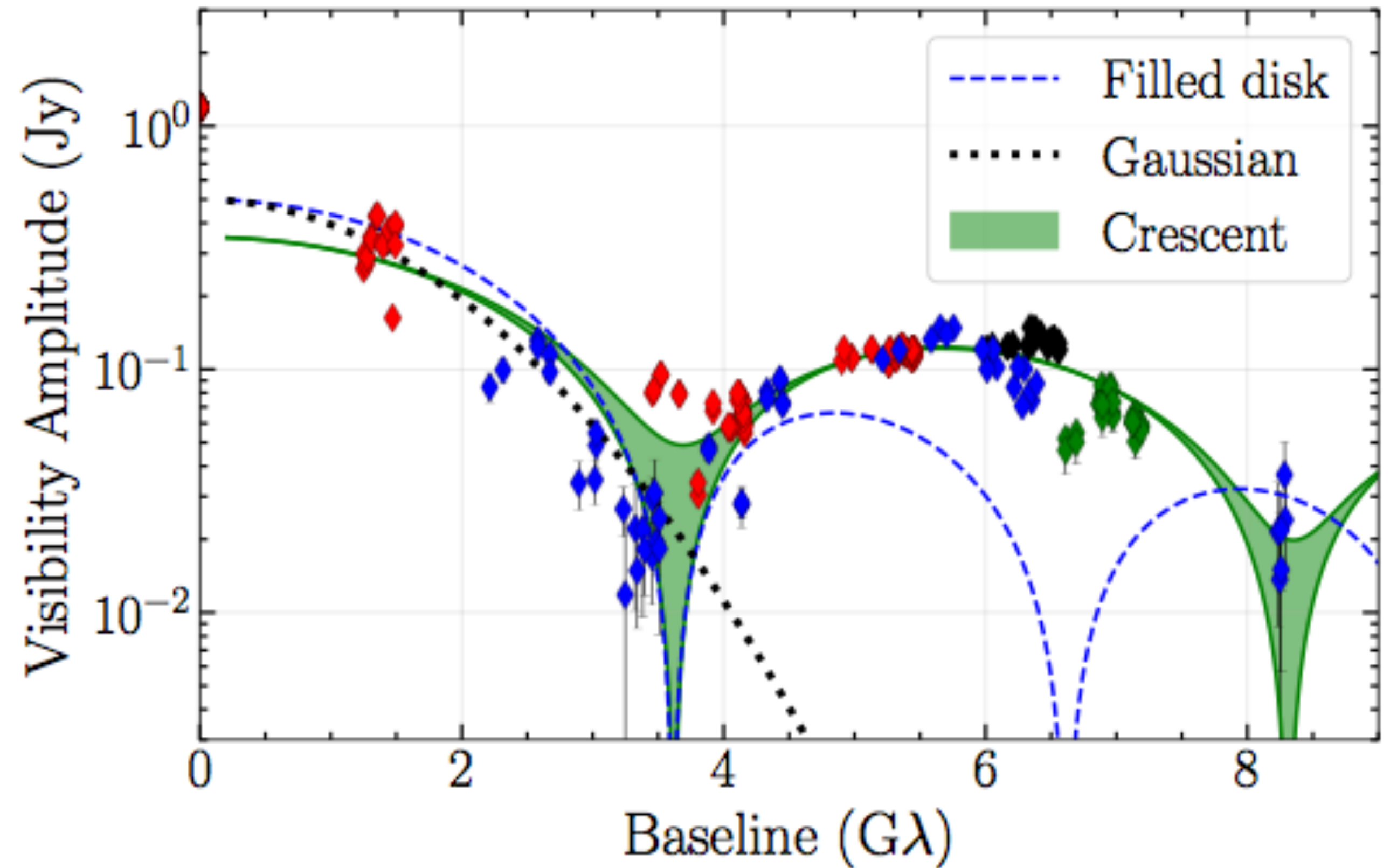
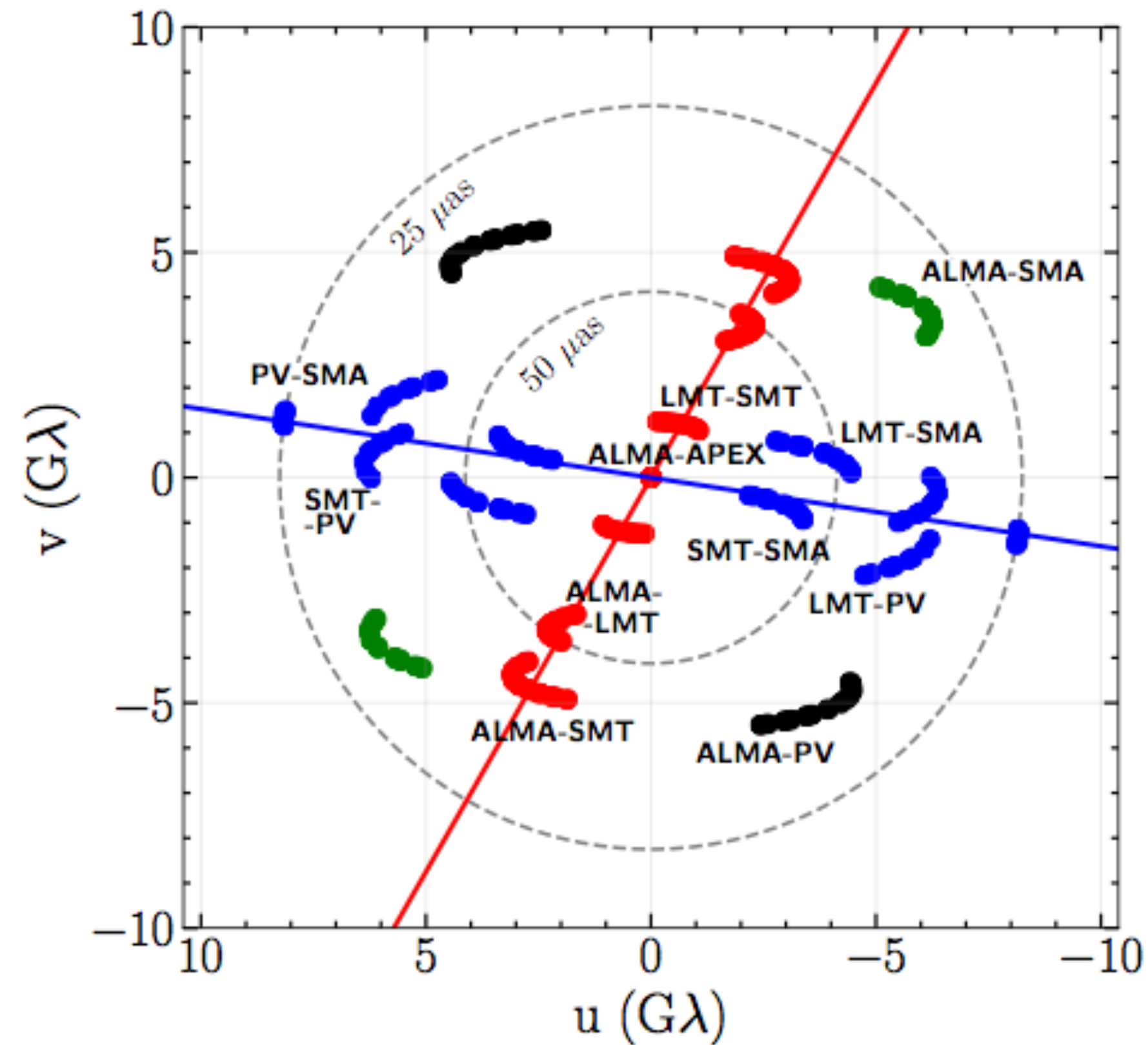
Behind the image: first EHT results - Oliver Porth. Saclay SAp seminar, May 21st 2019



Event Horizon Telescope

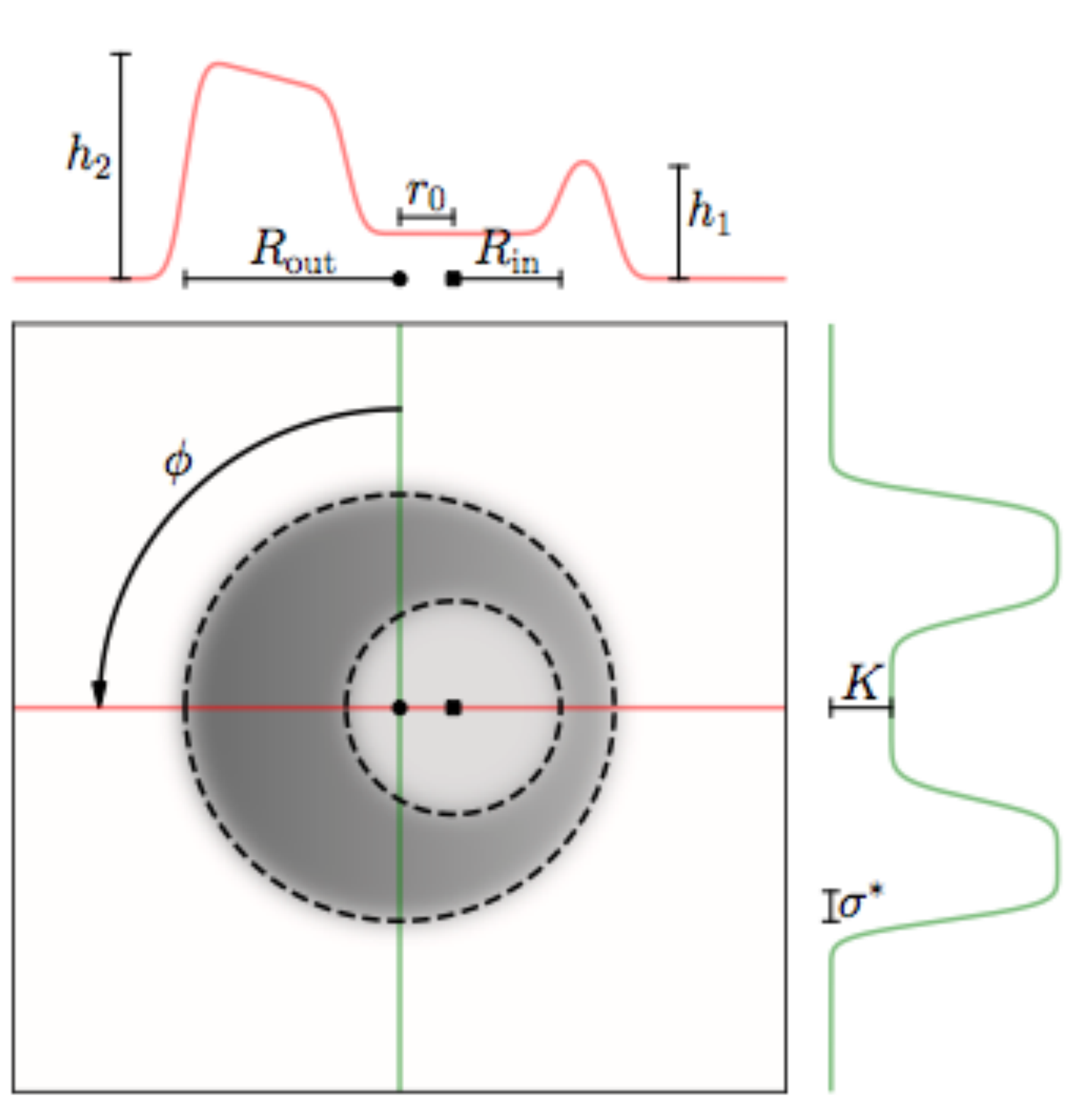
Behind the image: first EHT results - Oliver Porth. Saclay SAp seminar, May 21st 2019

EHT 2017 M87 data look consistent with an asymmetric ring (“crescent”)

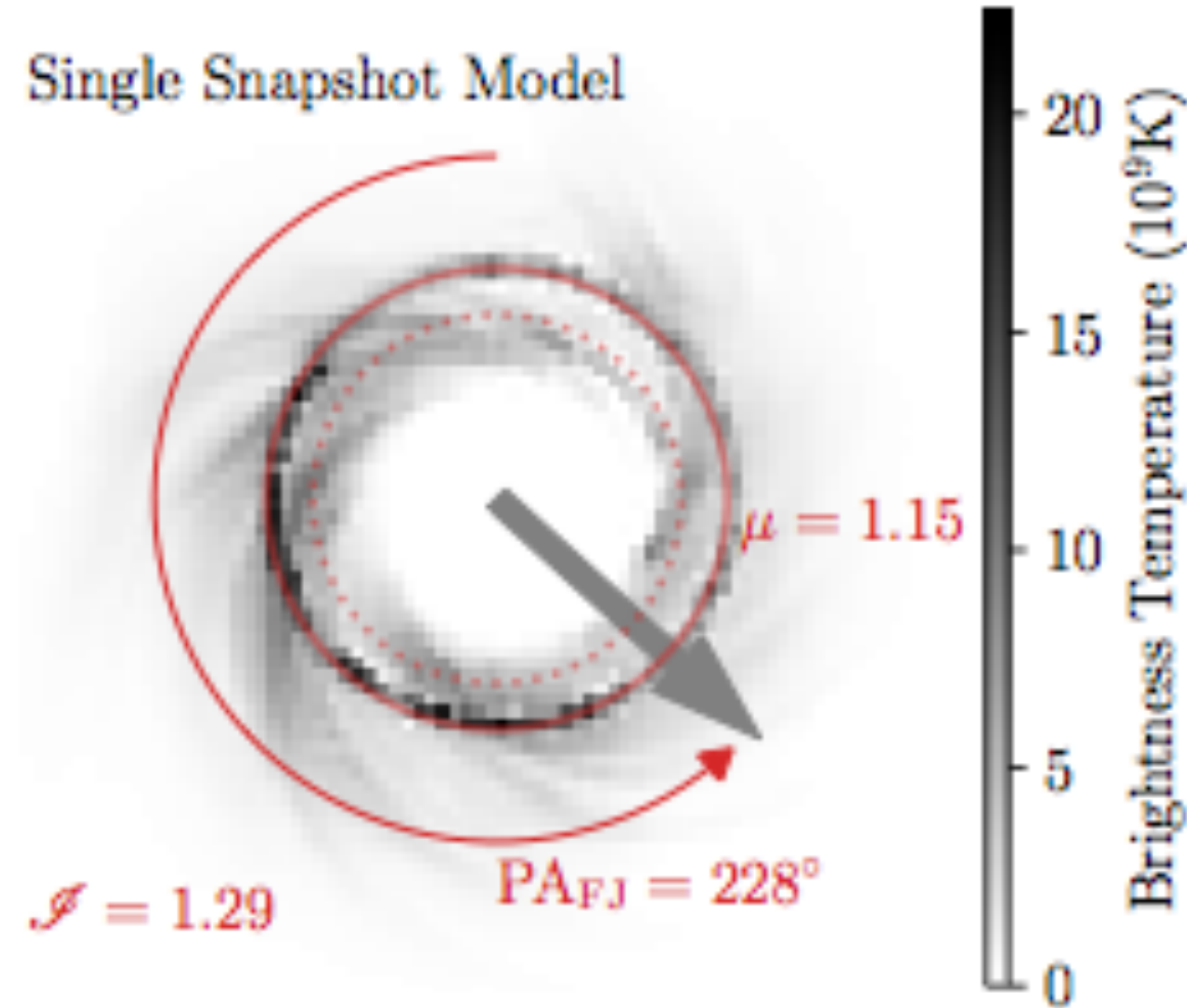


Quantify M87 source properties

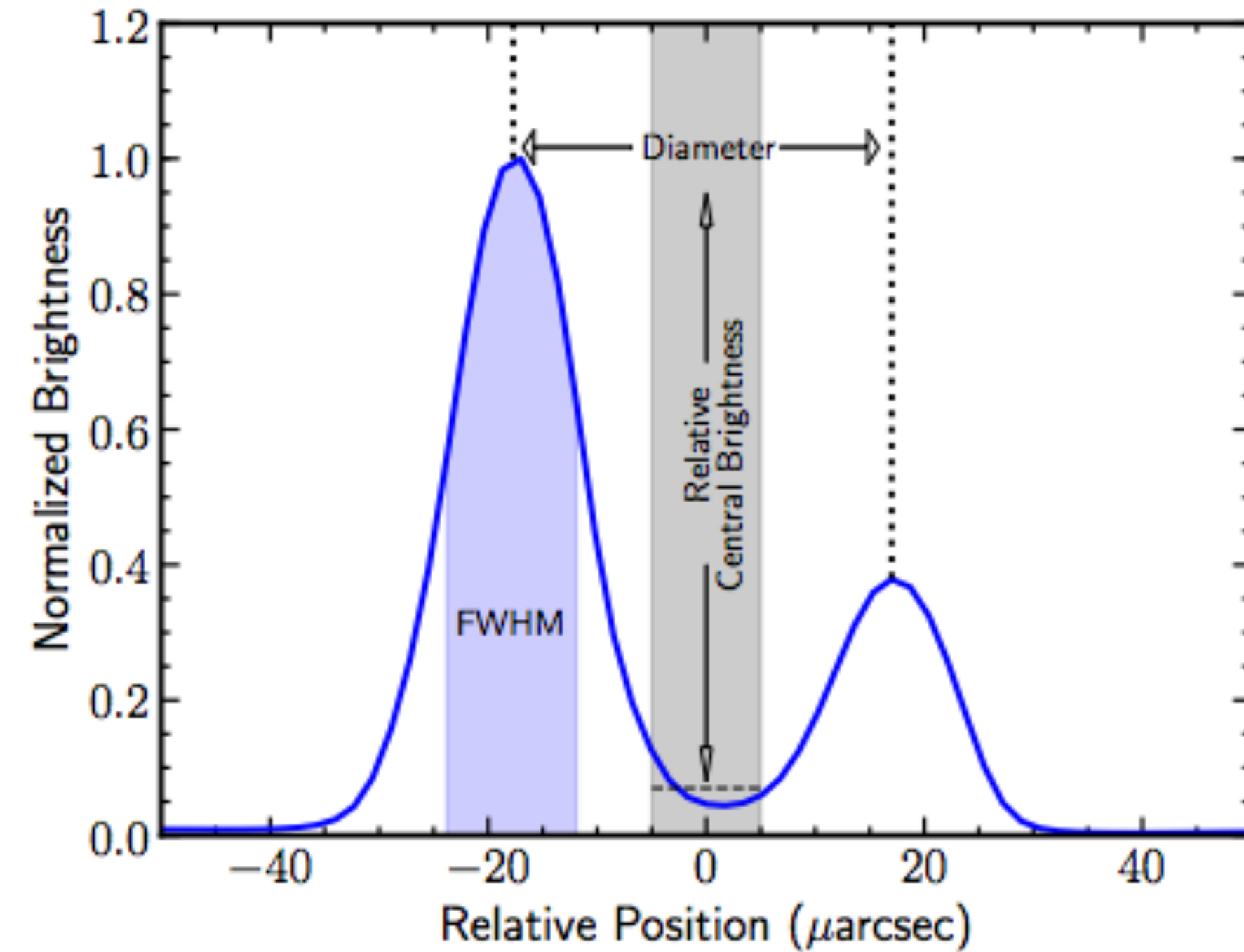
Fit geometric models



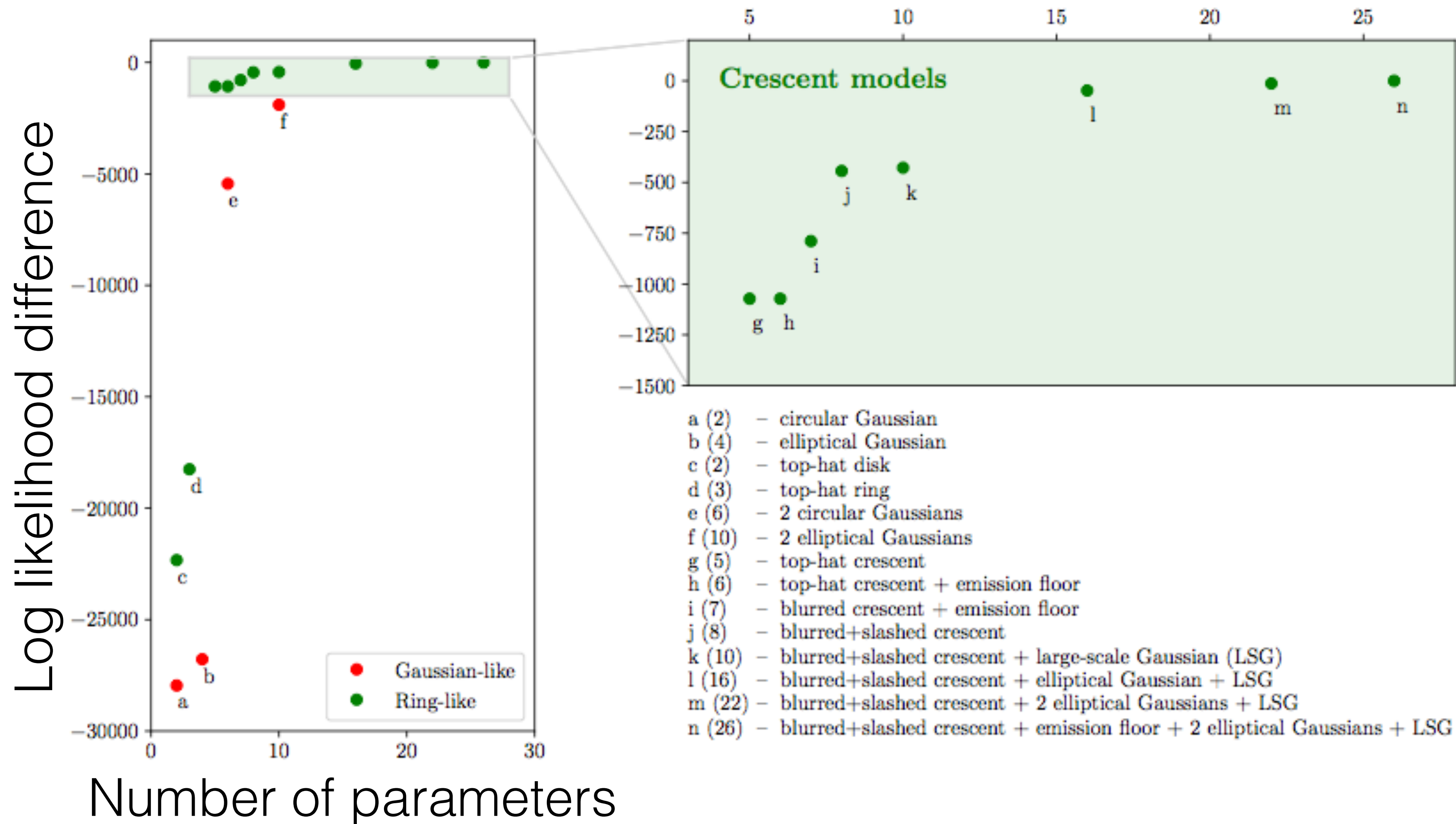
Fit GRMHD models



Extract image parameters



Geometric model fitting: crescents overwhelmingly preferred over other simple shapes



Theoretical models

- ▶ Global **General Relativistic Magnetohydrodynamic** (GRMHD) and radiative transfer (GRRT) simulations
- ▶ End-to-end modelling pipeline:
 - ▶ from picking the **spacetime, atmospheric effects** to **parameter estimation**
- ▶ Dominating uncertainties:
 - ▶ stochastic nature of the **turbulent** flows
 - ▶ **plasma physics**: electron heating, radiation reaction and particle acceleration

Theoretical models

- ▶ Global **General Relativistic Magnetohydrodynamic** (GRMHD) and radiative transfer (GRRT) simulations
- ▶ End-to-end modelling pipeline:
 - ▶ from picking the **spacetime, atmospheric effects** to **parameter estimation**
- ▶ Dominating uncertainties:
 - ▶ stochastic nature of the **turbulent** flows
 - ▶ **plasma physics**: electron heating, radiation reaction and particle acceleration

Simulation Library: 43 GRMHD numerical simulations

- ▶ $\dot{M}/\dot{M}_{\text{Edd}} \lesssim 10^{-5}$: Radiatively inefficient (RIAF), no cooling and radiative feedback
- ▶ 3D GRMHD simulations from: BHAC, iharm3d, KORAL, H-AMR

▶ Two accretion states:

▶ **SANE** (Standard and Normal Evolution)

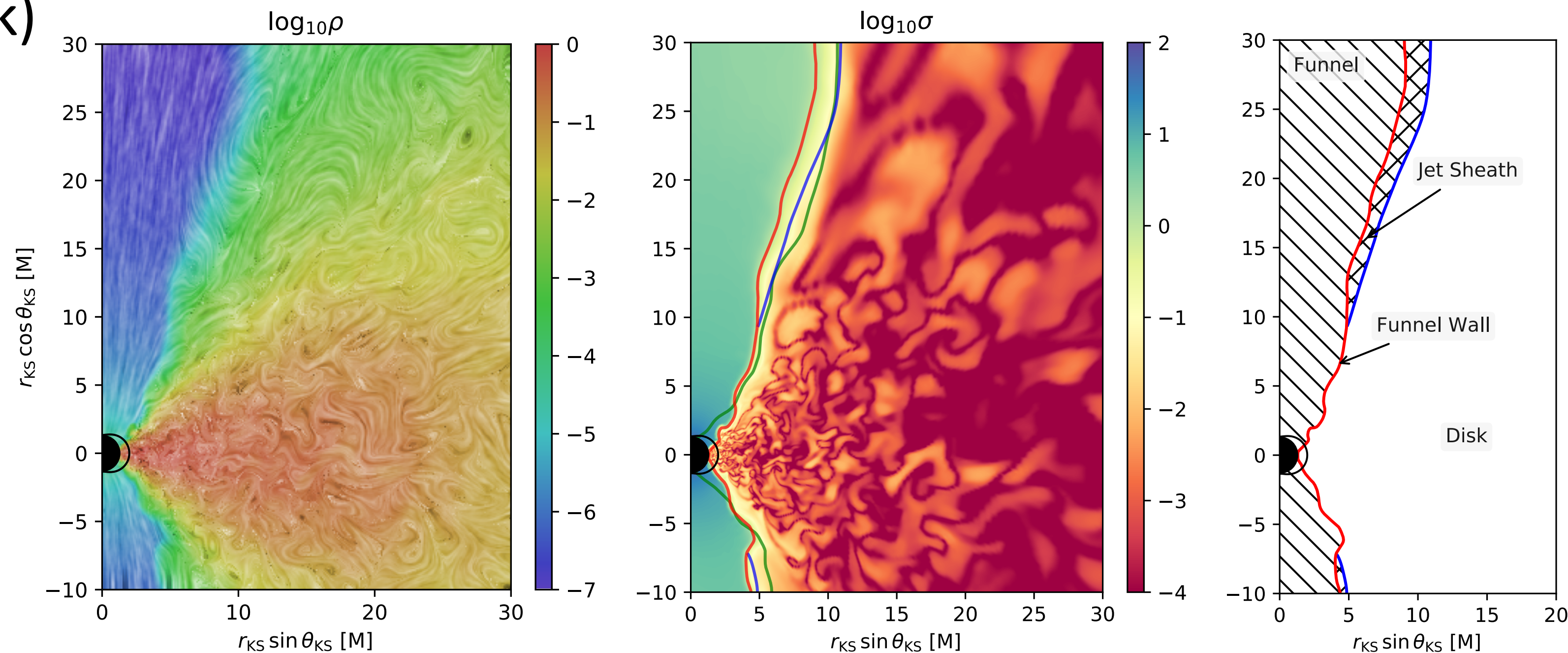
▶ **MAD** (Magnetically Arrested Disk)

▶ Spin parameter:

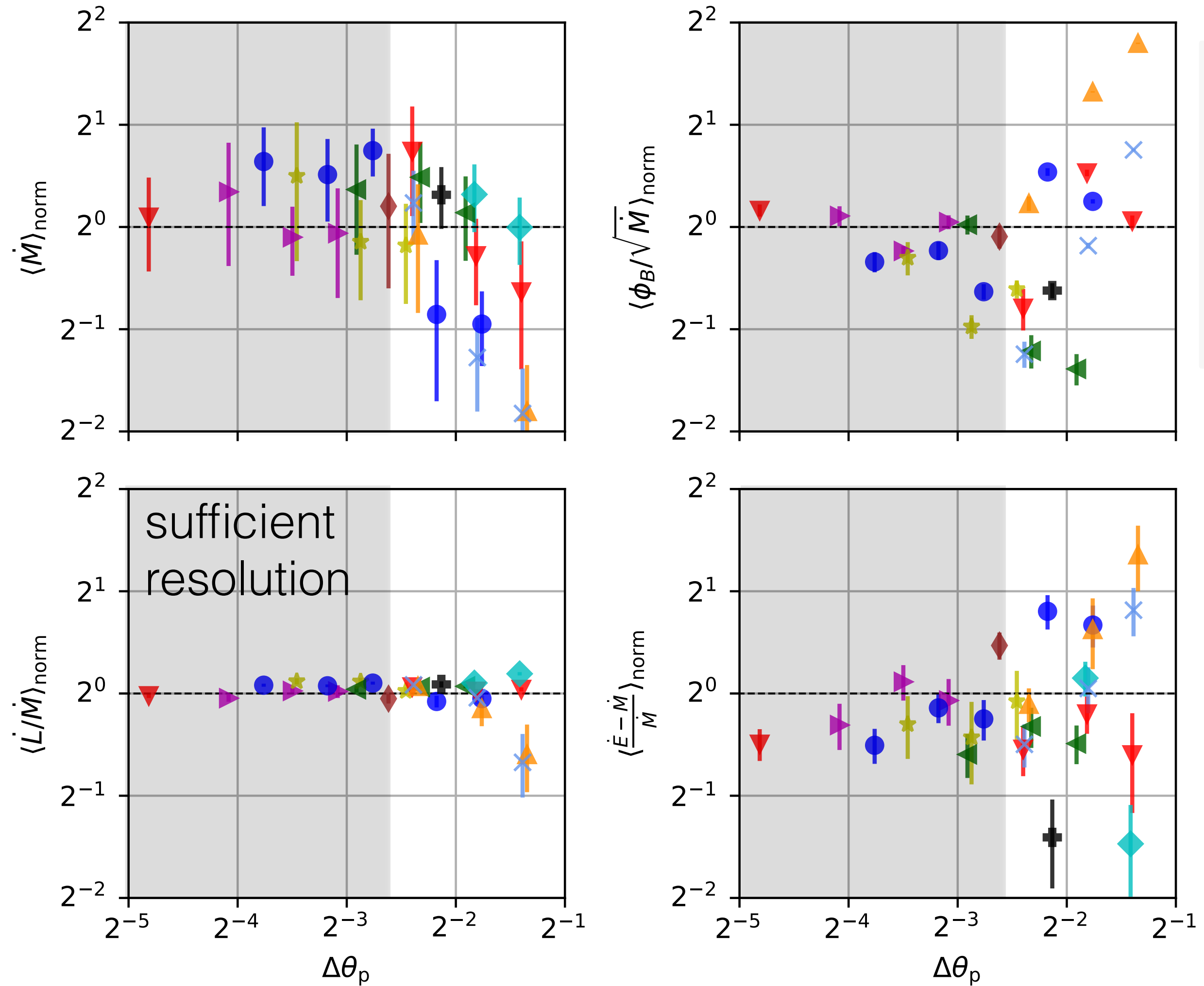
▶ SANE: **-0.94, -0.5, 0, 0.5, 0.75, 0.88, 0.94, 0.97, 0.98**

▶ MAD: **-0.94, -0.5, 0, 0.5, 0.75, 0.94**

SANE morphology (OP, ...Bugli... et al. 2019)



Event Horizon GRMHD Code Comparison Project



- ▶ Assess systematics:
- ▶ Algorithms
- ▶ grids
- ▶ boundary conditions

Codes can be used interchangeably once sufficient resolution is employed

Typically:

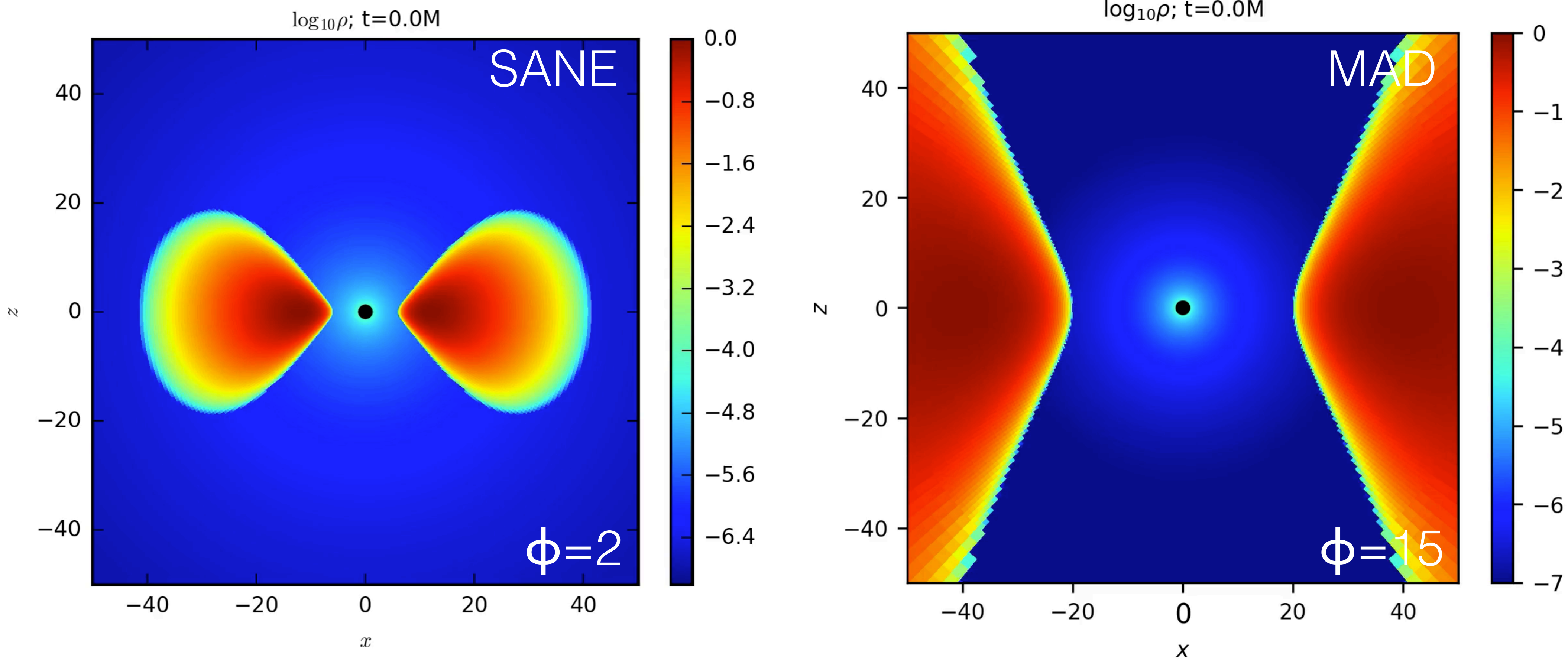
**192³, PPM reconstruction,
100K cpu hours (500EUR)**

OP, ...Bugli... et al. (arXiv: 1904.04923)



Event Horizon Telescope

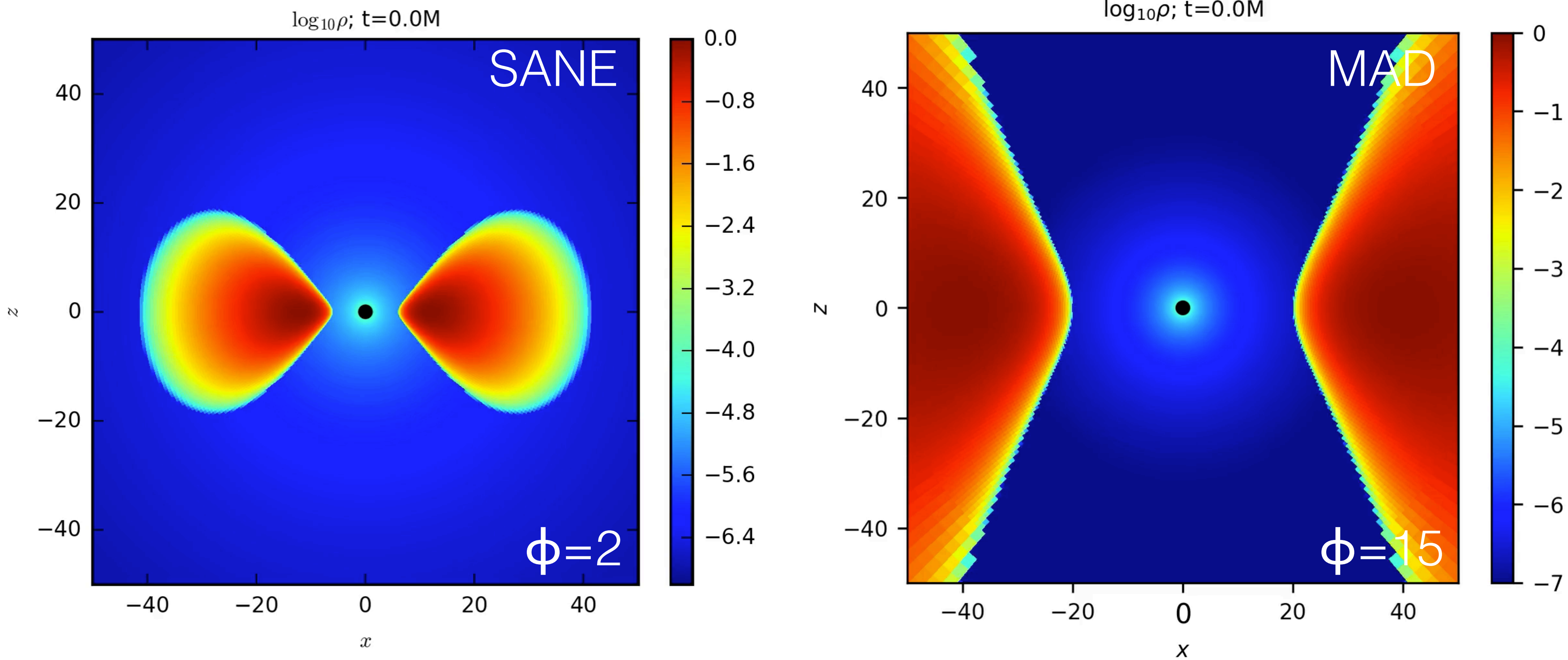
The hair of accreting black holes: magnetic flux



$$\phi = \frac{\int B^r dA_{\text{Horizon}}}{\sqrt{\dot{M}}}$$

Maximum BH magnetic flux: $\phi_{\text{max}}=15$

The hair of accreting black holes: magnetic flux



$$\phi = \frac{\int B^r dA_{\text{Horizon}}}{\sqrt{\dot{M}}}$$

Maximum BH magnetic flux: $\phi_{\text{max}}=15$



Tchekhovskoy et al. 2011, McKinney et al. 2012

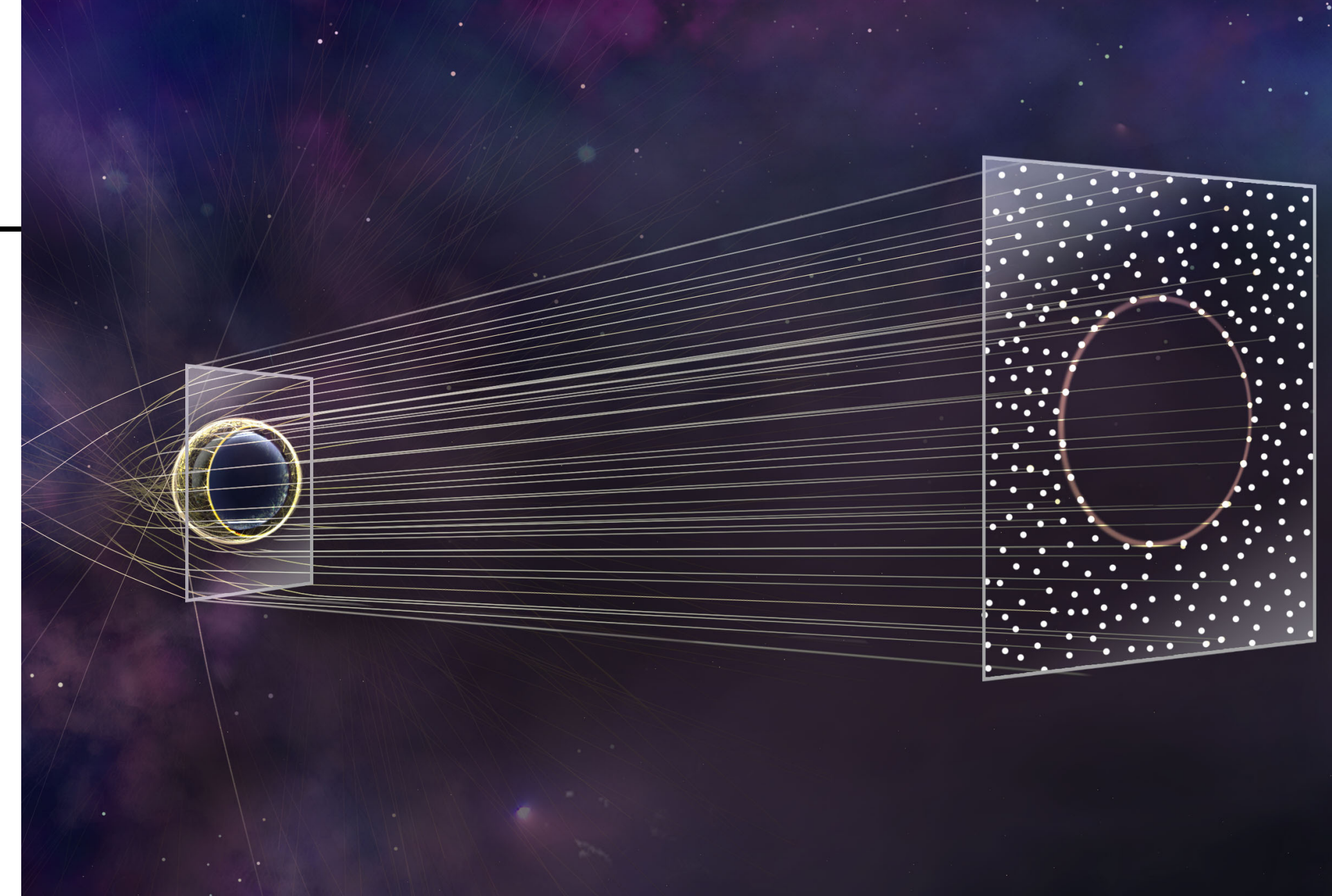
Image Library: > 60,000 images

- ▶ 1.3mm modeled images from: *ipole*, RAPTOR, BHOSS
- ▶ **100-500 samples** per GRMHD simulation
- ▶ Observer inclination angles:
 $i=12, 17, 22, 158, 163, 168$ deg

- ▶ Thermal electrons (Moscibrodzka+, 2016):

$$\frac{T_i}{T_e} = R_{\text{high}} \frac{\beta_p^2}{1 + \beta_p^2} + \frac{1}{1 + \beta_p^2}$$

- ▶ Electrons colder at high plasma beta (disk), warmer in low plasma beta (jet)

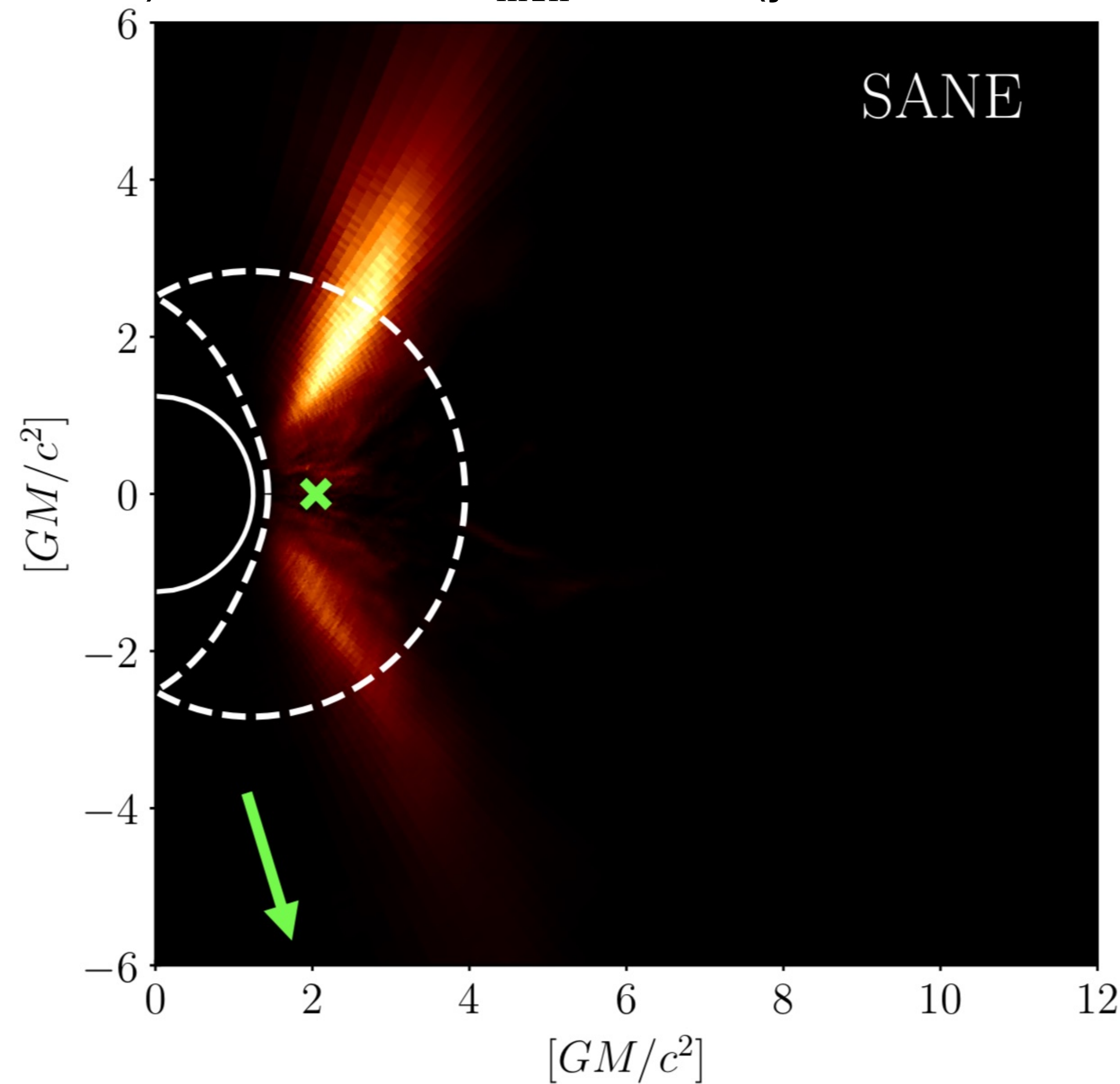
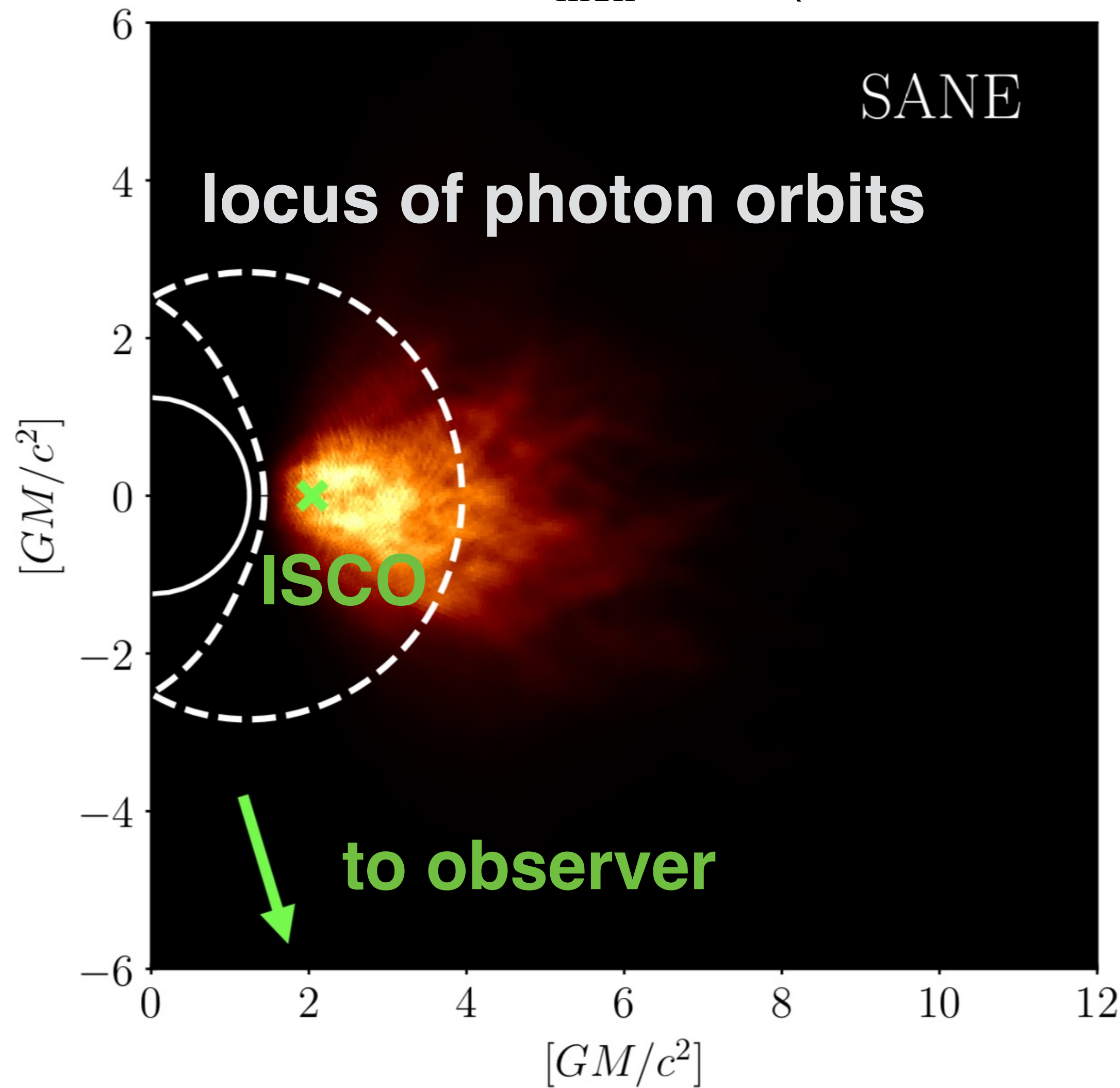


Ion/electron temperature ratio depends on **$R_{\text{high}}=(1, 10, 20, 40, 80, 160)$** , plasma beta $\beta_p \equiv P_g/P_{\text{mag}}$.

Where do mm photons originate? (SANE, $a = 0.94$)

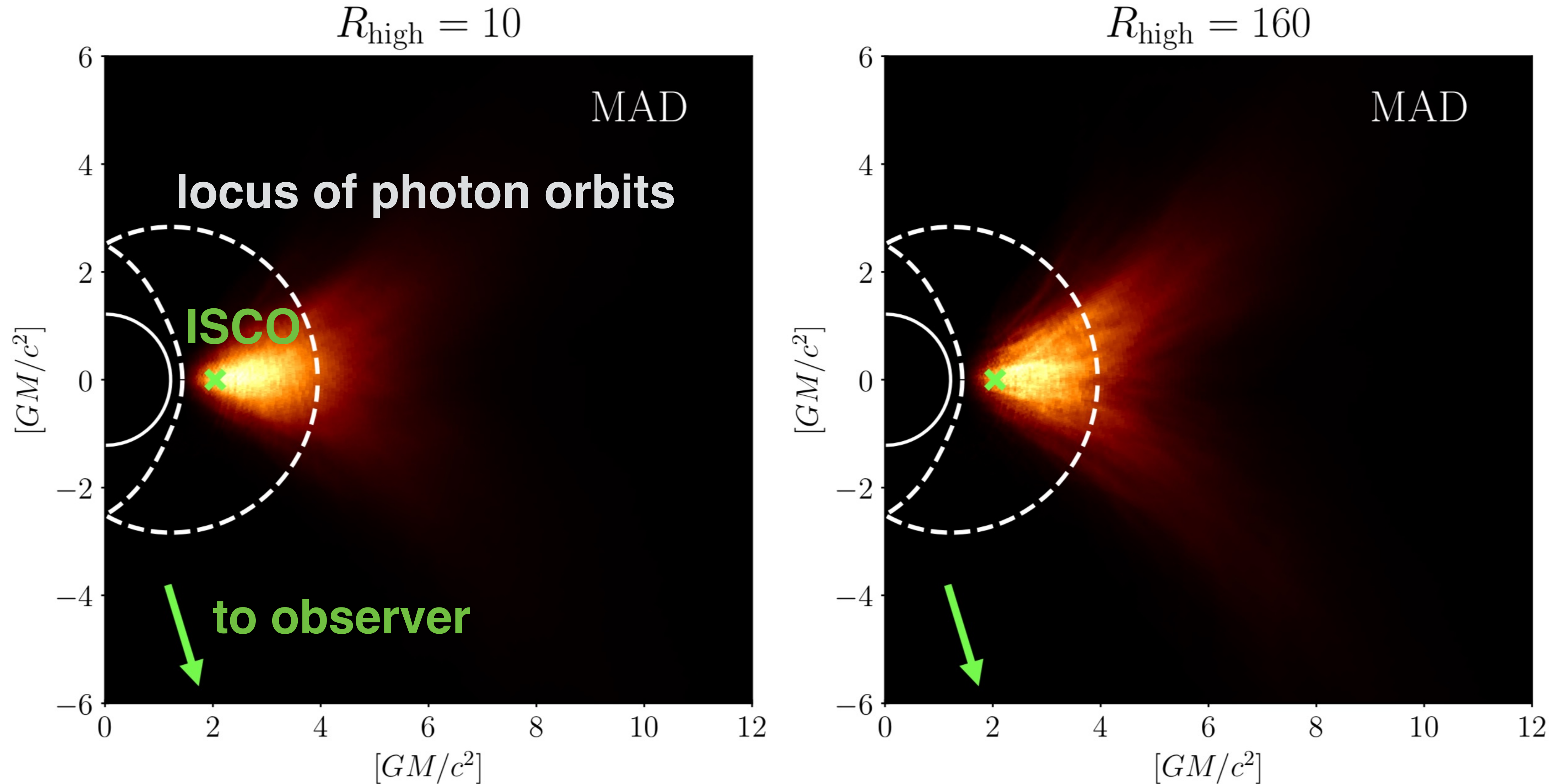
$R_{\text{high}} = 10$ (disk dominated)

$R_{\text{high}} = 160$ (jet dominated)



Event Horizon Telescope

Where do mm photons originate? (MAD, $a = 0.94$)



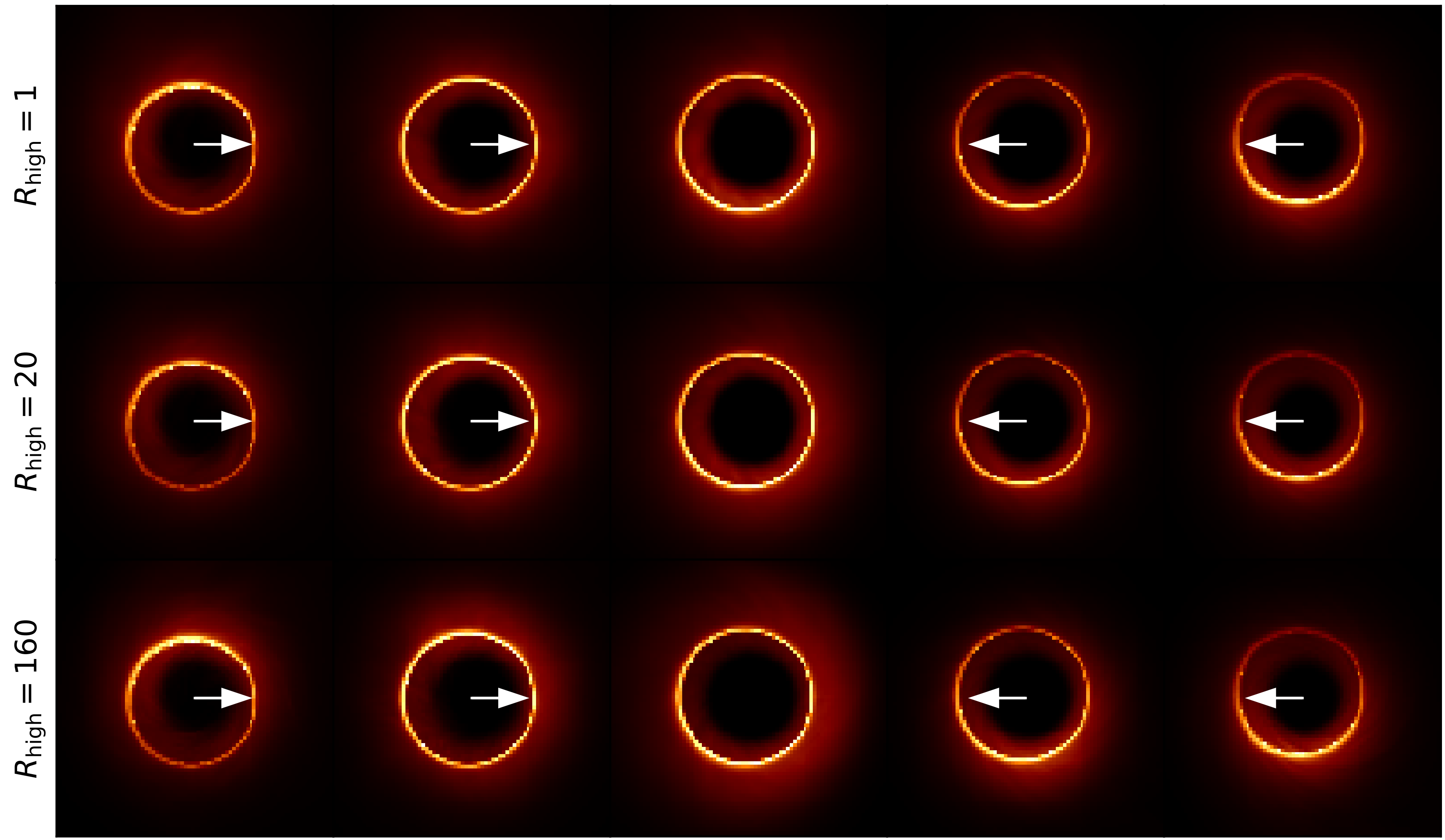
Overview of image library: Time-averaged Images (MAD)

$a_* = -0.94$ $a_* = -0.5$ $a_* = 0$ $a_* = +0.5$ $a_* = +0.94$

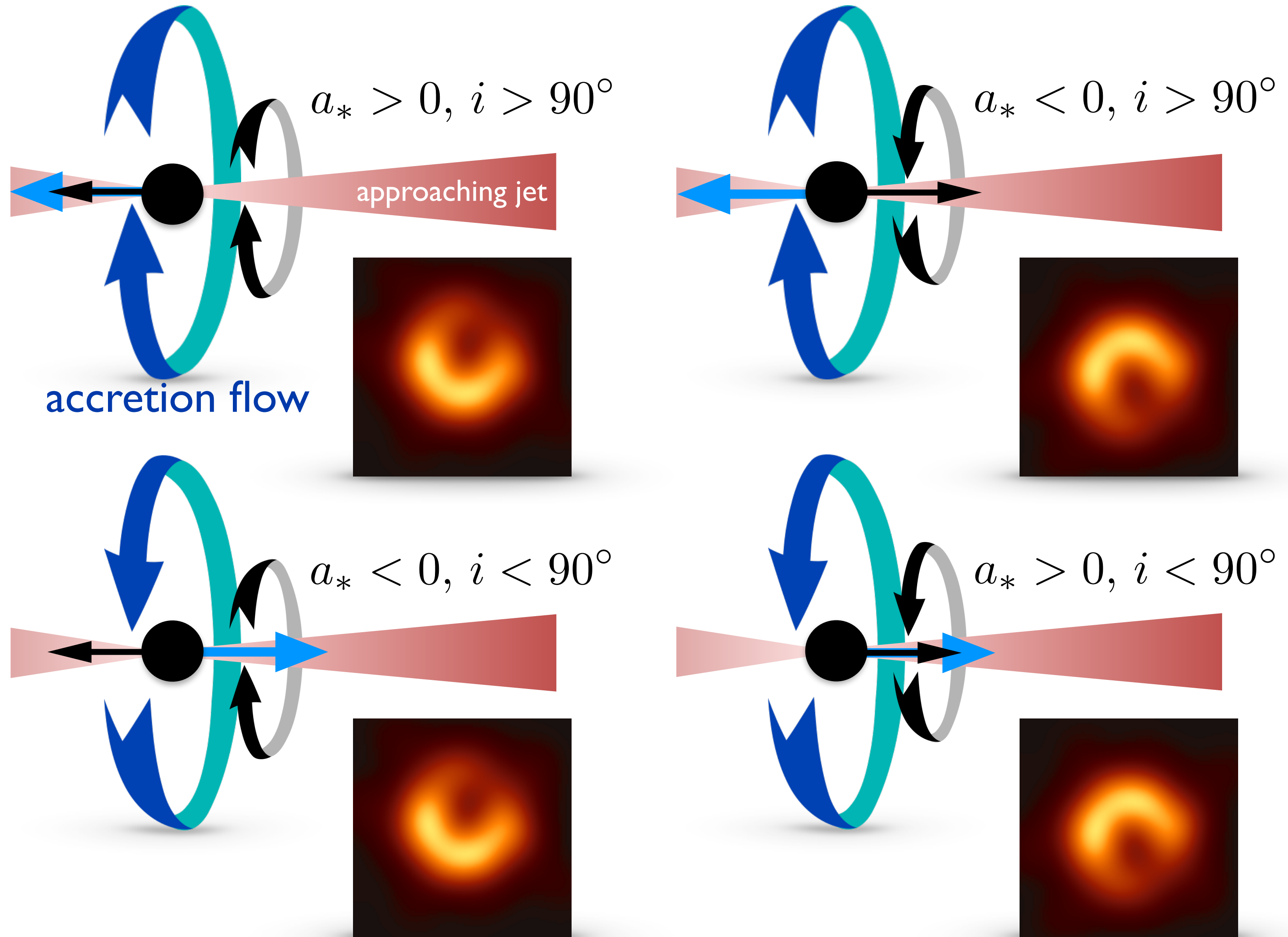


black hole
rotational axis

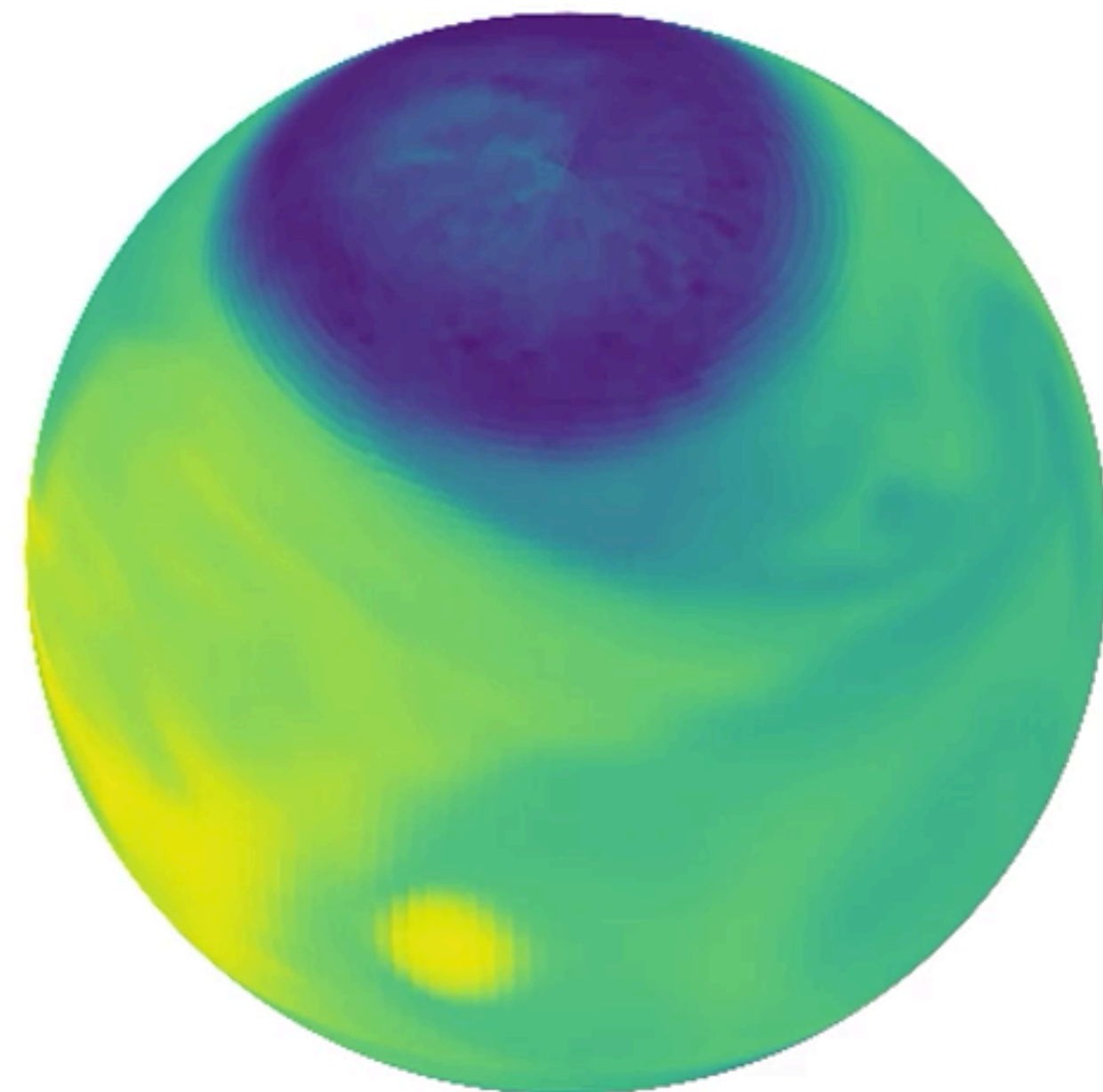
**the forward jet is
pointed to the right
in all panels*



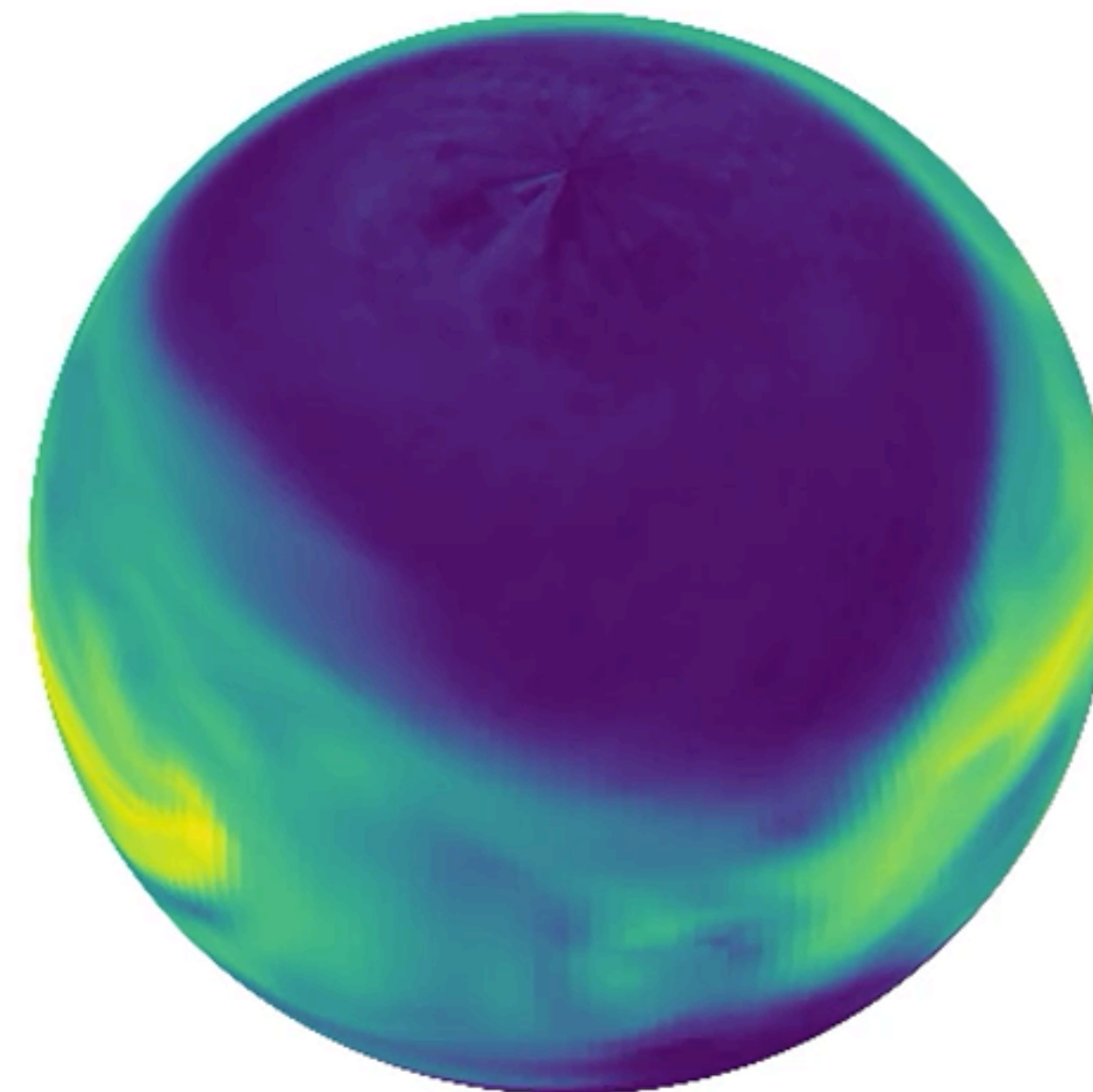
Ring Asymmetry and Black Hole Spin



Spherical Projection of Density Evolution



MAD, $a = -0.94$



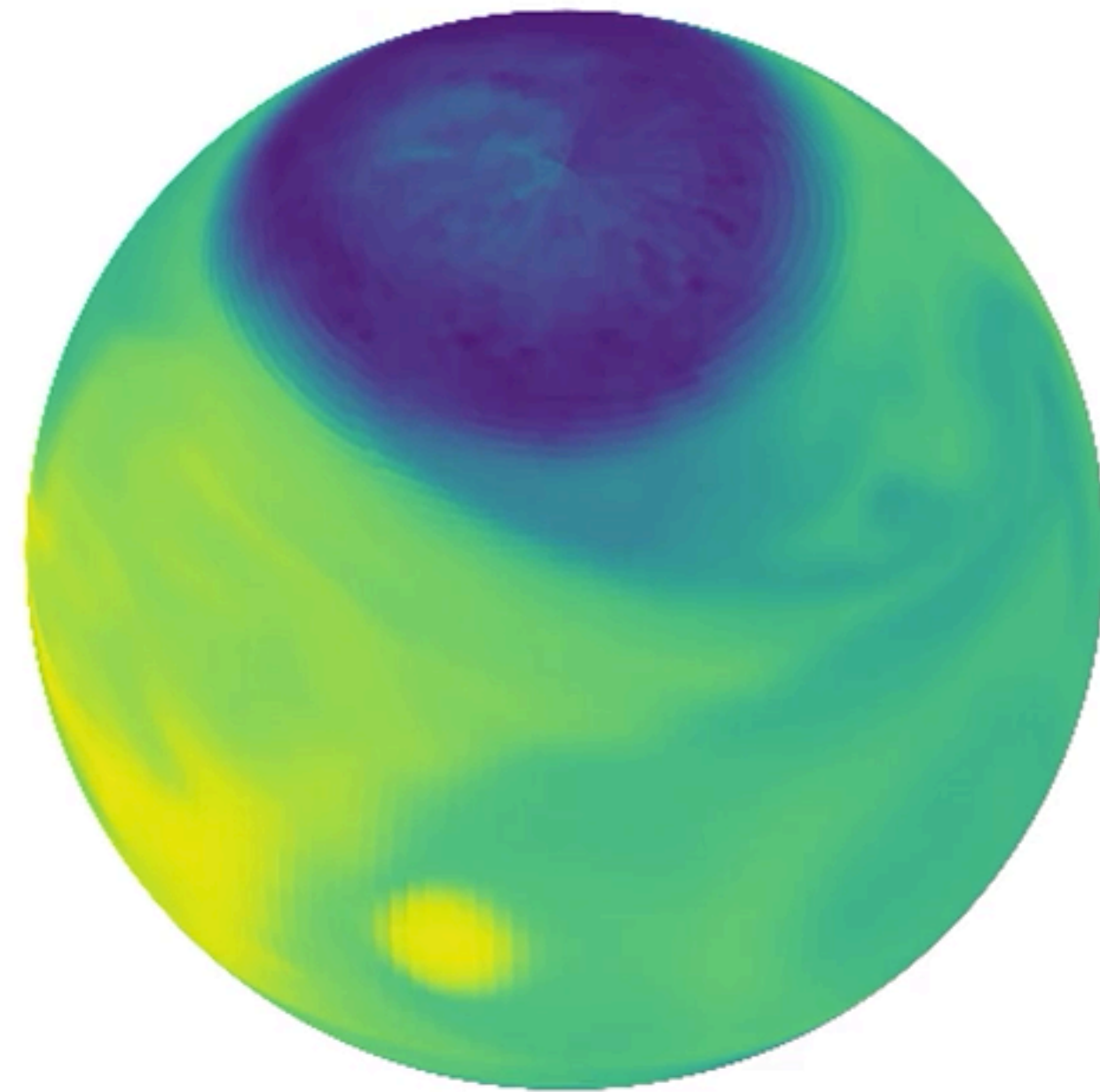
MAD, $a = +0.94$

color shows
 $\log(\rho)$
on surface
 $r = 10 \text{ GM}/c^2$

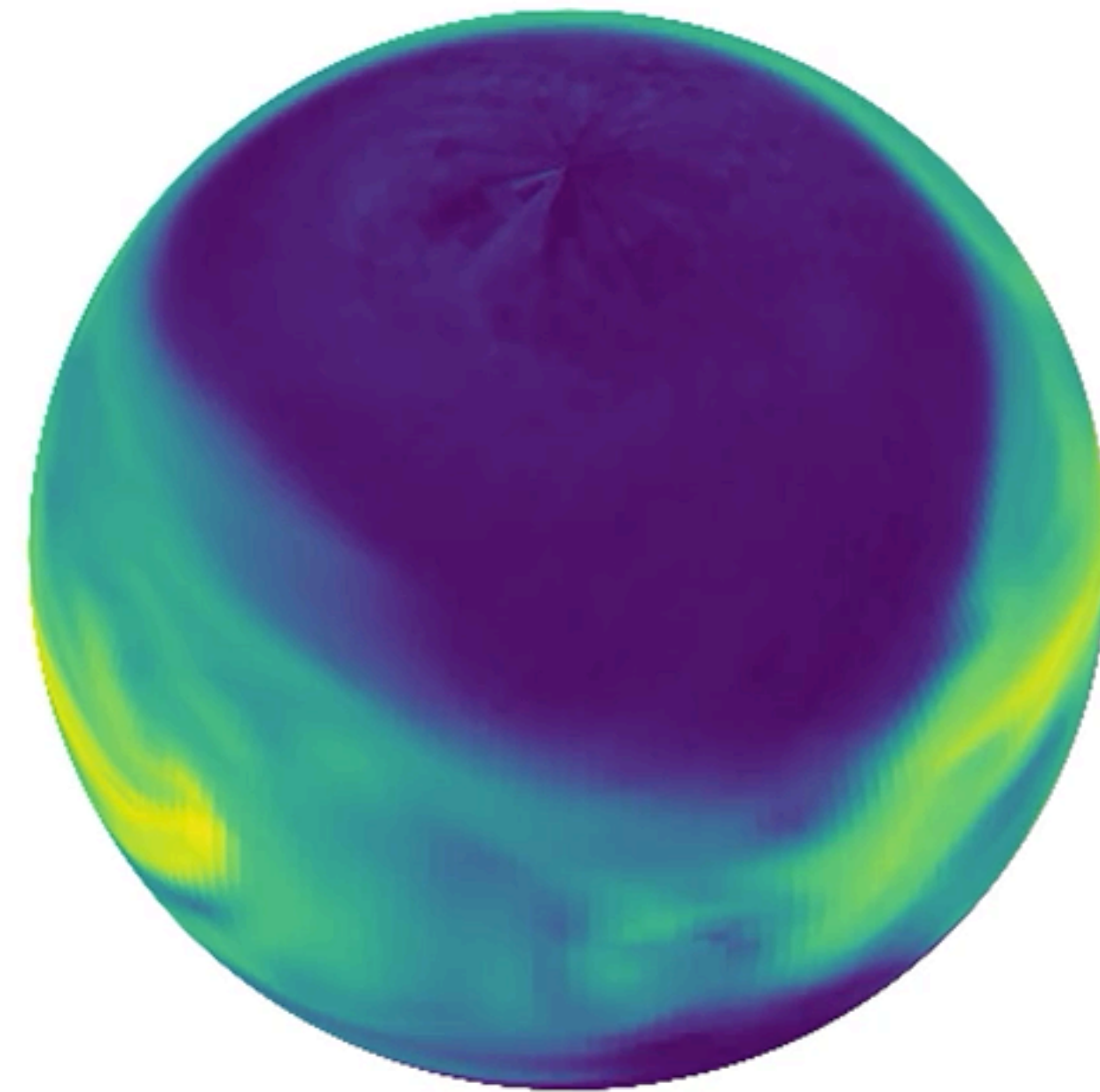
pole to equator
contrast $\sim 10^5$



Spherical Projection of Density Evolution



MAD, $a = -0.94$



MAD, $a = +0.94$

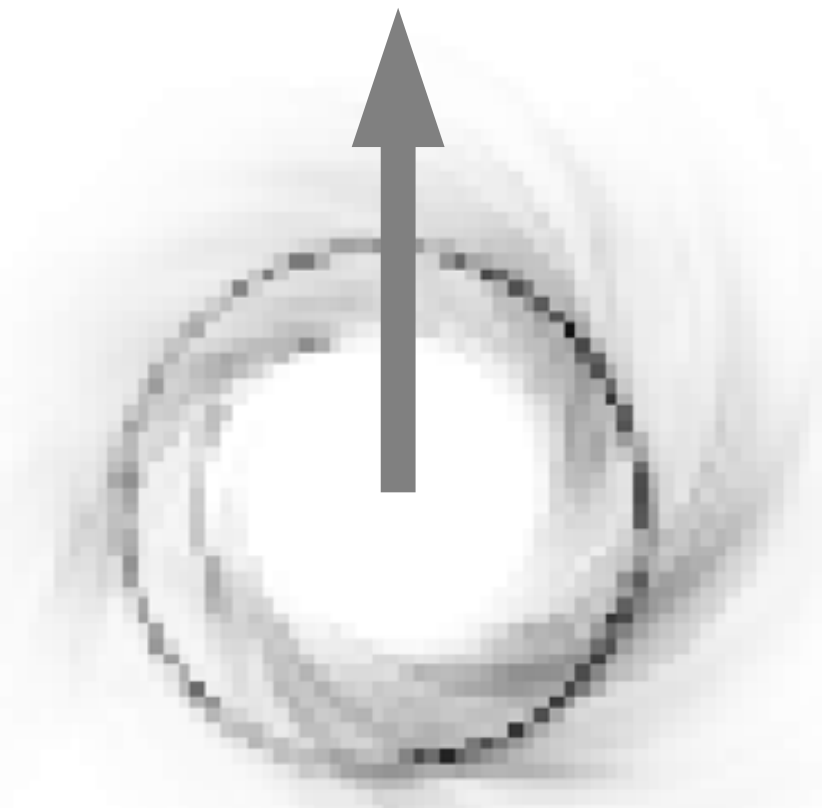
color shows
 $\log(\rho)$
on surface
 $r = 10 \text{ GM}/c^2$

pole to equator
contrast $\sim 10^5$

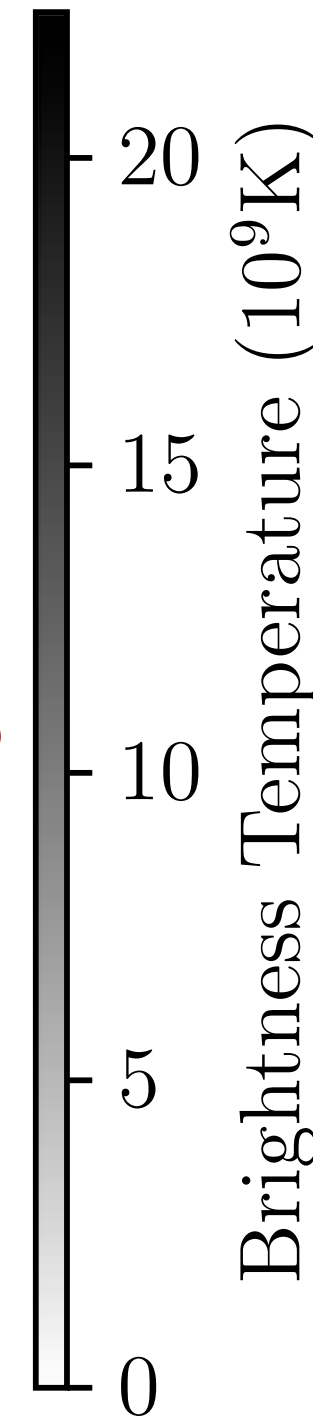
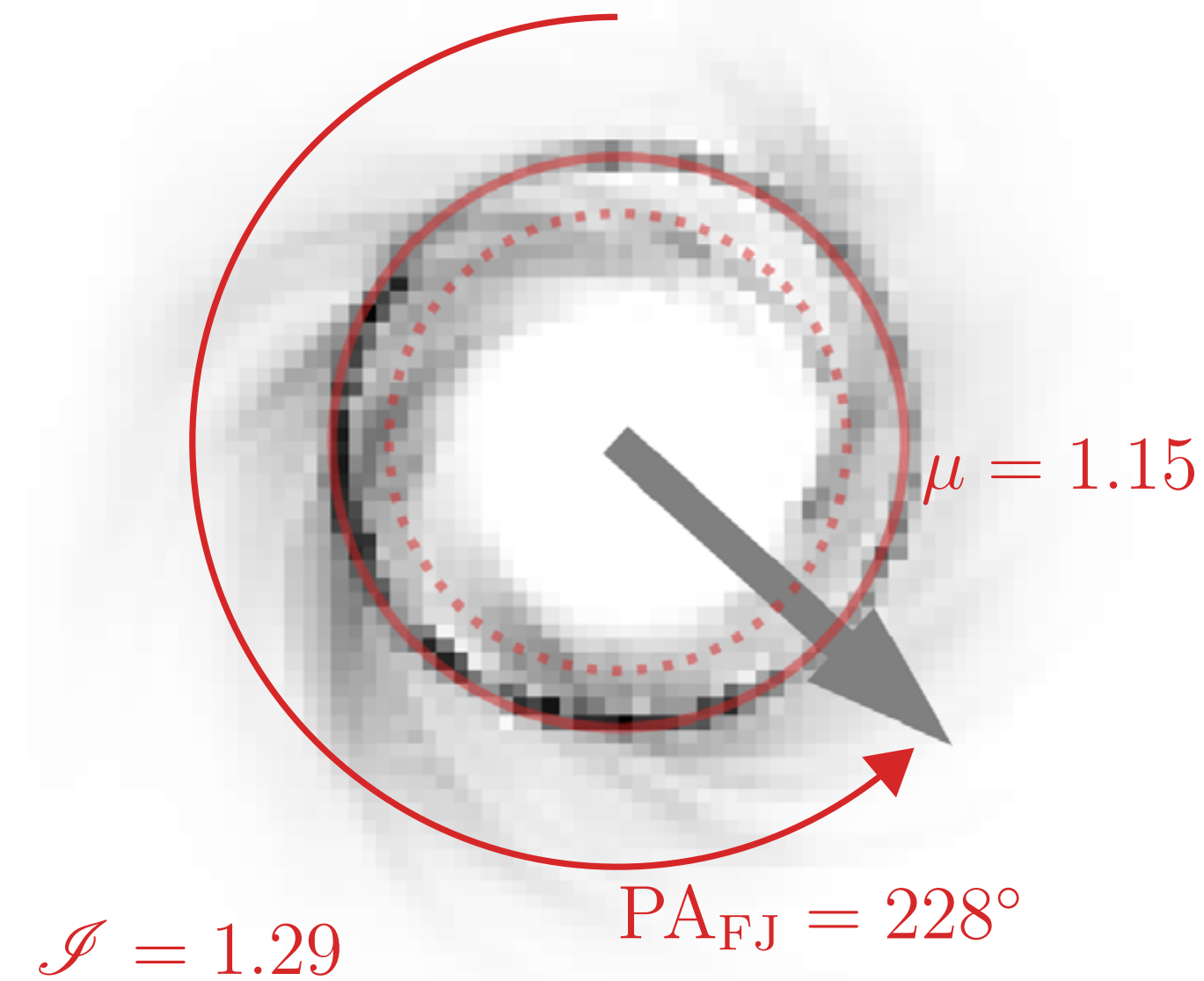


Single snapshot model: fitting GRMHD data

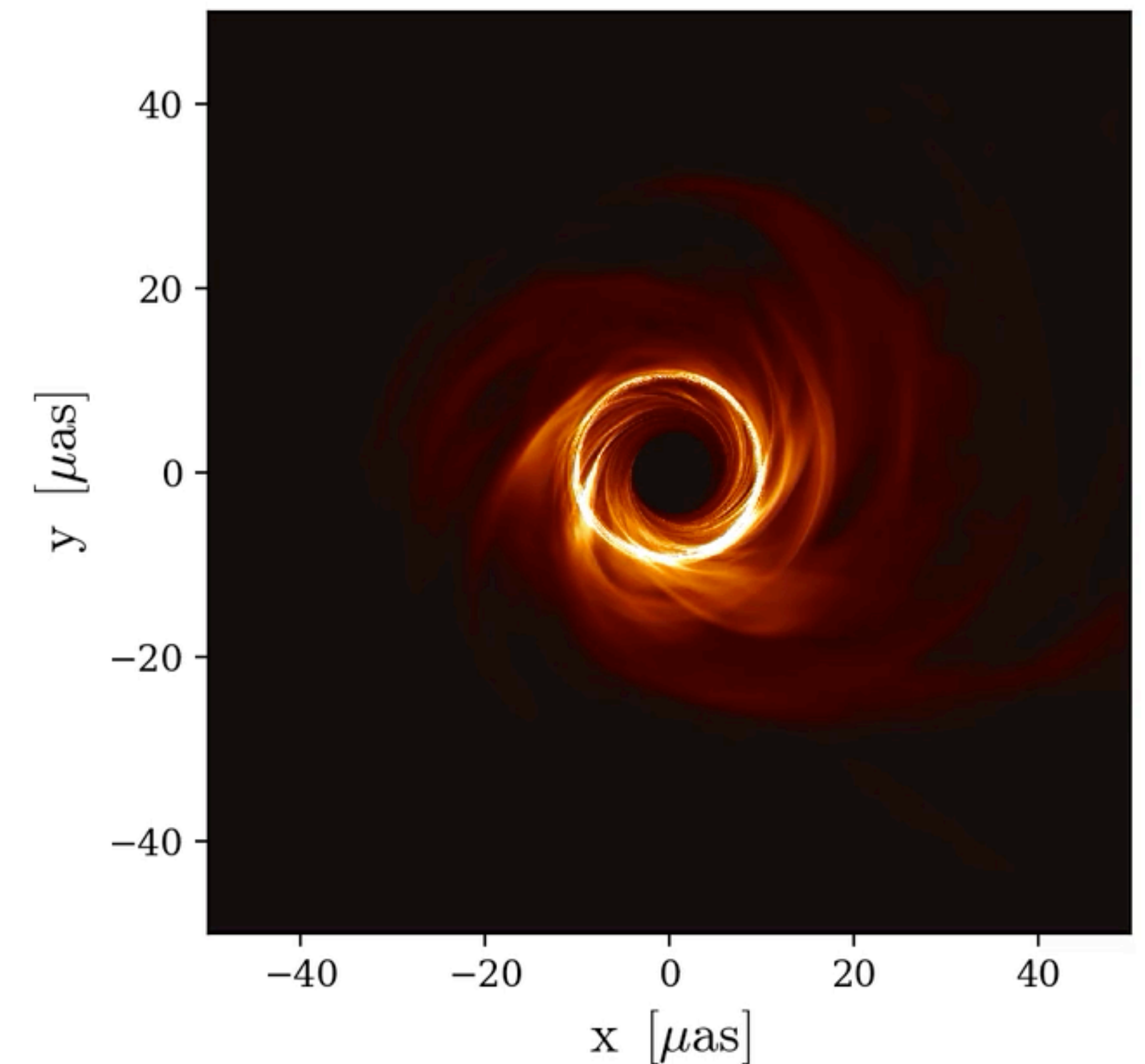
Input Snapshot



Single Snapshot Model



+ 1759.3 days



G. Wong, B. Prather, C. Gammie (Illinois)

Free parameters: M/D, flux density, position angle PA, gain at each VLBI station

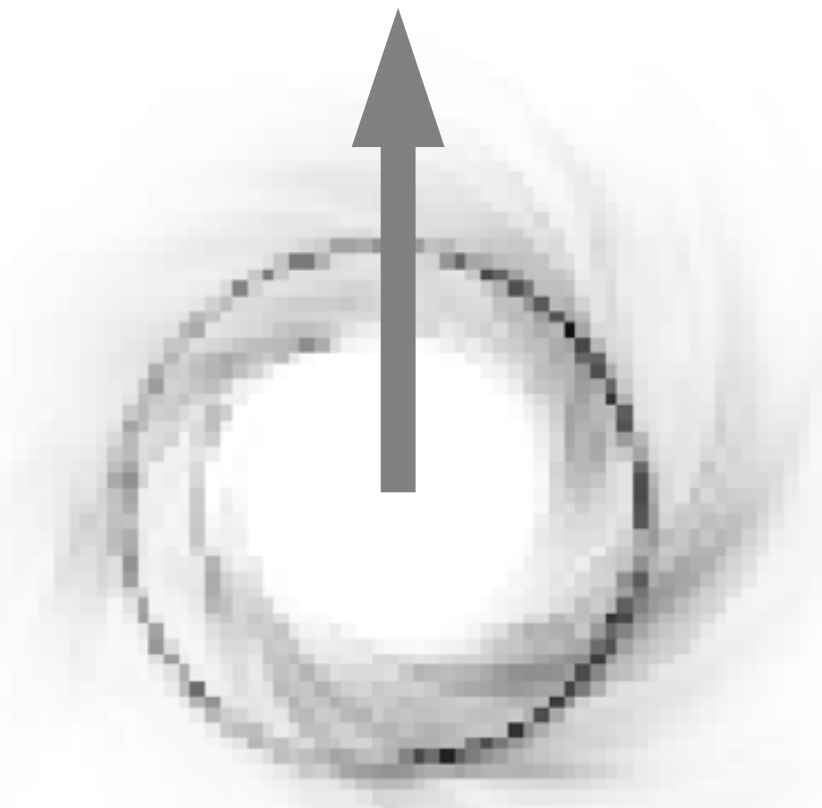
Two pipelines: THEMIS (MCMC), GENA (Evolutionary Algorithm)



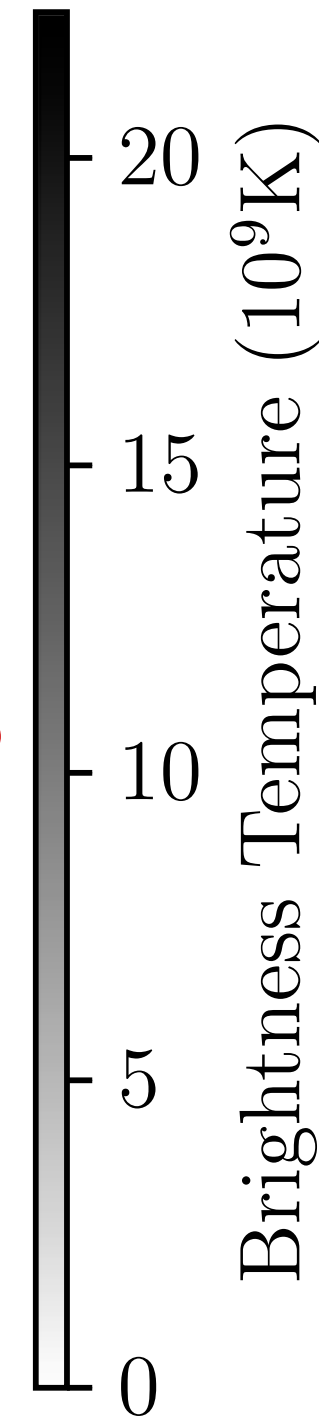
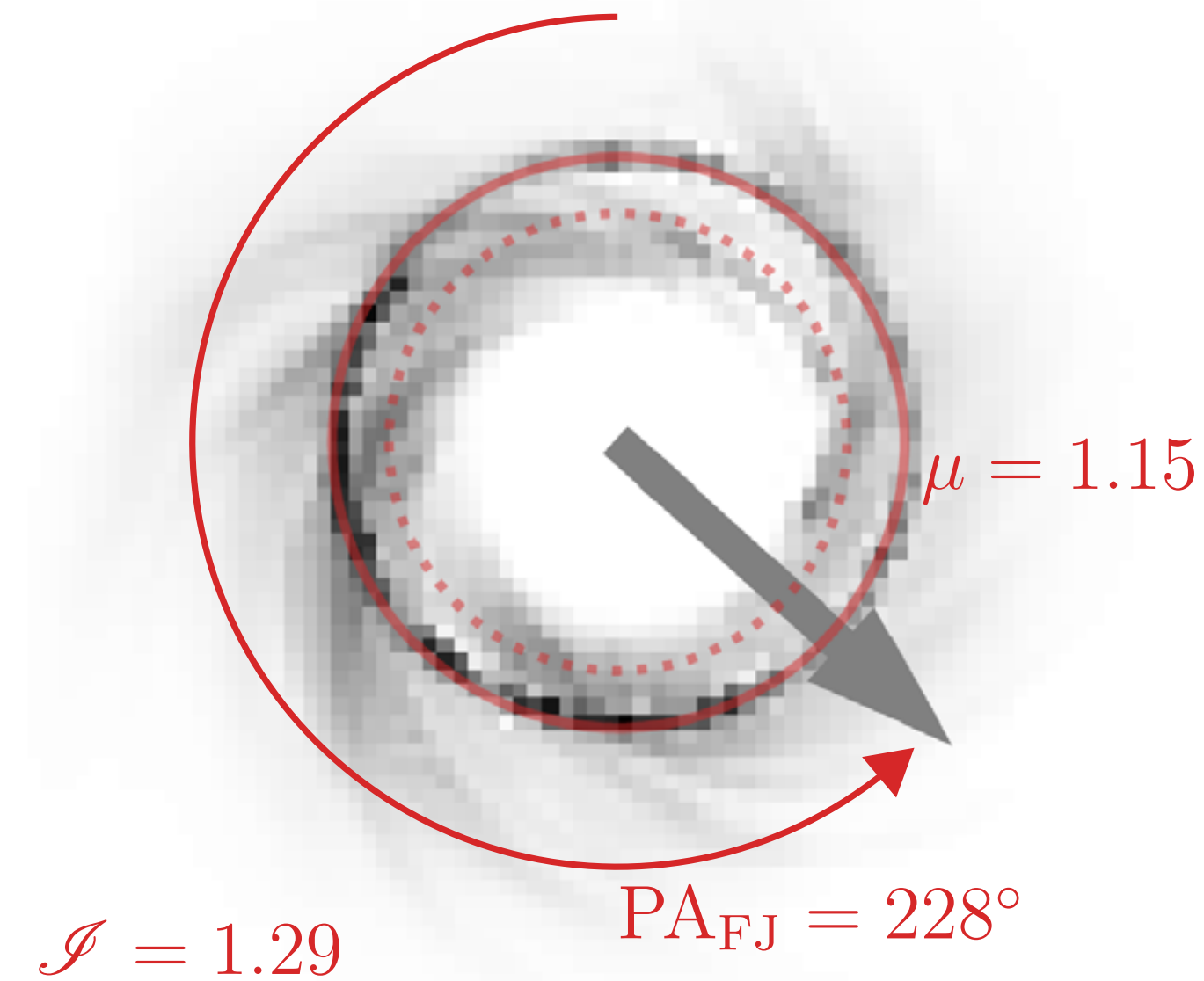
Event Horizon Telescope

Single snapshot model: fitting GRMHD data

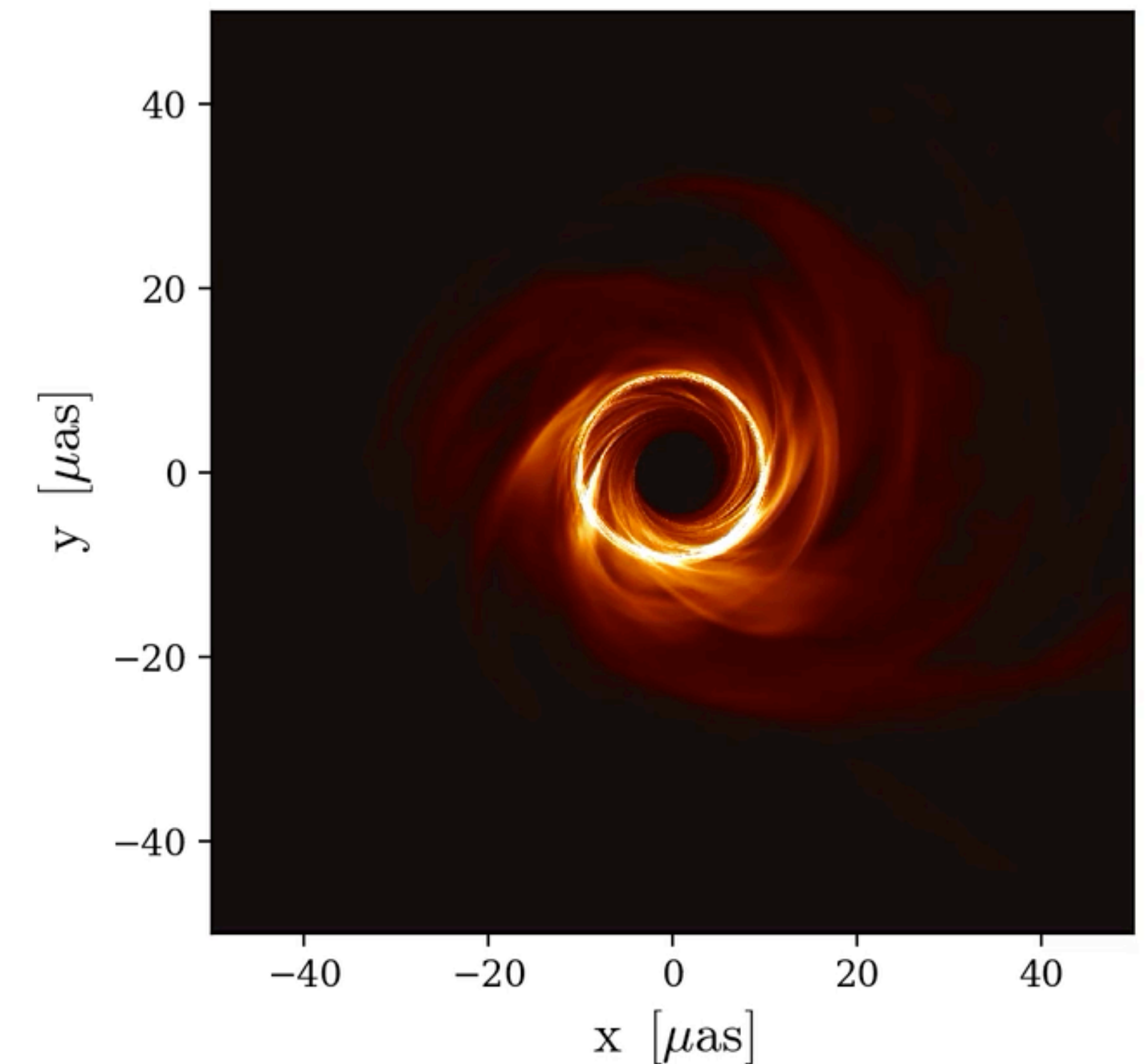
Input Snapshot



Single Snapshot Model



+ 1759.3 days



G. Wong, B. Prather, C. Gammie (Illinois)

Free parameters: M/D , flux density, position angle PA, gain at each VLBI station

Two pipelines: THEMIS (MCMC), GENA (Evolutionary Algorithm)



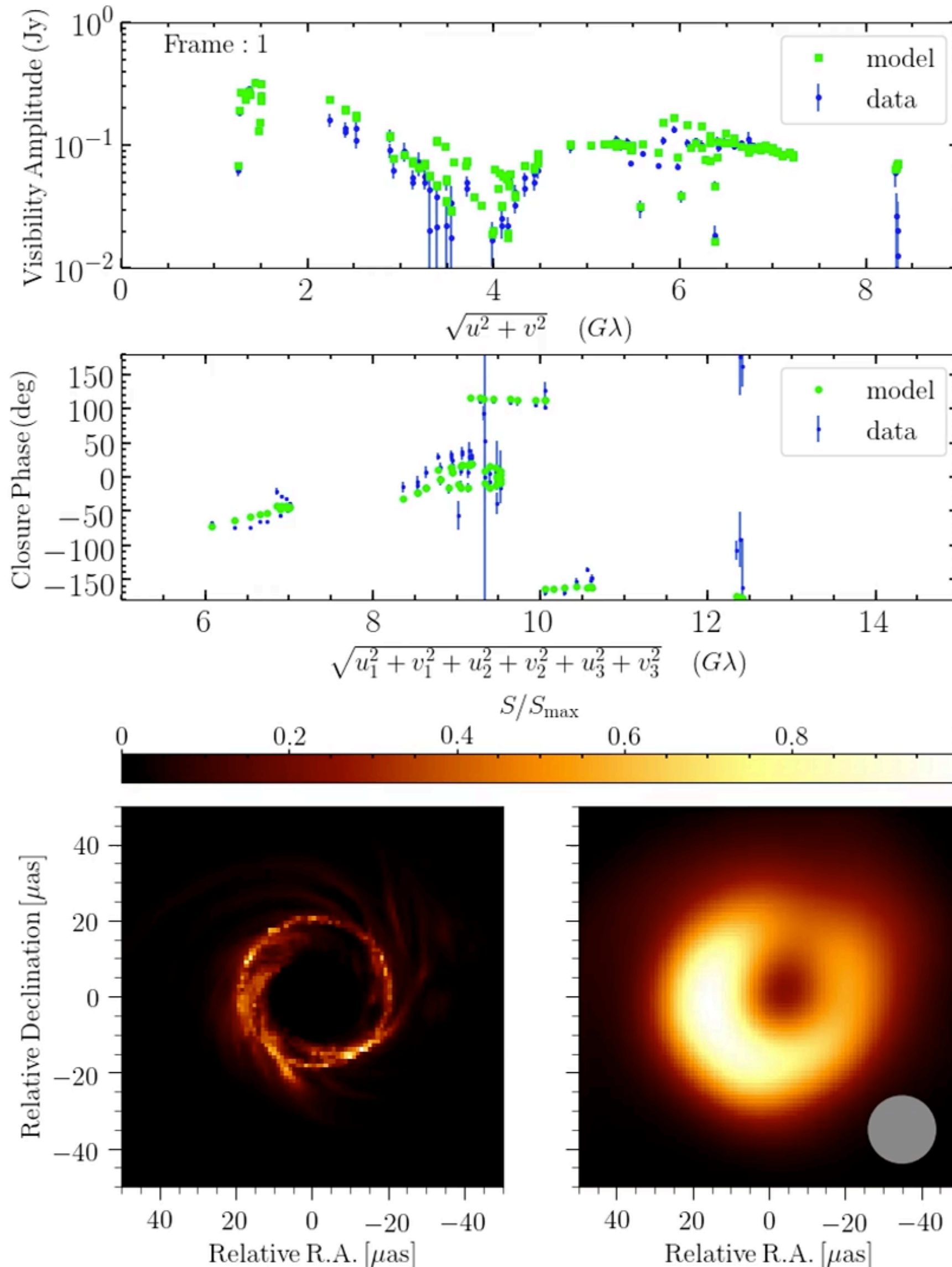
Event Horizon Telescope

Fitting Time-Dependent Model to EHT observations

visibility
amplitude
(VA)

Closure
phase (CP)

GRMHD image
(left) & convolved
image (right)



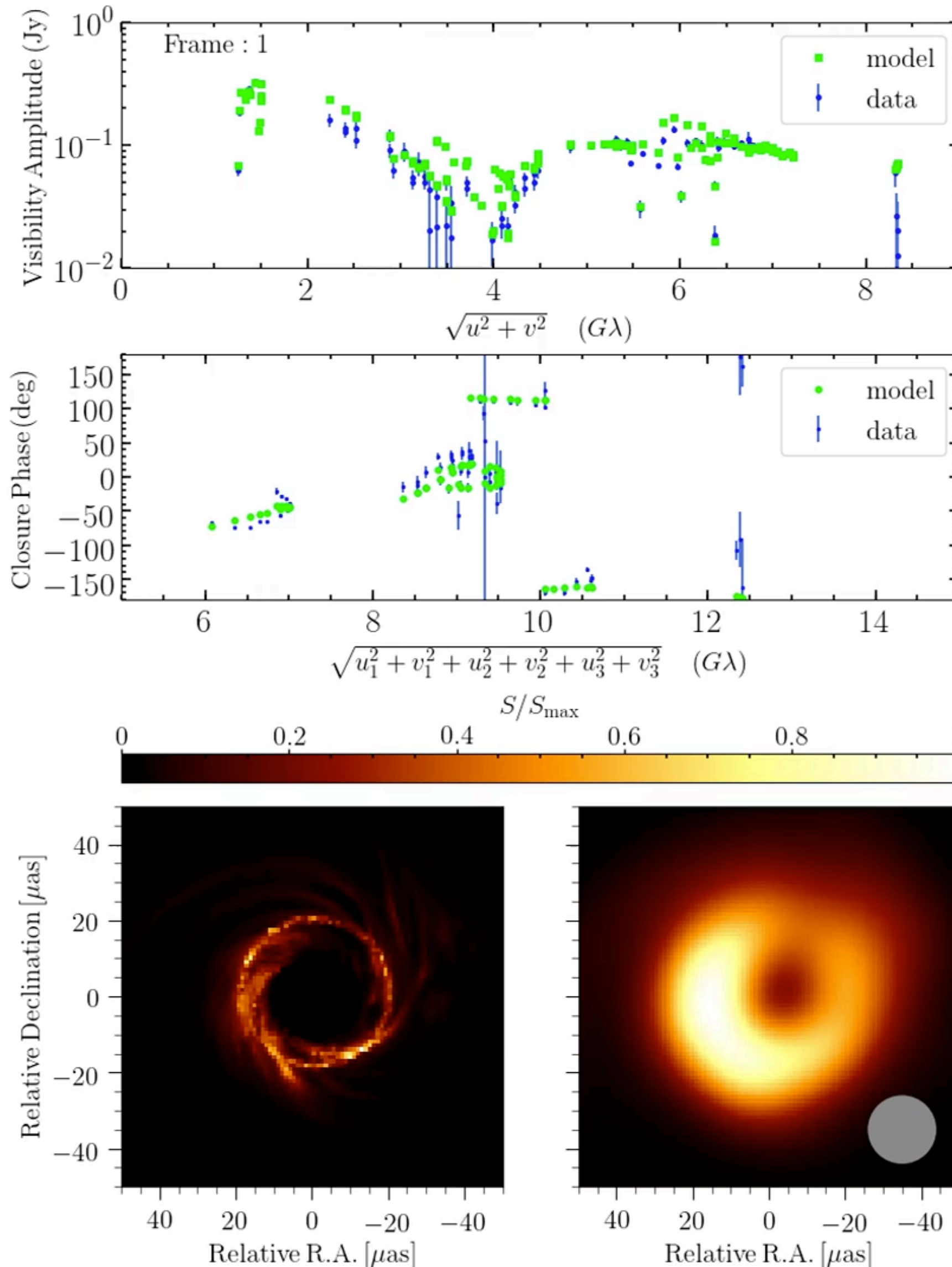
- ▶ Reduced chi-square comparison: **stochastic fluctuations** in the GRMHD model *not a single formally acceptable fit* (best χ^2 : 1.79)
- ▶ Average Imaging Scoring to **test the consistency** of the GRMHD models to data

Fitting Time-Dependent Model to EHT observations

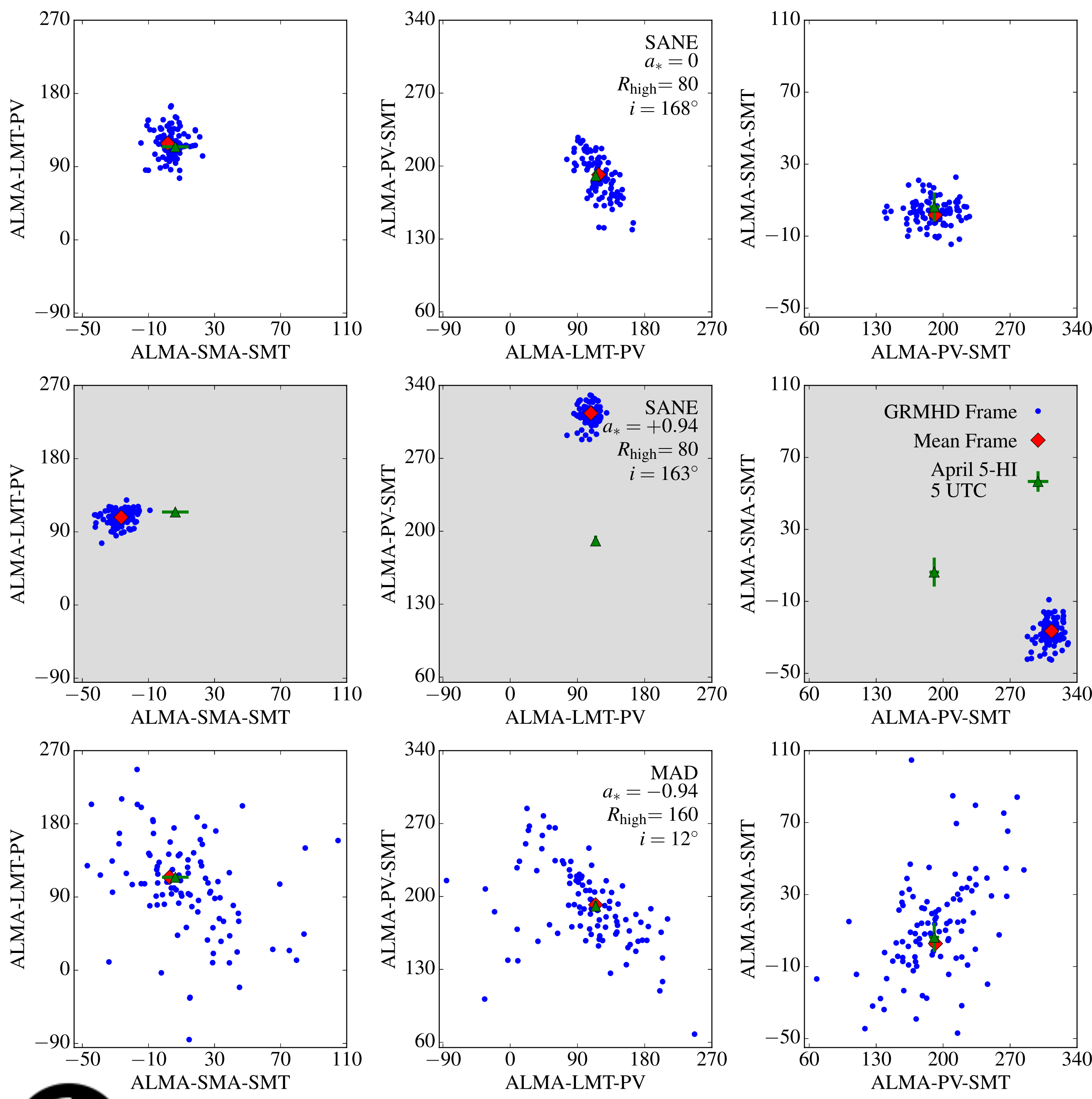
visibility
amplitude
(VA)

Closure
phase (CP)

GRMHD image
(left) & convolved
image (right)

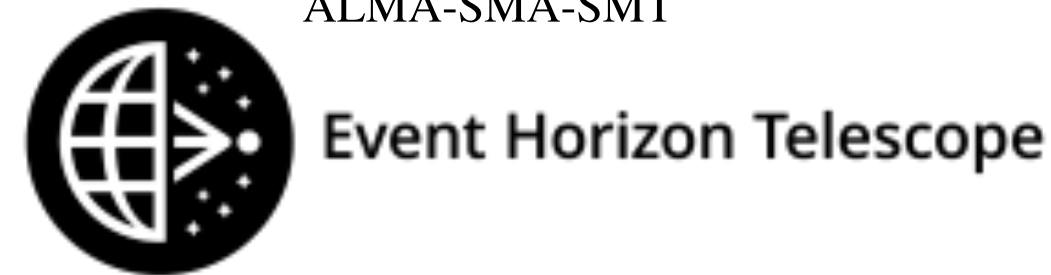
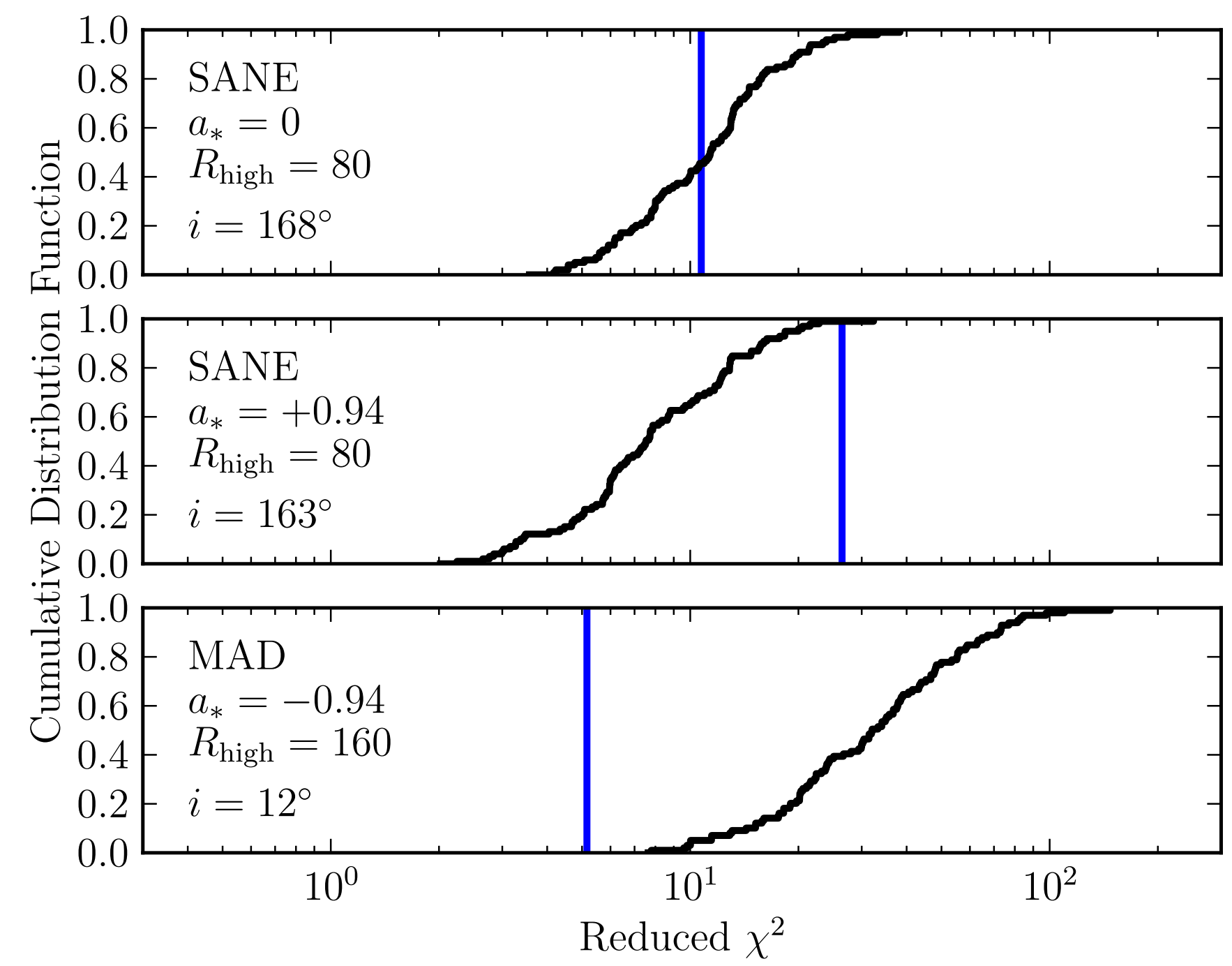


- ▶ Reduced chi-square comparison: **stochastic fluctuations** in the GRMHD model *not a single formally acceptable fit* (best χ^2 : 1.79)
- ▶ Average Imaging Scoring to **test the consistency** of the GRMHD models to data



Average image scoring (AIS):
*check if the data is consistent
 with being drawn from a
 given simulation model*

reject model if $\langle p \rangle \leq 1\%$



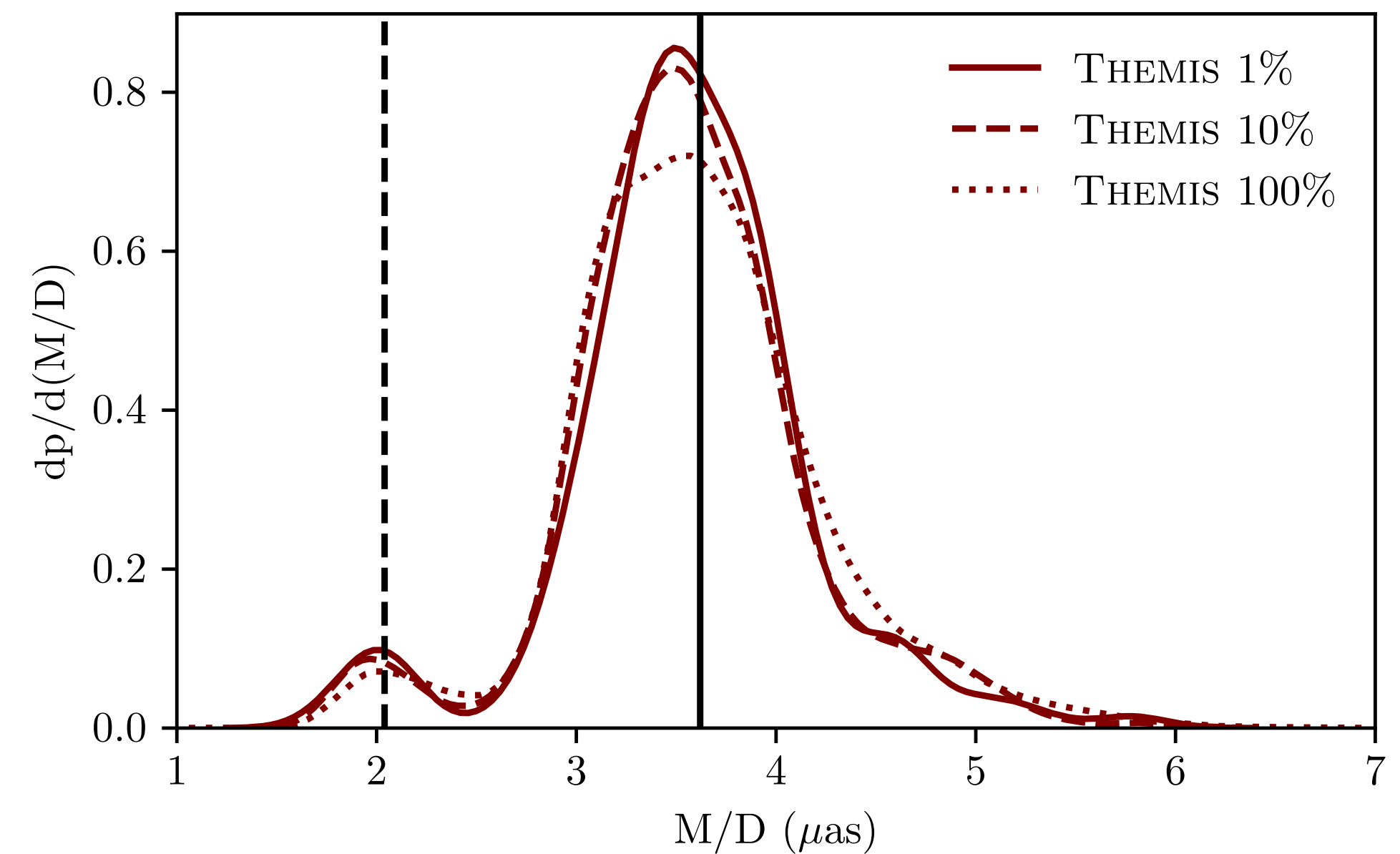
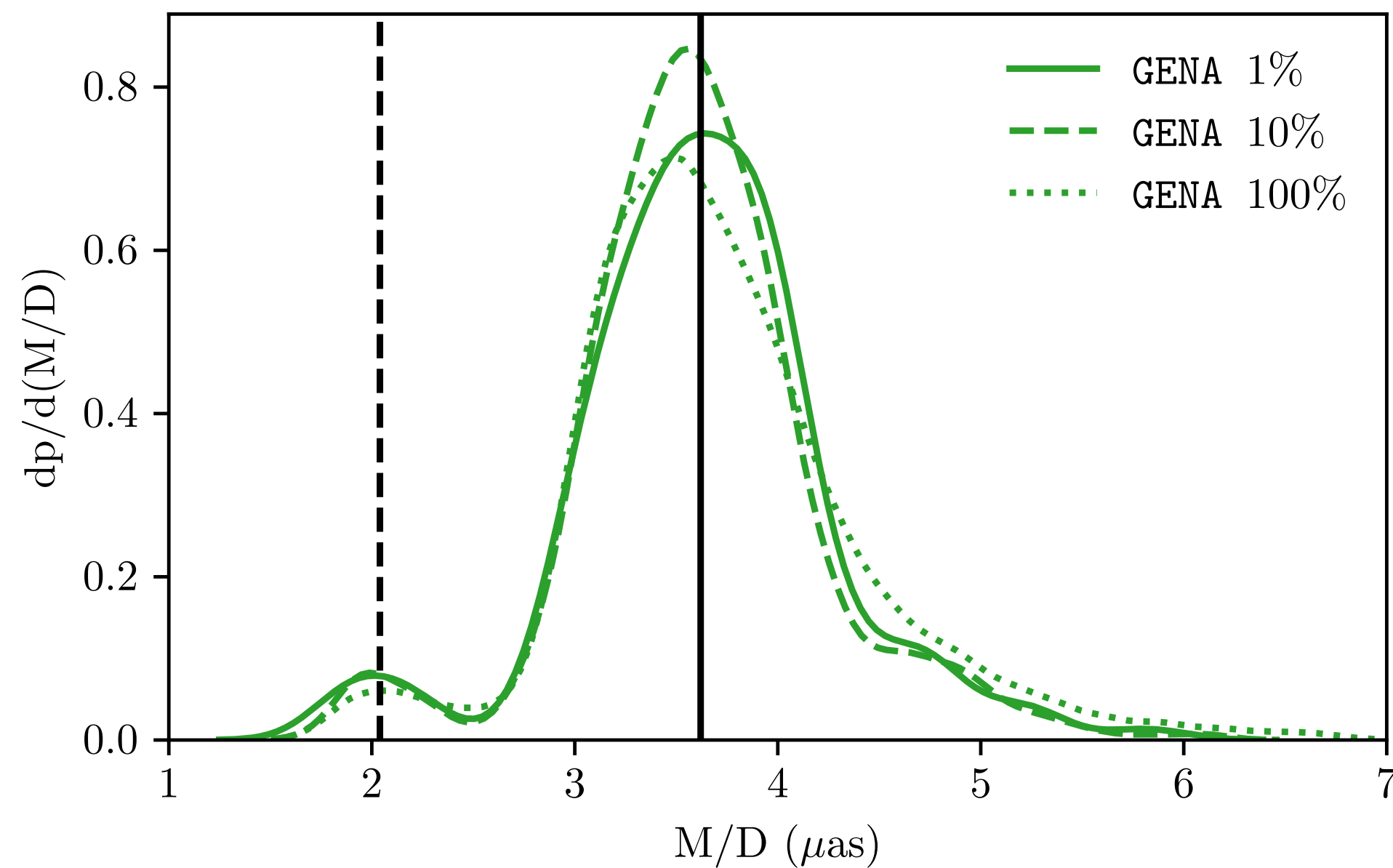
Average Image Scoring Summary

Flux ^b	a_* ^c	$\langle p \rangle$ ^d	N_{model} ^e	MIN(p) ^f	MAX(p) ^g
SANE	-0.94	0.33	24	0.01	0.88
SANE	-0.5	0.19	24	0.01	0.73
SANE	0	0.23	24	0.01	0.92
SANE	0.5	0.51	30	0.02	0.97
SANE	0.75	0.74	6	0.48	0.98
SANE	0.88	0.65	6	0.26	0.94
SANE	0.94	0.49	24	0.01	0.92
SANE	0.97	0.12	6	0.06	0.40
MAD	-0.94	0.01	18	0.01	0.04
MAD	-0.5	0.75	18	0.34	0.98
MAD	0	0.22	18	0.01	0.62
MAD	0.5	0.17	18	0.02	0.54
MAD	0.75	0.28	18	0.01	0.72
MAD	0.94	0.21	18	0.02	0.50

- ▶ Compare:
data - $\langle \text{model} \rangle$
model - $\langle \text{model} \rangle$
using Themis-AIS
- ▶ Rejects $a = -0.94$ MAD models
- ▶ This model exhibit highest morphological variability

Distribution of Best-Fit Black Hole Angular Size

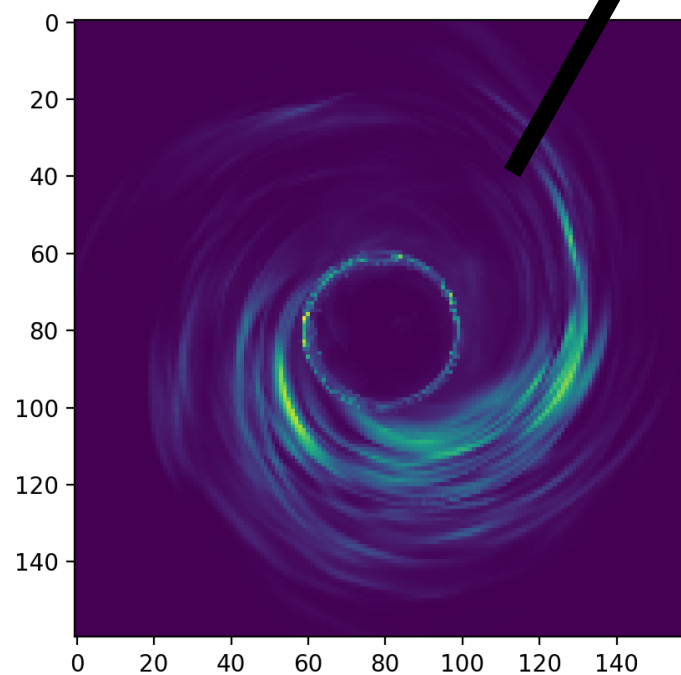
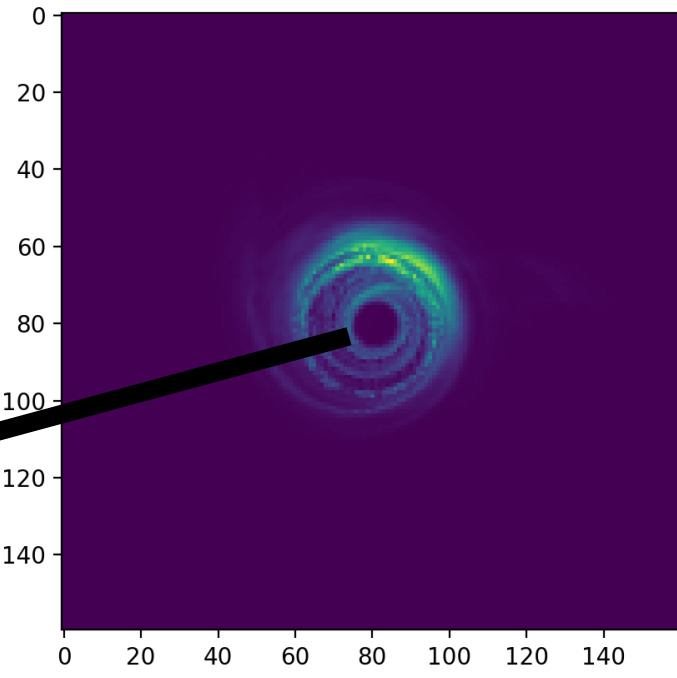
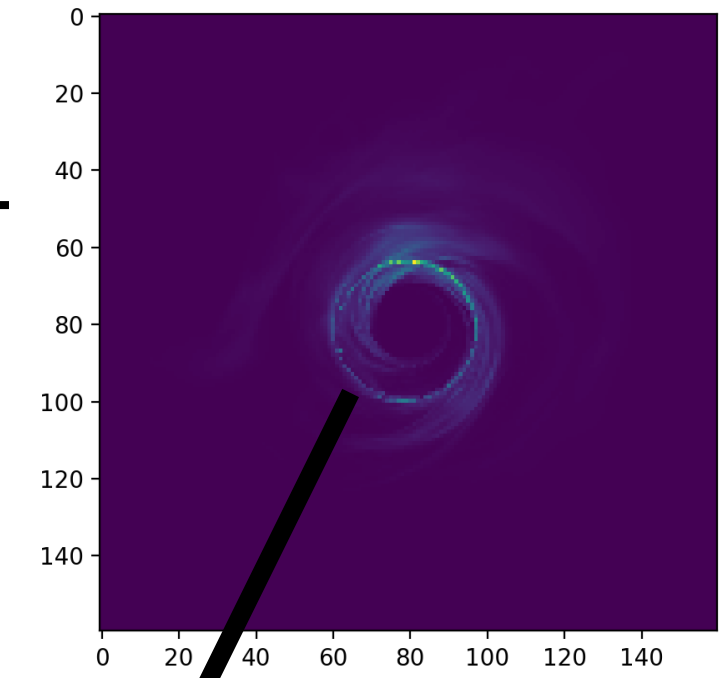
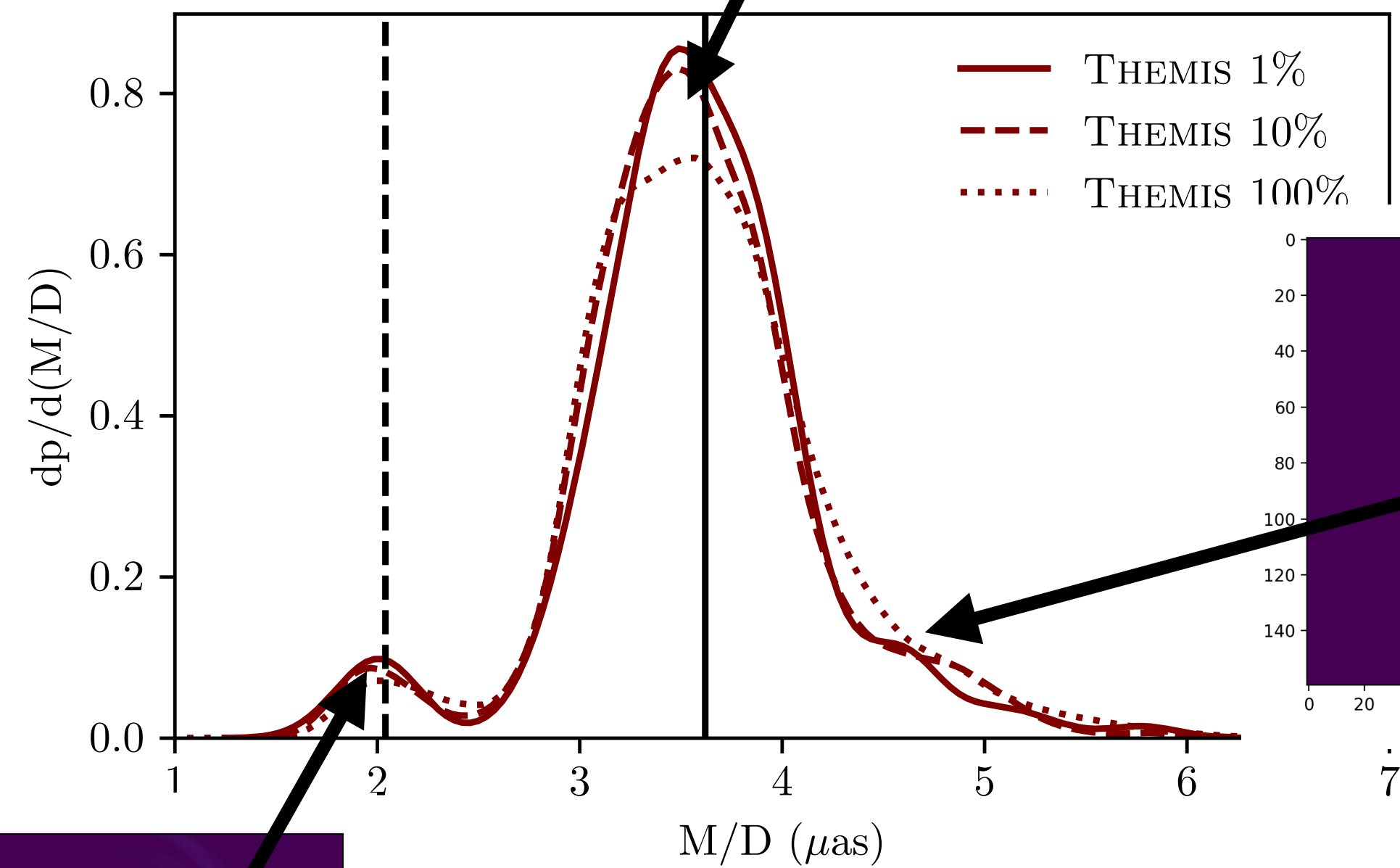
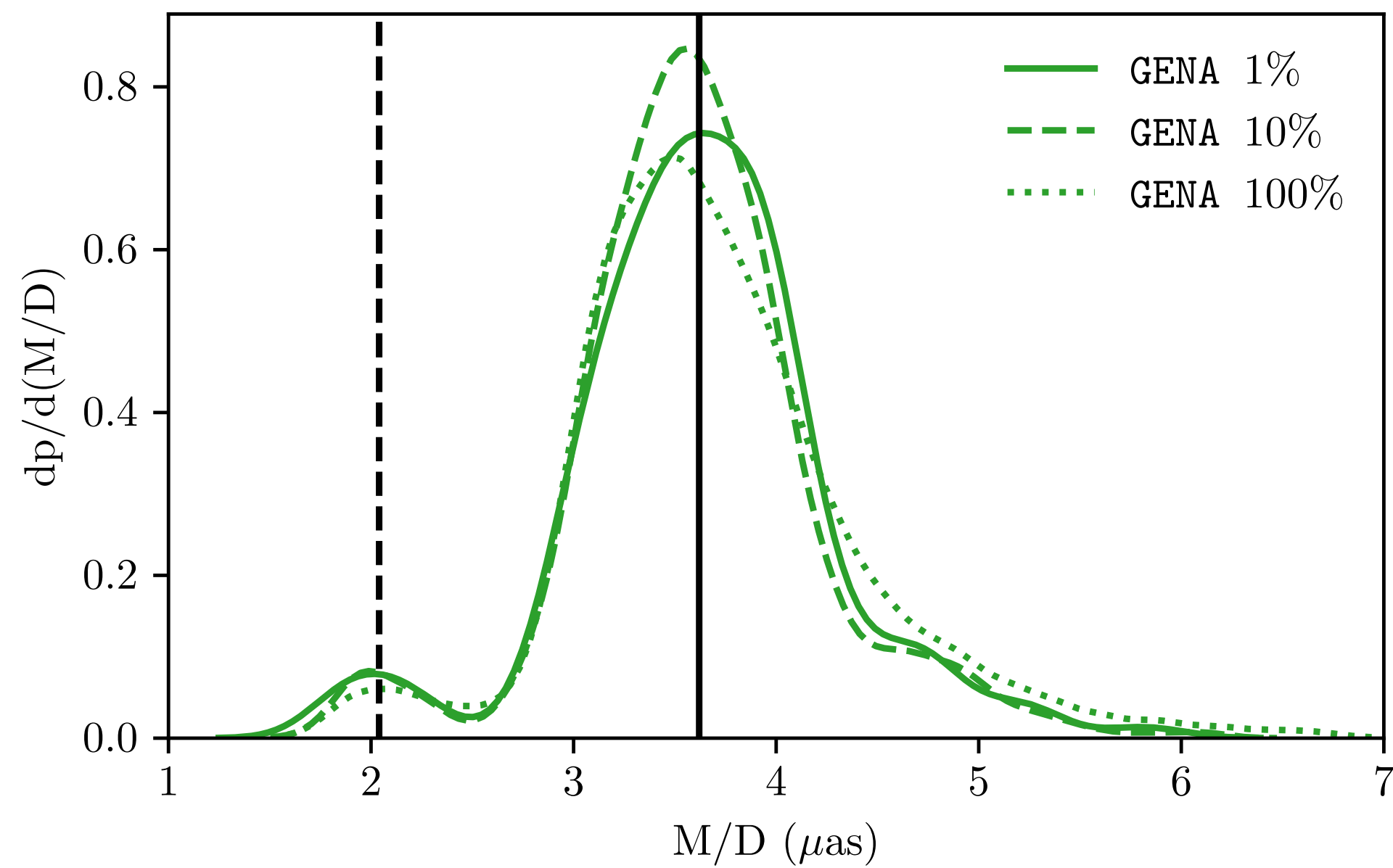
- ▶ The distribution peaks close to $M/D \sim 3.6 \mu\text{as}$ with a width of $\sim 0.5 \mu\text{as}$



- ▶ Consistent with stellar mass estimate

Distribution of Best-Fit Black Hole Angular Size

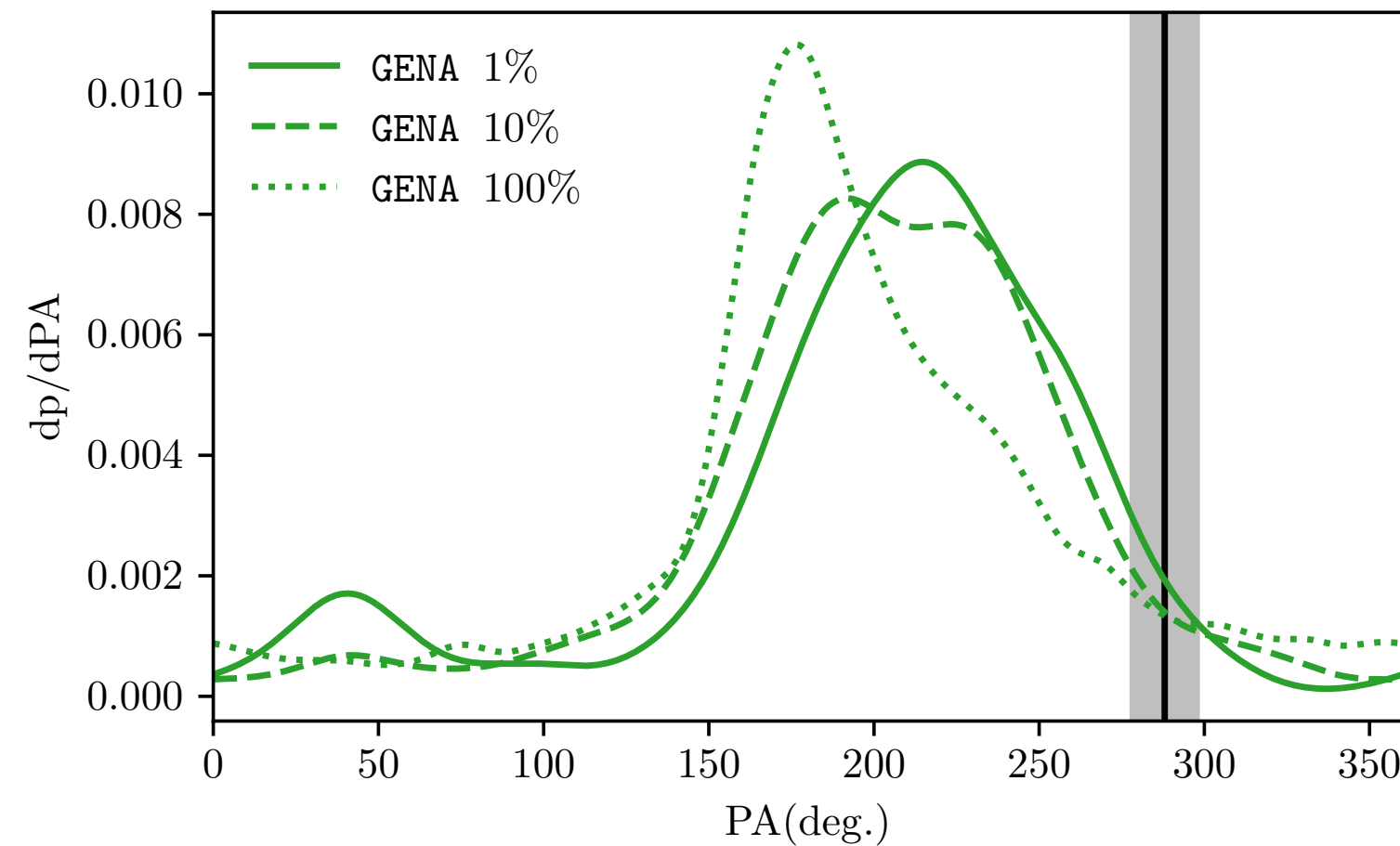
- ▶ The distribution peaks close to $M/D \sim 3.6 \mu\text{as}$ with a width of $\sim 0.5 \mu\text{as}$



- ▶ Consistent with stellar mass estimate

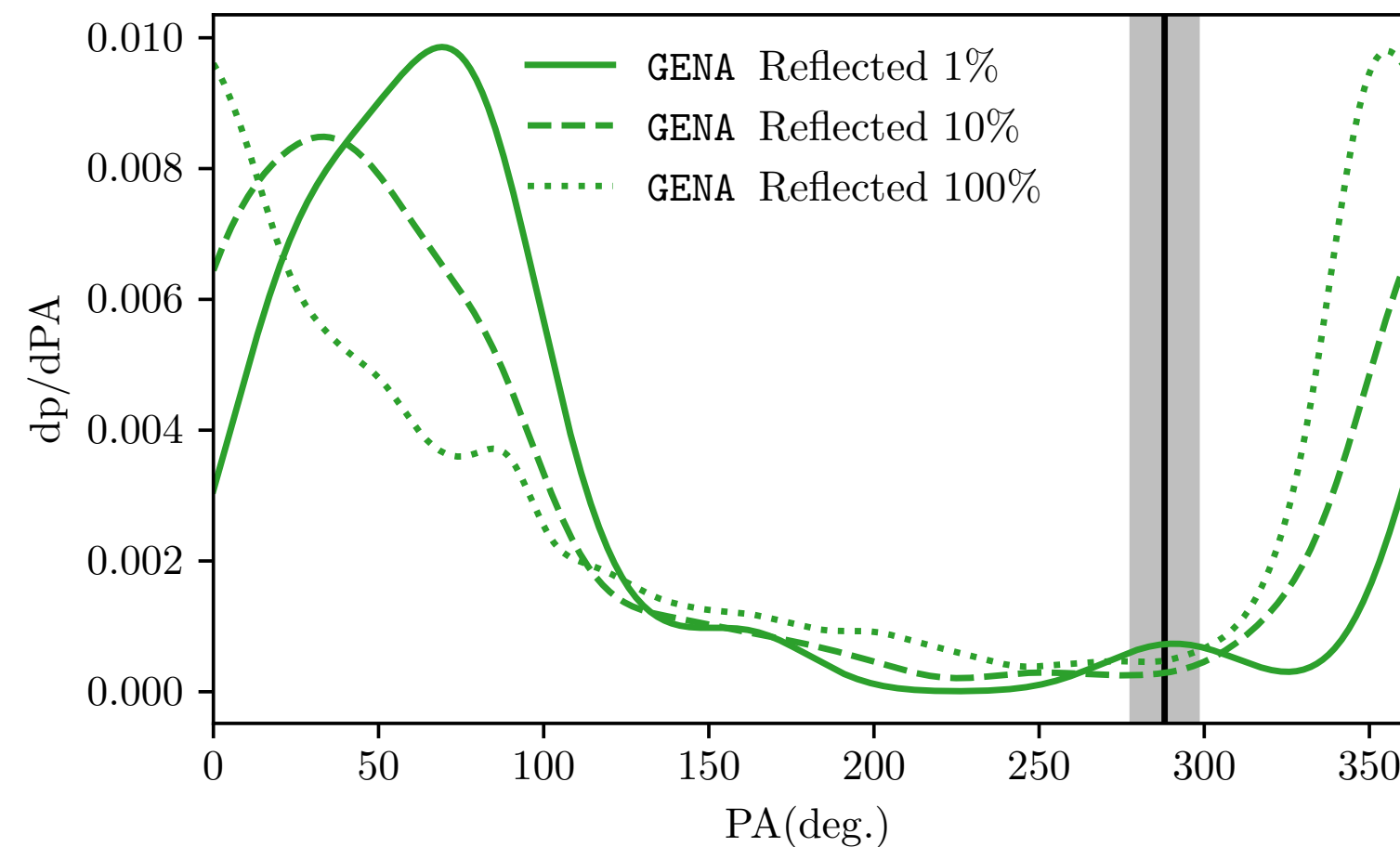
Distribution of Model Best-Fit Position Angle

BH spin vector pointing away from Earth



- ▶ Large scale jet orientation lies on the shoulder of the spin-away models ($\langle \text{PA} \rangle \sim 200$ deg, $\sigma_{\text{PA}} \sim 55$ deg)
- ▶ Large scale jet orientation lies off the shoulder of the spin-toward models

BH spin vector pointing toward Earth



- ▶ **BH spin-away models are favoured**
- ▶ Width of distributions arises from brightness fluctuations in the ring

Further constraints 1 - 3:

1. Radiative Equilibrium:

- ▶ Calculate radiative efficiency, $\epsilon \equiv L_{\text{bol}}/(\dot{M}c^2)$
- ▶ Reject model if $\epsilon > \epsilon(\text{classical thin disk model})$; inconsistent; would cool quickly
- ▶ **Rejects** MAD models with $a \geq 0$ and $R_{\text{high}} = 1$ (hot midplane electrons)

2. X-ray constraint

- ▶ X-ray data: simultaneously Chandra, NuSTAR observations during EHT2017 Campaign
 - ▶ 2-10 keV luminosity: $L_x = 4.4 \pm 0.1 \times 10^{40}$ erg/s
- ▶ Reject models that consistently *overproduce* X-ray
- ▶ Overluminous model: **rejects** SANE with $R_{\text{high}} \leq 20$.

3. Jet power

- ▶ Constraint $P_{\text{jet}} > P_{\text{jet,min}} = 10^{42}$ erg/s **rejects all $a=0$ models**
- ▶ Most $|a| > 0$ MAD models acceptable
- ▶ P_{jet} dominated by **extraction of black hole spin** energy through Blandford-Znajek process

Constraint Summary

- ▶ Applied AIS, consistency of radiative equilibrium, max X-ray luminosity, and minimum jet power
- ▶ Most SANE models fail, except $a = -0.94$ and $a = 0.94$ models with large R_{high}
- ▶ Large fraction of MAD model pass, except $a = 0$ models and small R_{high} models

SANE

	flux ¹	a_* ²	R_{high} ³	AIS ⁴	ϵ ⁵	L_X ⁶	P_{jet} ⁷	
SANE	-0.94	1	1	Fail	Pass	Pass	Pass	Fail
SANE	-0.94	10	10	Pass	Pass	Pass	Pass	Pass
SANE	-0.94	20	20	Pass	Pass	Pass	Pass	Pass
SANE	-0.94	40	40	Pass	Pass	Pass	Pass	Pass
SANE	-0.94	80	80	Pass	Pass	Pass	Pass	Pass
SANE	-0.94	160	160	Fail	Pass	Pass	Pass	Fail
SANE	-0.5	1	1	Pass	Pass	Fail	Fail	Fail
SANE	-0.5	10	10	Pass	Pass	Fail	Fail	Fail
SANE	-0.5	20	20	Pass	Pass	Pass	Fail	Fail
SANE	-0.5	40	40	Pass	Pass	Pass	Fail	Fail
SANE	-0.5	80	80	Fail	Pass	Pass	Fail	Fail
SANE	-0.5	160	160	Pass	Pass	Pass	Fail	Fail
SANE	0	1	1	Pass	Pass	Pass	Fail	Fail
SANE	0	10	10	Pass	Pass	Pass	Fail	Fail
SANE	0	20	20	Pass	Pass	Fail	Fail	Fail
SANE	0	40	40	Pass	Pass	Pass	Fail	Fail
SANE	0	80	80	Pass	Pass	Pass	Fail	Fail
SANE	0	160	160	Pass	Pass	Pass	Fail	Fail
SANE	+0.5	1	1	Pass	Pass	Pass	Fail	Fail
SANE	+0.5	10	10	Pass	Pass	Pass	Fail	Fail
SANE	+0.5	20	20	Pass	Pass	Pass	Fail	Fail
SANE	+0.5	40	40	Pass	Pass	Pass	Fail	Fail
SANE	+0.5	80	80	Pass	Pass	Pass	Fail	Fail
SANE	+0.5	160	160	Pass	Pass	Pass	Fail	Fail
SANE	+0.94	1	1	Pass	Fail	Pass	Fail	Fail
SANE	+0.94	10	10	Pass	Fail	Pass	Fail	Fail
SANE	+0.94	20	20	Pass	Pass	Pass	Fail	Fail
SANE	+0.94	40	40	Pass	Pass	Pass	Fail	Fail
SANE	+0.94	80	80	Pass	Pass	Pass	Pass	Pass
SANE	+0.94	160	160	Pass	Pass	Pass	Pass	Pass

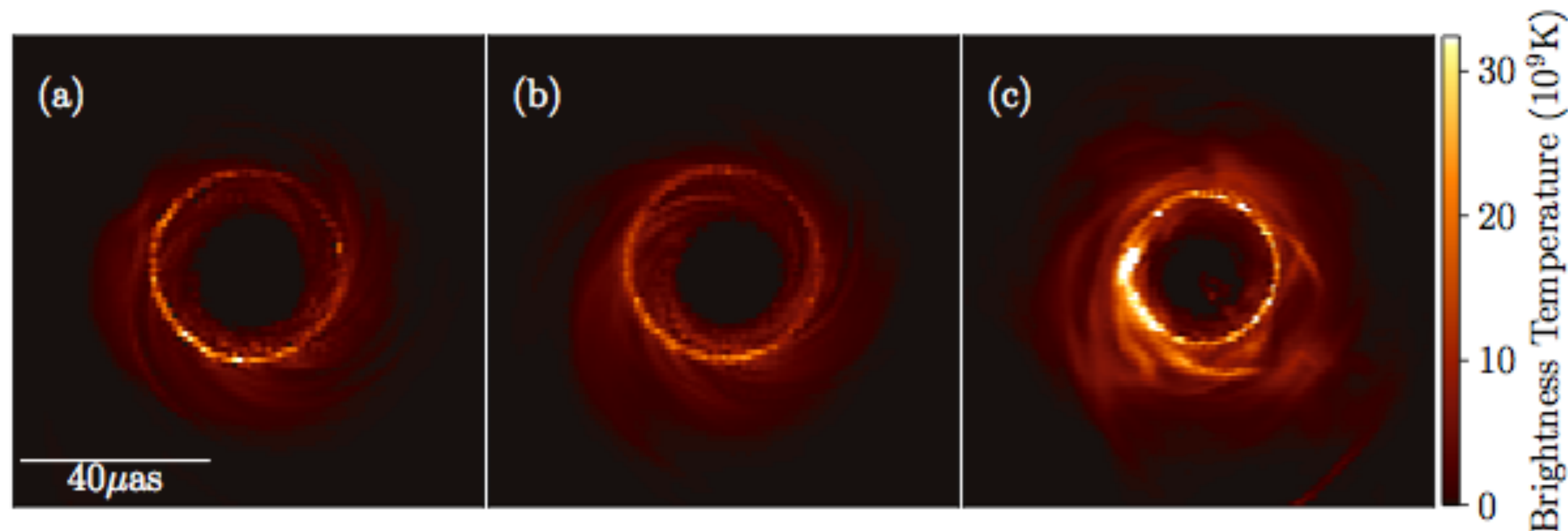
MAD

	flux ¹	a_* ²	R_{high} ³	AIS ⁴	ϵ ⁵	L_X ⁶	P_{jet} ⁷	
MAD	-0.94	1	1	Fail	Fail	Pass	Pass	Fail
MAD	-0.94	10	10	Fail	Pass	Pass	Pass	Fail
MAD	-0.94	20	20	Fail	Pass	Pass	Pass	Fail
MAD	-0.94	40	40	Fail	Pass	Pass	Pass	Fail
MAD	-0.94	80	80	Fail	Pass	Pass	Pass	Fail
MAD	-0.94	160	160	Fail	Pass	Pass	Pass	Fail
MAD	-0.5	1	1	Pass	Fail	Pass	Fail	Fail
MAD	-0.5	10	10	Pass	Pass	Pass	Fail	Fail
MAD	-0.5	20	20	Pass	Pass	Pass	Pass	Pass
MAD	-0.5	40	40	Pass	Pass	Pass	Pass	Pass
MAD	-0.5	80	80	Pass	Pass	Pass	Pass	Pass
MAD	-0.5	160	160	Pass	Pass	Pass	Pass	Pass
MAD	0	1	1	Pass	Fail	Pass	Fail	Fail
MAD	0	10	10	Pass	Pass	Pass	Fail	Fail
MAD	0	20	20	Pass	Pass	Pass	Fail	Fail
MAD	0	40	40	Pass	Pass	Pass	Fail	Fail
MAD	0	80	80	Pass	Pass	Pass	Fail	Fail
MAD	0	160	160	Pass	Pass	Pass	Fail	Fail
MAD	+0.5	1	1	Pass	Fail	Pass	Fail	Fail
MAD	+0.5	10	10	Pass	Pass	Pass	Pass	Pass
MAD	+0.5	20	20	Pass	Pass	Pass	Pass	Pass
MAD	+0.5	40	40	Pass	Pass	Pass	Pass	Pass
MAD	+0.5	80	80	Pass	Pass	Pass	Pass	Pass
MAD	+0.5	160	160	Pass	Pass	Pass	Pass	Pass
MAD	+0.94	1	1	Pass	Fail	Fail	Pass	Fail
MAD	+0.94	10	10	Pass	Fail	Pass	Pass	Fail
MAD	+0.94	20	20	Pass	Pass	Pass	Pass	Pass
MAD	+0.94	40	40	Pass	Pass	Pass	Pass	Pass
MAD	+0.94	80	80	Pass	Pass	Pass	Pass	Pass
MAD	+0.94	160	160	Pass	Pass	Pass	Pass	Pass



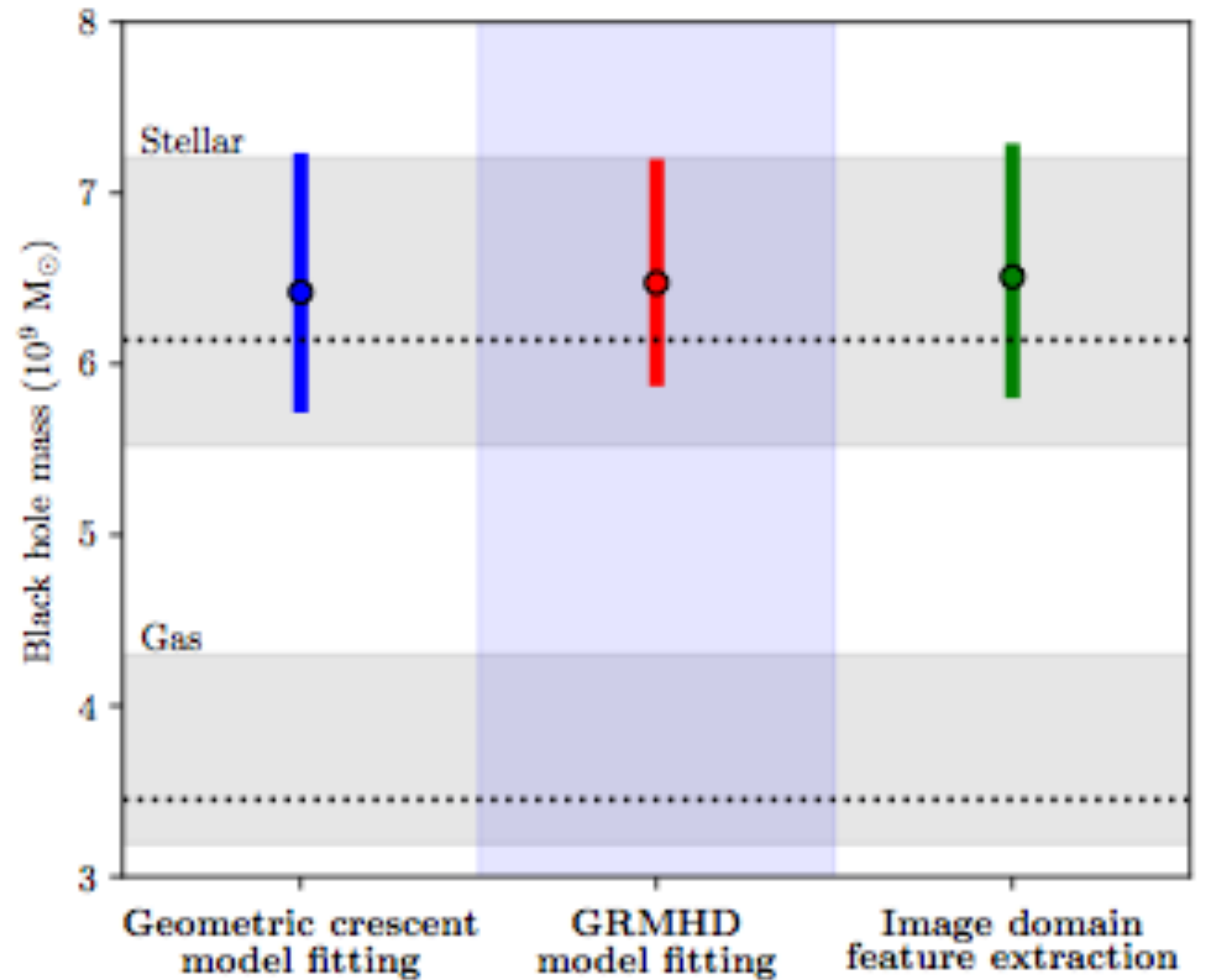
From diameter to black hole mass

- ▶ Observed diameter should scale with $\theta_g = \frac{GM}{c^2 D}$: $\hat{d} = \alpha \theta_g$
- ▶ Naive approach: assume measured diameter corresponds to photon ring
alpha = 9.6-10.4 (Johannsen & Psaltis 2010)
- ▶ **Calibrate** alpha by fitting geometric models to a set of GRMHD models where Θ_g is known: $\alpha = 11.5 \pm 10\%$



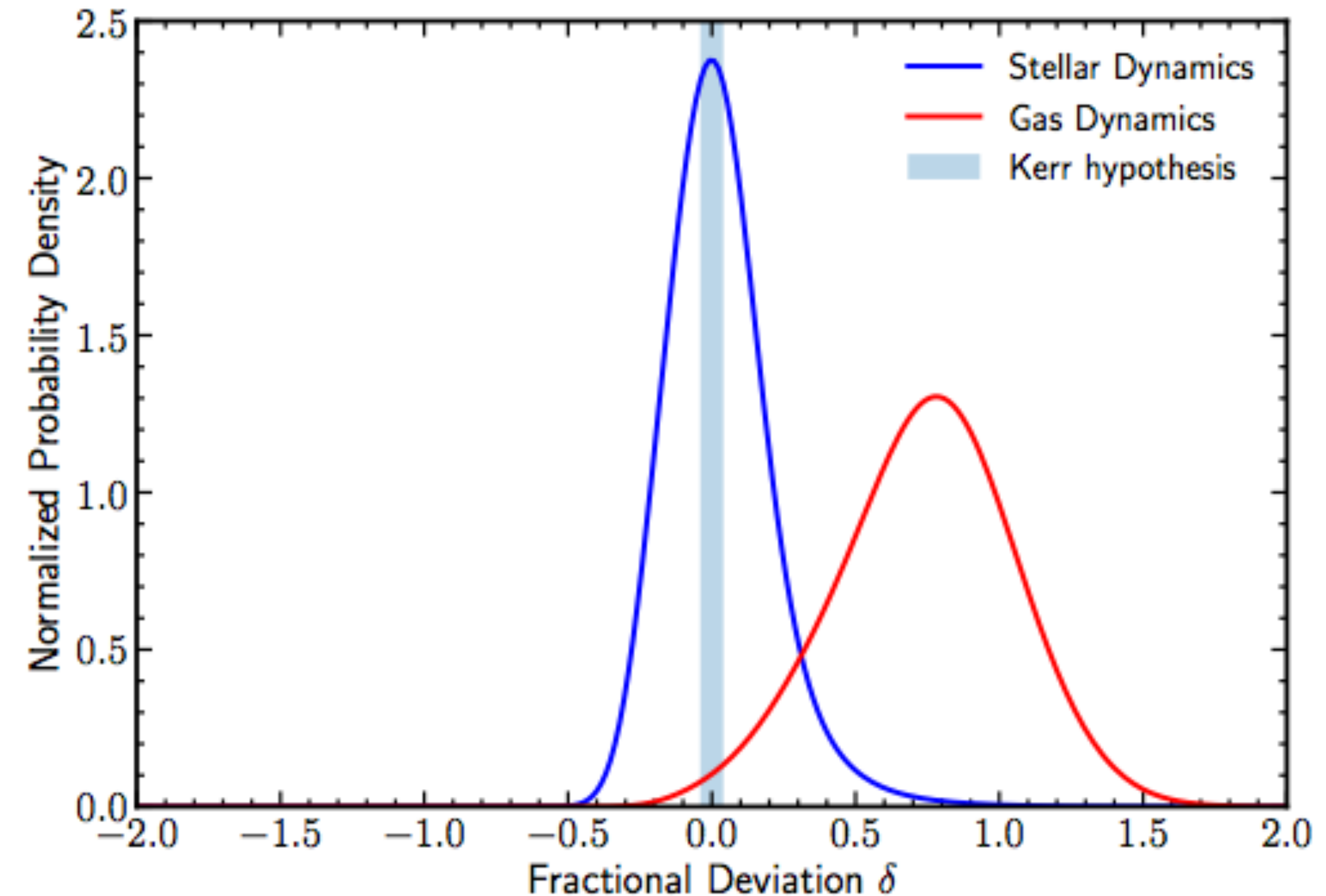
The black hole mass of M87

- Convert Θ_g to M using $D = 16.8 \pm 0.7$ Mpc
- $M = 6.5 \pm 0.7 \times 10^9 M_{\odot}$
- Three methods in excellent agreement
- Systematic error in calibration of α dominates in all cases
- Excellent agreement with stellar dynamics mass estimate (Gebhardt+2011)

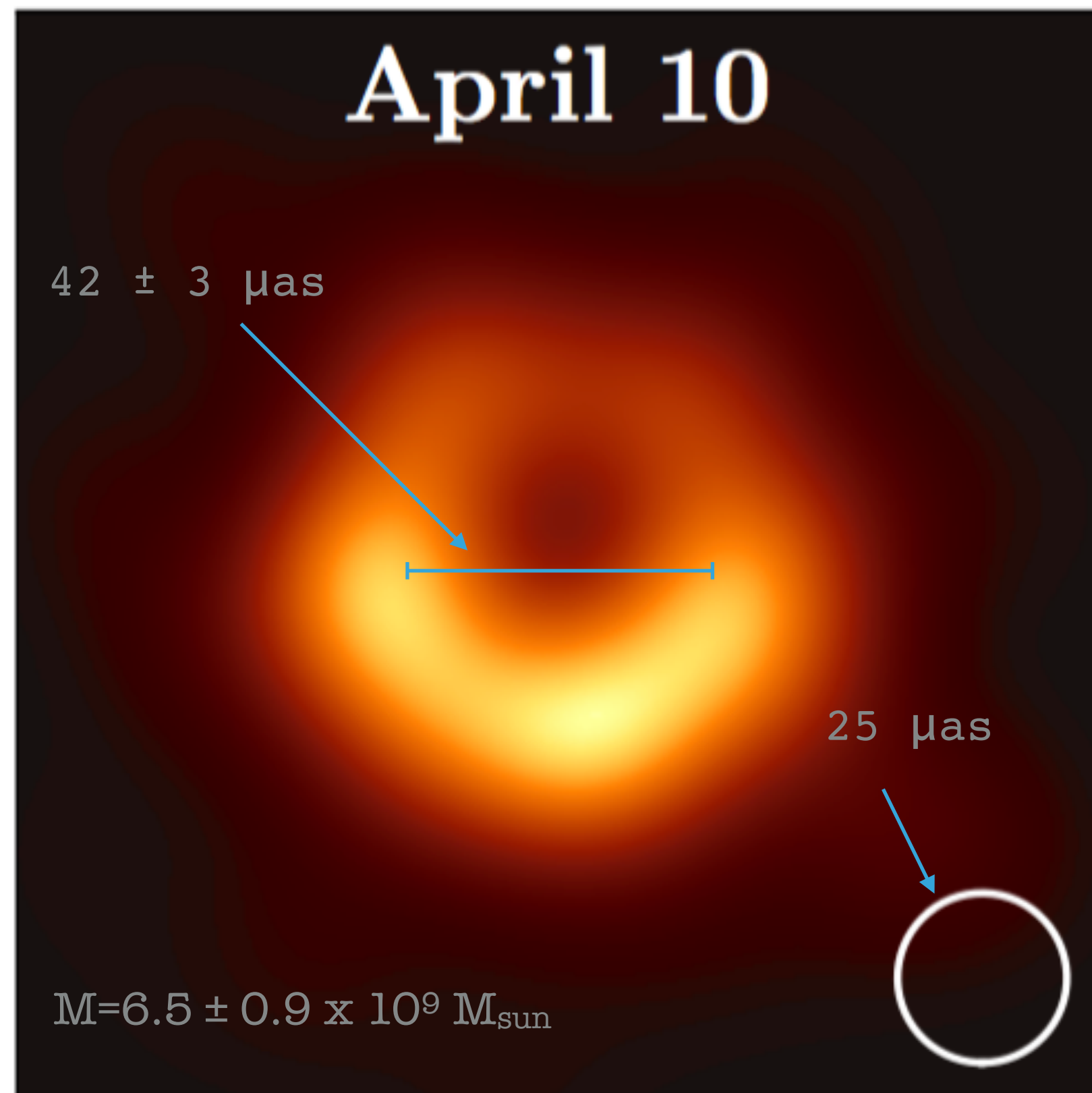


Towards tests of GR: null hypothesis test

- ▶ Consistency of the mass estimate with stellar dynamics means our results are completely consistent with general relativity



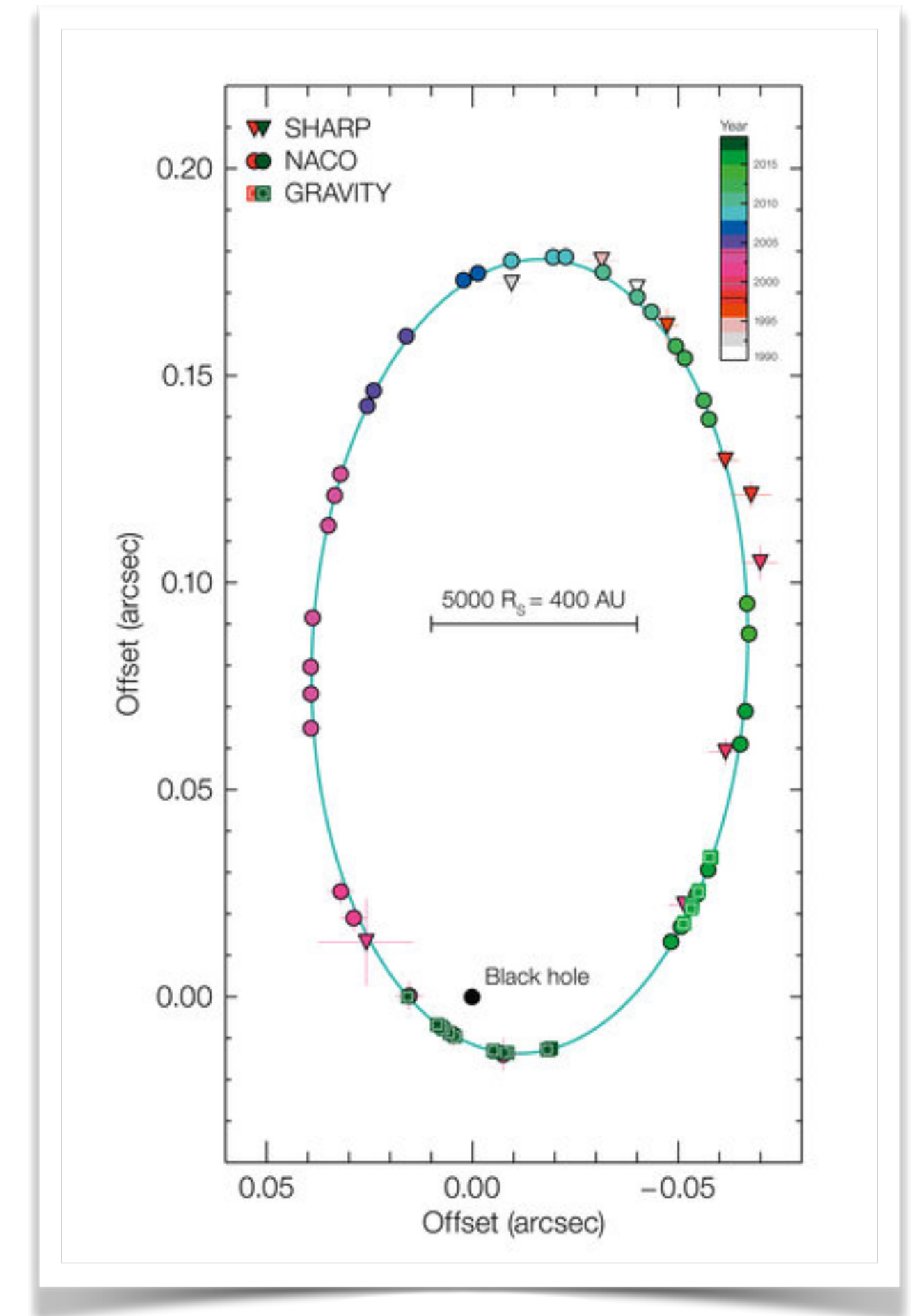
Conclusions first analysis



- ▶ M87 at 1mm: **Crescent-like structure** with diameter $42 \pm 3 \mu\text{as}$
- ▶ Black hole mass **$6.5 \pm 0.2|_{\text{stat}} \pm 0.7|_{\text{sys}} 10^9 M_{\text{sun}}$** (Consistent with stellar mass estimate)
- ▶ Image consistent with **strongly lensed emission** at the photon-orbit
- ▶ Models show that the jet forms due to **extraction of spin-energy** from the black hole (Blandford Znajek mechanism)
- ▶ Emission co-rotates with spin: **Spin points away from earth**
- ▶ Non-spinning models ruled out
- ▶ So far all points towards a **Kerr- black hole**.

EHT Science in the pipeline (2017 & 2018 campaigns)

- ▶ M87*
 - ▶ **Polarisation**: Jet launching, breaking degeneracies
 - ▶ **Multi-wavelength**: jet dynamics
- ▶ SgrA*
 - ▶ **Variability** requires more complex analysis
 - ▶ Interstellar scattering seems OK
 - ▶ **Better constrained** test of General Relativity
 - ▶ Jet launching in other targets

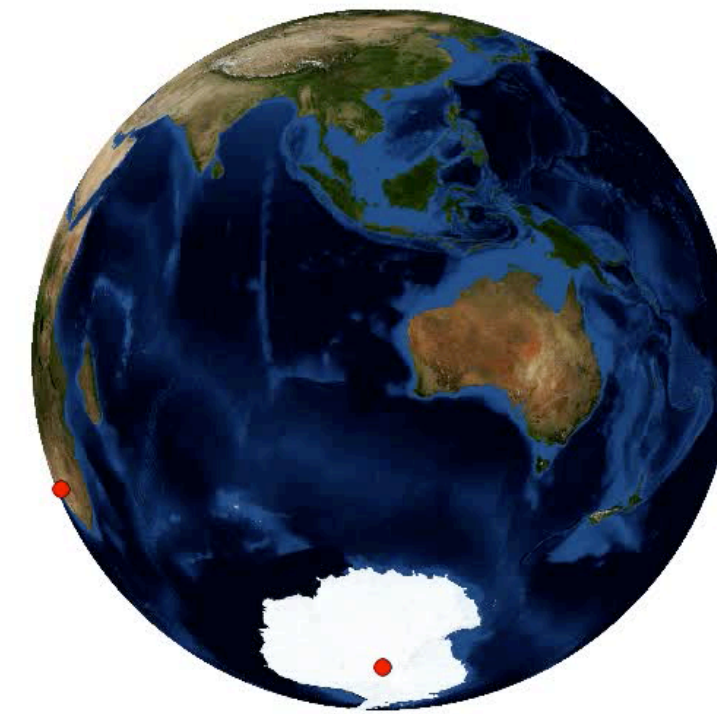


Mass and distance of SgrA* known accurately from Gravity measurements



Upcoming EHT science, near future

- ▶ More science applications:
 - ▶ Dynamical imaging
 - ▶ Variability, IR- and X-ray flares
 - ▶ Other AGN
 - ▶ Galactic Centre pulsars, masers
- ▶ Technical improvements
 - ▶ Sensitivity, Polarisation,
 - ▶ Observe at 345 GHz
 - ▶ Additional telescopes
 - ▶ Greenland, Llama, **AMT**

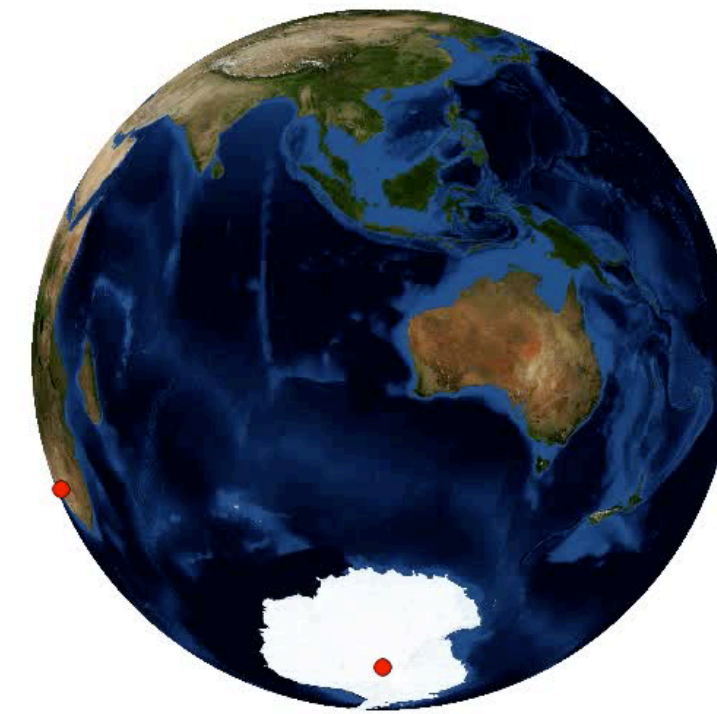


Further targets:

Cen A, 3C273, OJ287, NGC1052

Upcoming EHT science, near future

- ▶ More science applications:
 - ▶ Dynamical imaging
 - ▶ Variability, IR- and X-ray flares
 - ▶ Other AGN
 - ▶ Galactic Centre pulsars, masers
- ▶ Technical improvements
 - ▶ Sensitivity, Polarisation,
 - ▶ Observe at 345 GHz
 - ▶ Additional telescopes
 - ▶ Greenland, Llama, **AMT**

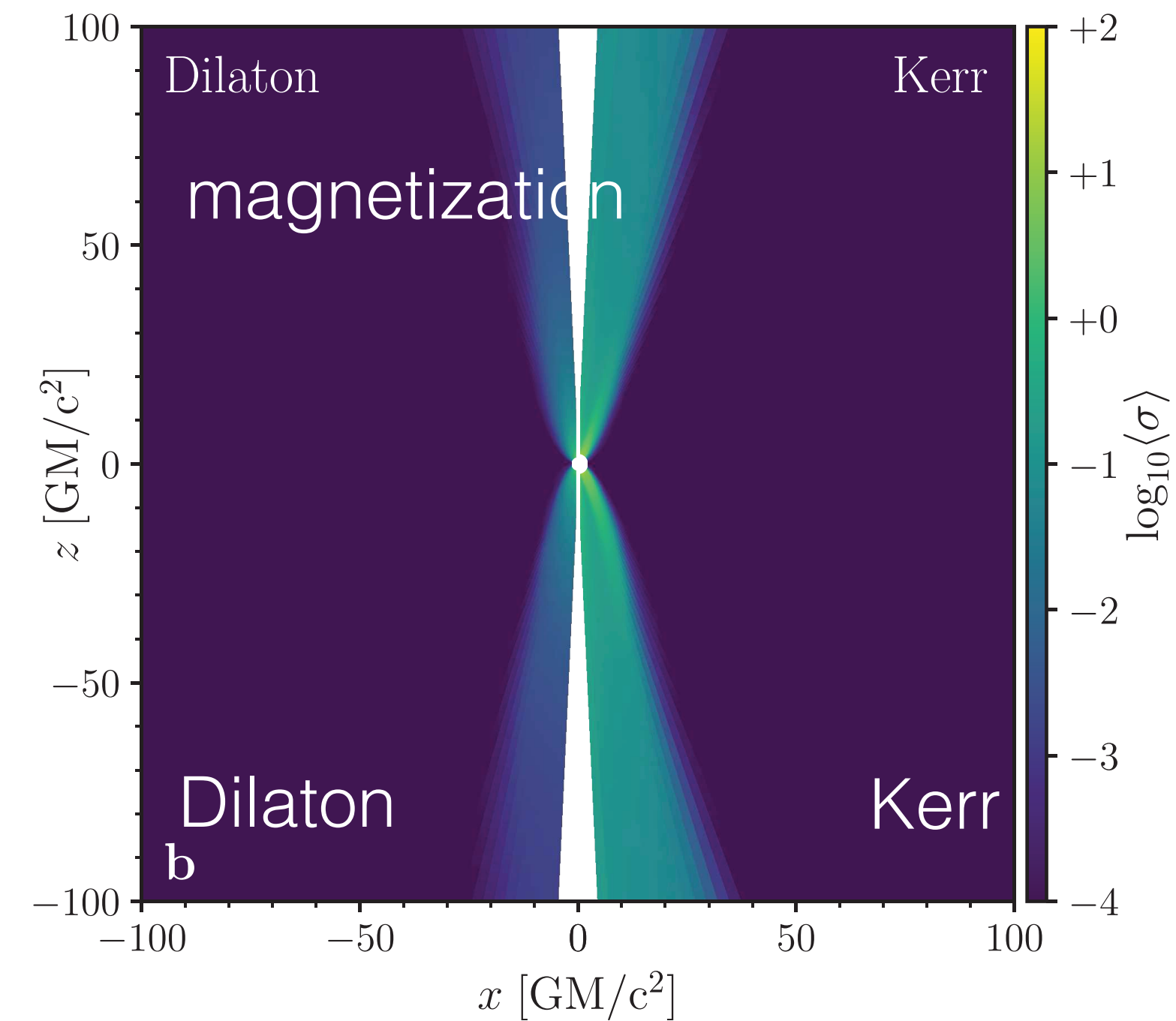
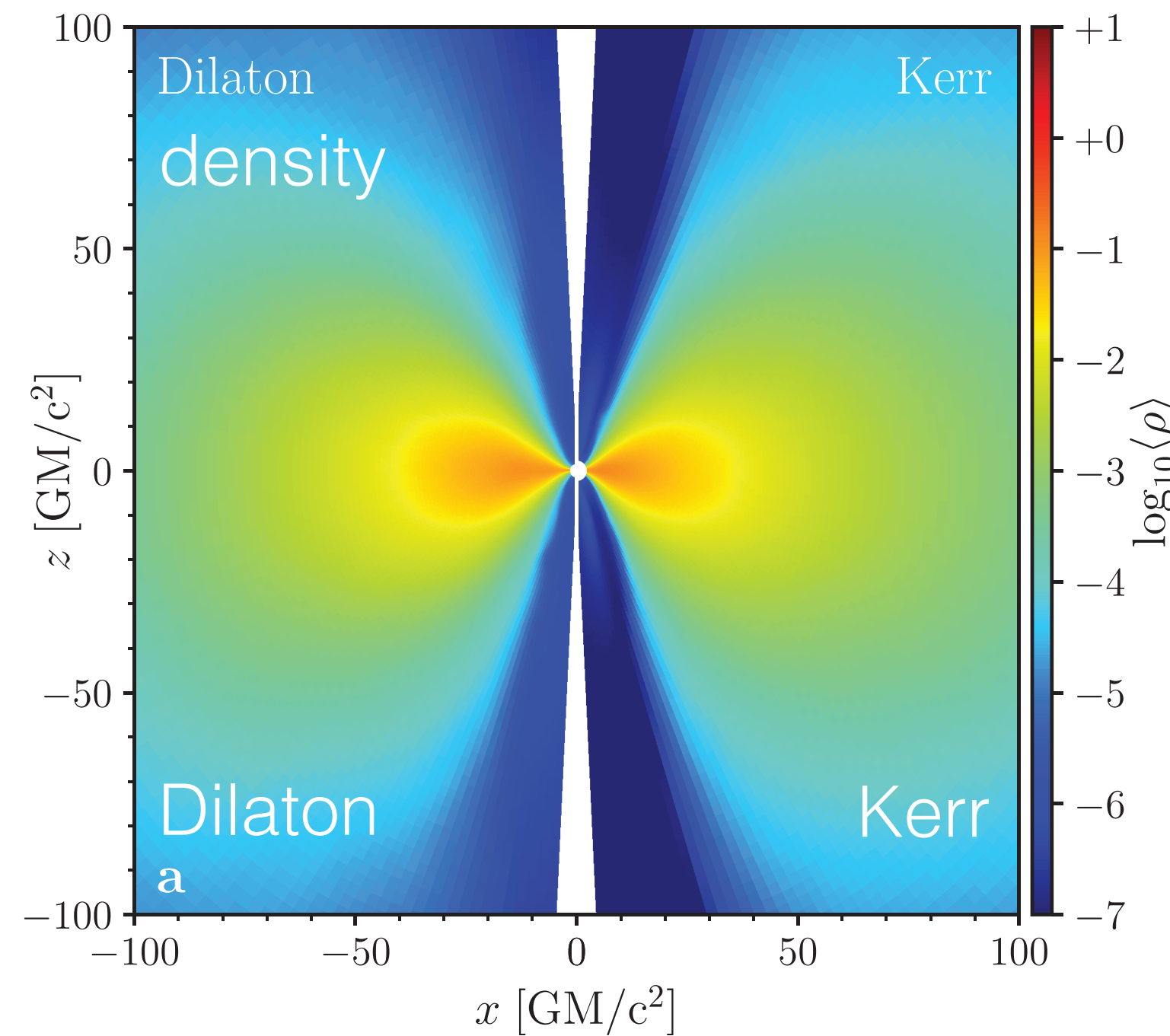


Further targets:

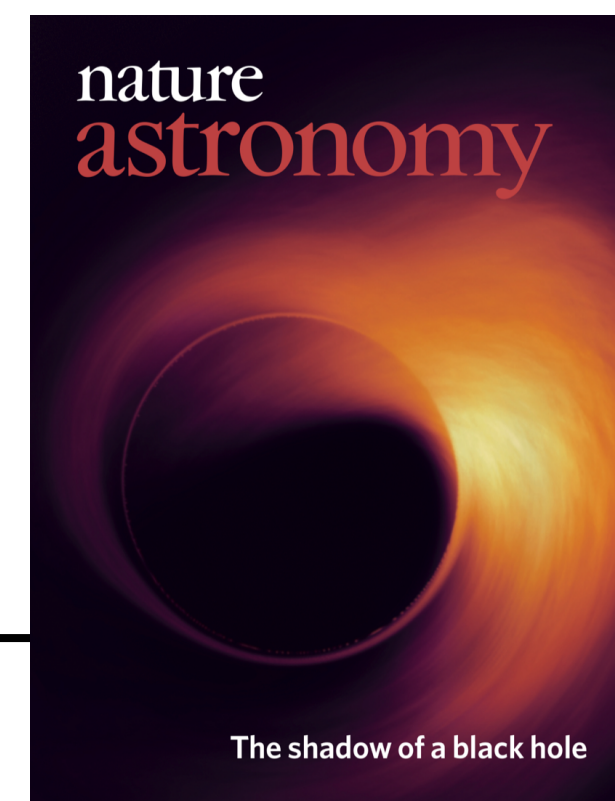
Cen A, 3C273, OJ287, NGC1052

non-GRMHD case: Dilaton BH

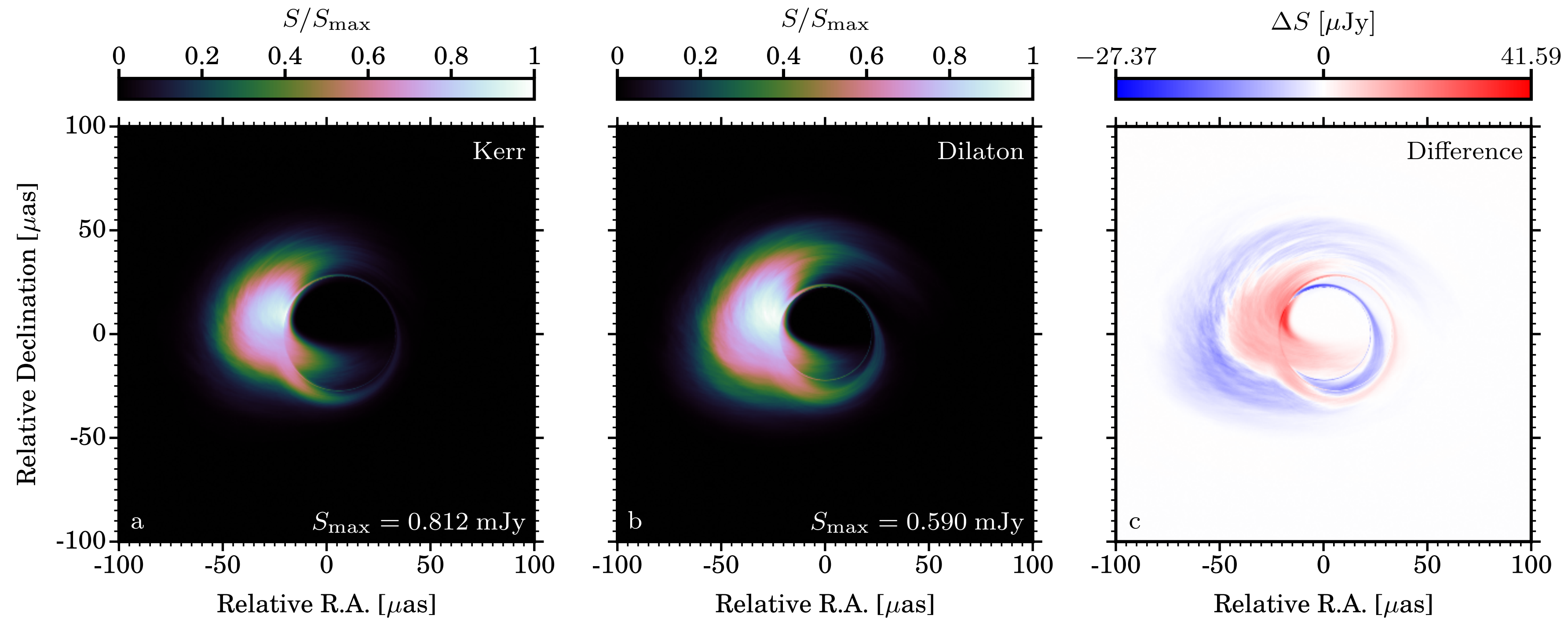
- 3D GRMHD simulations of magnetized torus accreting with a weak poloidal magnetic field loop onto **Kerr BH** ($a=0.6$) & **ISCO-matched dilaton BH** ($b=0.5$) by BHAC
- Azimuthal & time-averaged density (left) and magnetization (right)



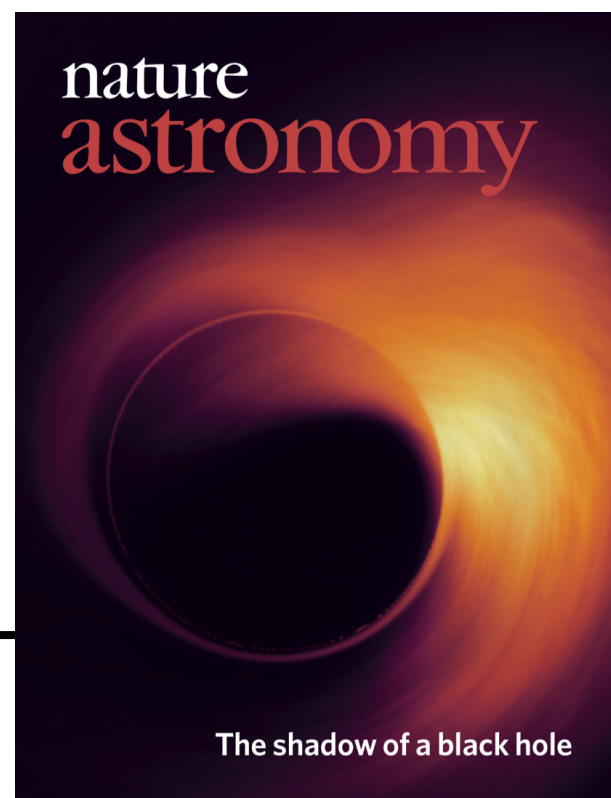
- Overall plasma behaviour is very similar in both cases but high magnetized jet spine region is different (dilaton BH is weaker than Kerr BH).



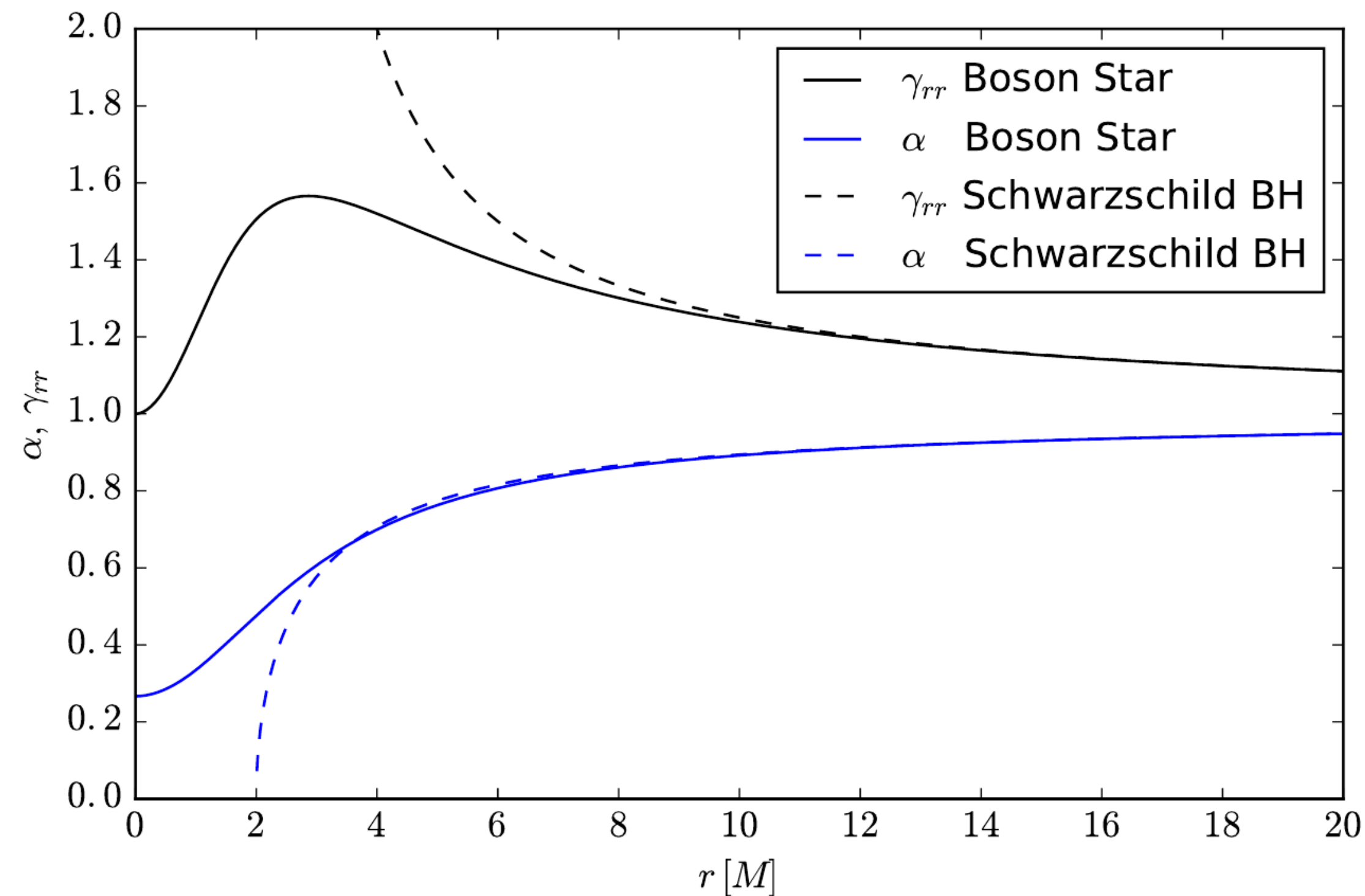
Dilaton-BH Shadow Images



- Emission model (fixed $T_i/T_e = 3$, $\dot{M} \sim 10^{-9} M_{\odot} \text{ yr}^{-1}$)
- BH shadow image is quite similar...
- Pixel-by-pixel difference shows *smaller shadow size* in dilaton BH (blue ring), and *offset & asymmetry of shadow* in Kerr (red ring)
- Differences small even in “*infinite-resolution images*”



Boson Stars: GRMHD



“Boson stars are macroscopic quantum states which are prevented from undergoing complete gravitational collapse by Heisenberg uncertainty principle “

Cardoso, Pani, Cadoni and Cavaglia (2008)

- So far: static configuration (e.g. Vincent et al., 2016)
=> **dynamical GRMHD simulations + GRRT**

- *Non-rotating Boson star*, minimally coupled self-gravitating scalar field

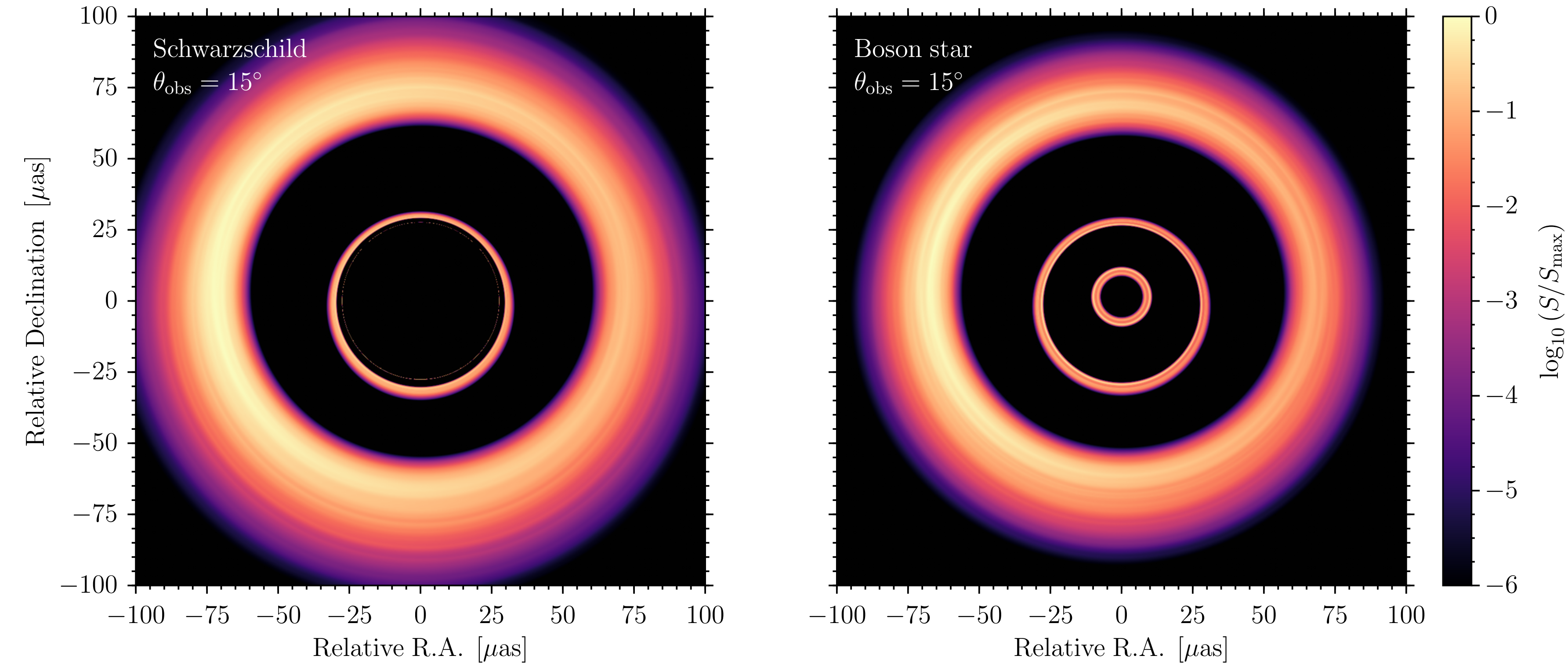
$$\mathcal{A} = \int d^4x \sqrt{-g} \left[\frac{R}{16\pi} - \frac{1}{2} \nabla_\mu \varphi \nabla^\mu \varphi^* + V(|\varphi|) \right]$$

$$V(|\varphi|) = \frac{1}{2} \frac{m^2}{M_P^4} |\varphi|^2 \quad m \simeq 10^{-17} \text{eV}/c^2$$

“mini-boson star”



Boson Stars: GRMHD



- *Non-rotating Boson star*, minimally coupled self-gravitating scalar field

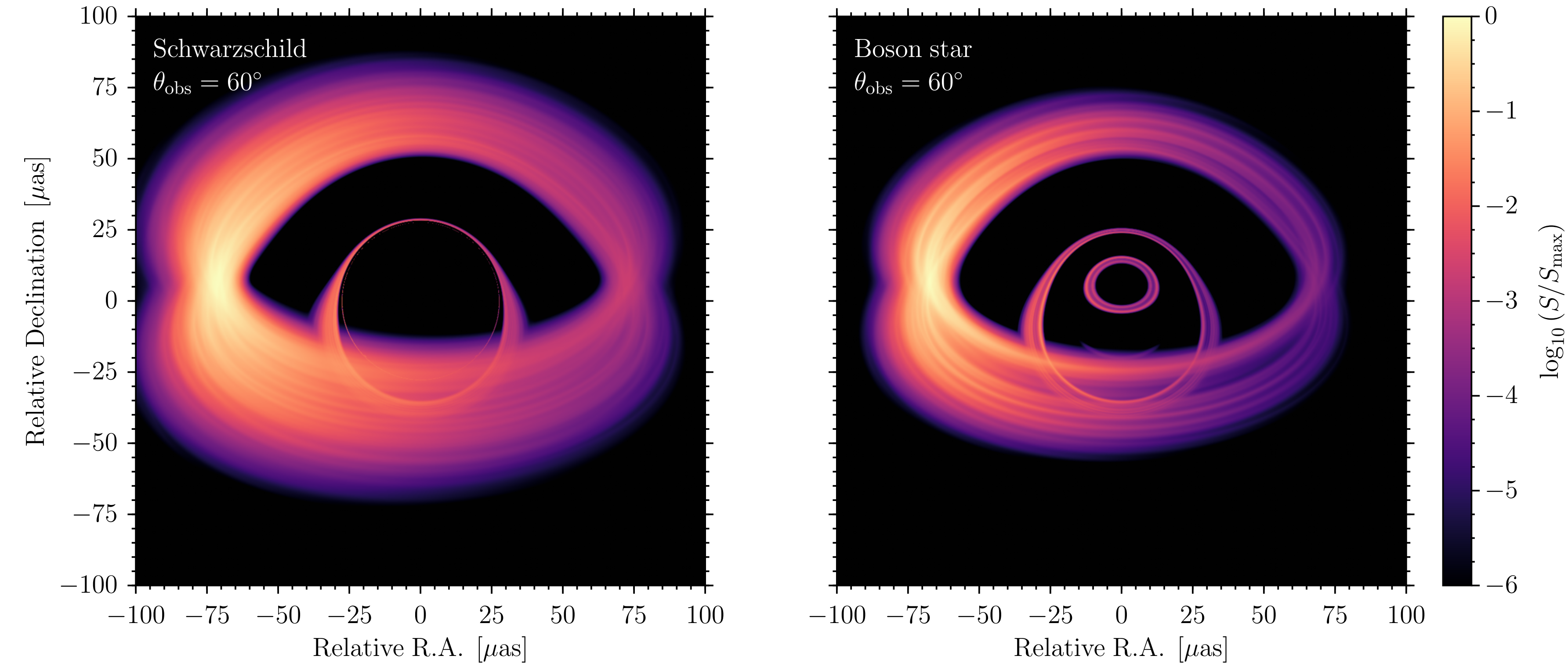
$$\mathcal{A} = \int d^4x \sqrt{-g} \left[\frac{R}{16\pi} - \frac{1}{2} \nabla_\mu \varphi \nabla^\mu \varphi^* + V(|\varphi|) \right]$$

$$V(|\varphi|) = \frac{1}{2} \frac{m^2}{M_P^4} |\varphi|^2 \quad m \simeq 10^{-17} \text{eV}/c^2$$

“mini-boson star”



Boson Stars: GRMHD



- *Non-rotating Boson star*, minimally coupled self-gravitating scalar field

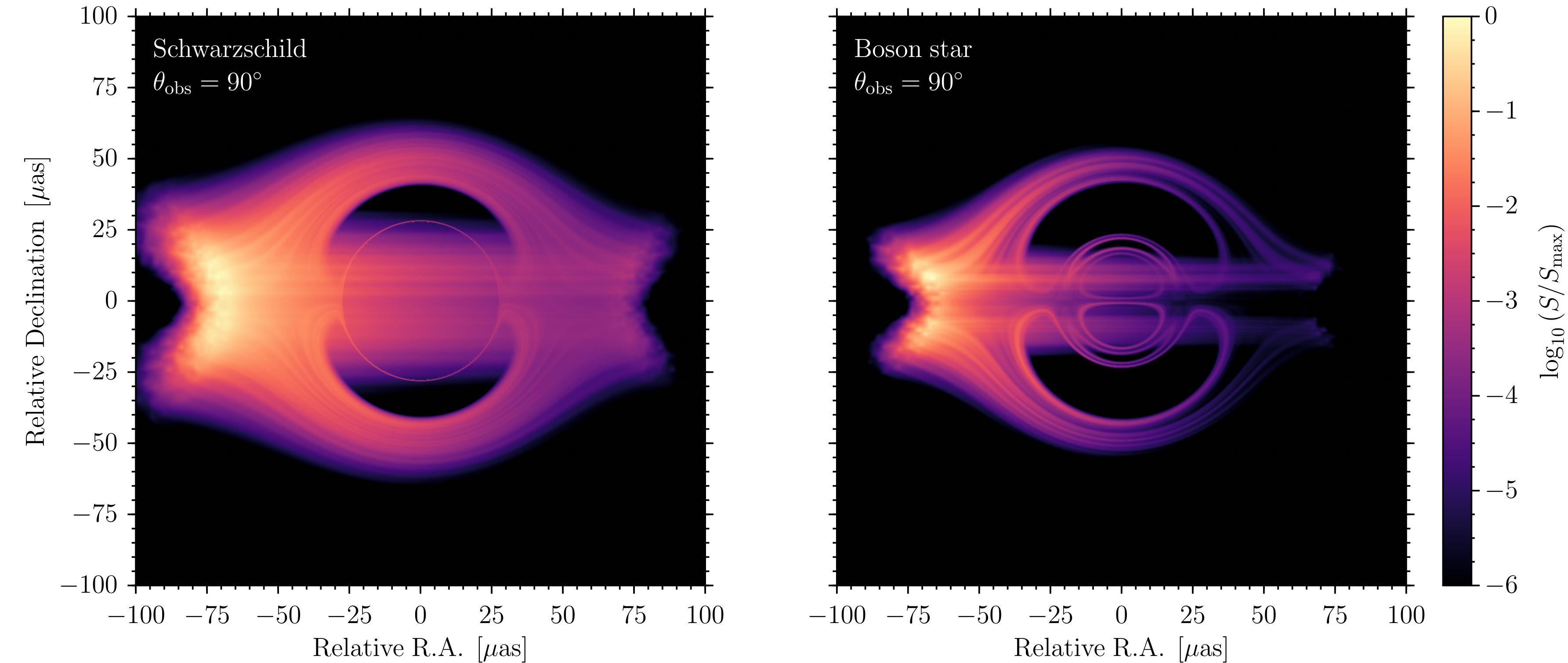
$$\mathcal{A} = \int d^4x \sqrt{-g} \left[\frac{R}{16\pi} - \frac{1}{2} \nabla_\mu \varphi \nabla^\mu \varphi^* + V(|\varphi|) \right]$$

$$V(|\varphi|) = \frac{1}{2} \frac{m^2}{M_P^4} |\varphi|^2 \quad m \simeq 10^{-17} \text{eV}/c^2$$

“mini-boson star”



Boson Stars: GRMHD



- *Non-rotating Boson star*, minimally coupled self-gravitating scalar field

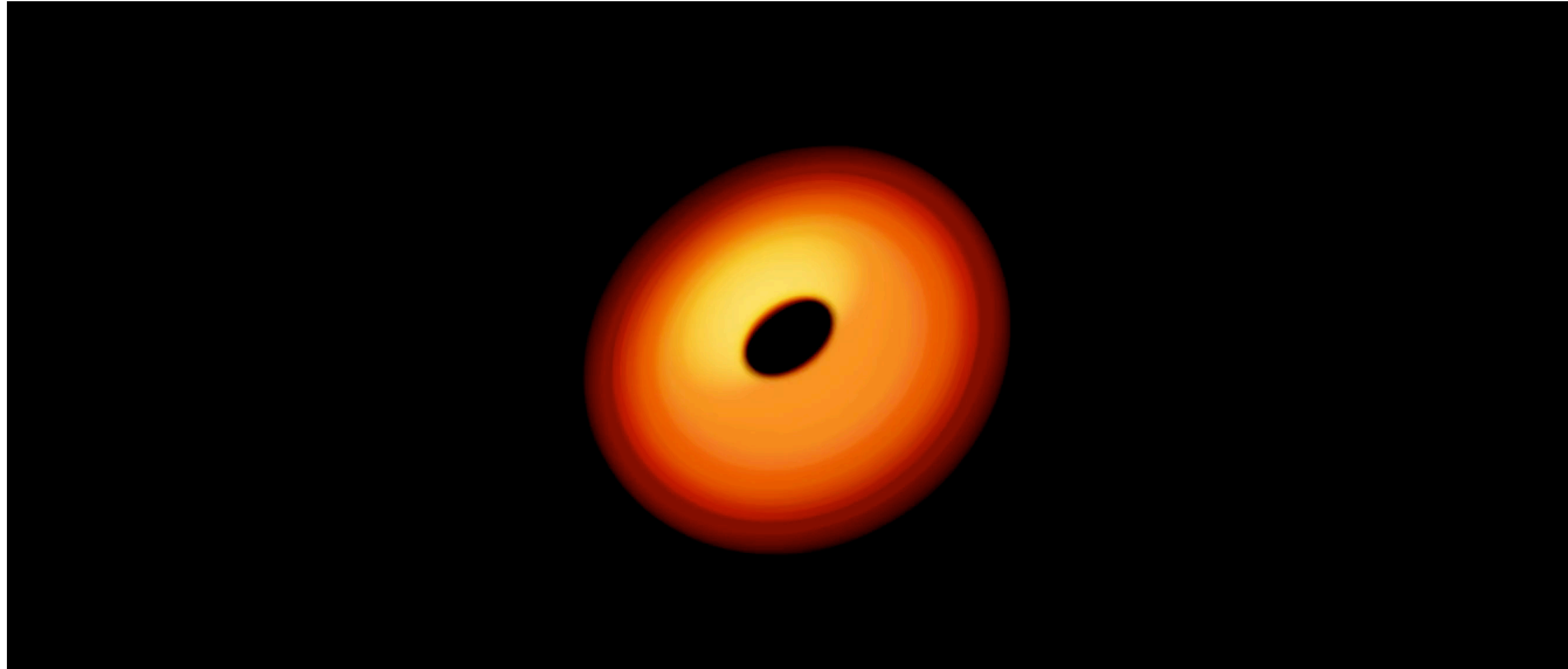
$$\mathcal{A} = \int d^4x \sqrt{-g} \left[\frac{R}{16\pi} - \frac{1}{2} \nabla_\mu \varphi \nabla^\mu \varphi^* + V(|\varphi|) \right]$$

$$V(|\varphi|) = \frac{1}{2} \frac{m^2}{M_P^4} |\varphi|^2 \quad m \simeq 10^{-17} \text{eV}/c^2$$

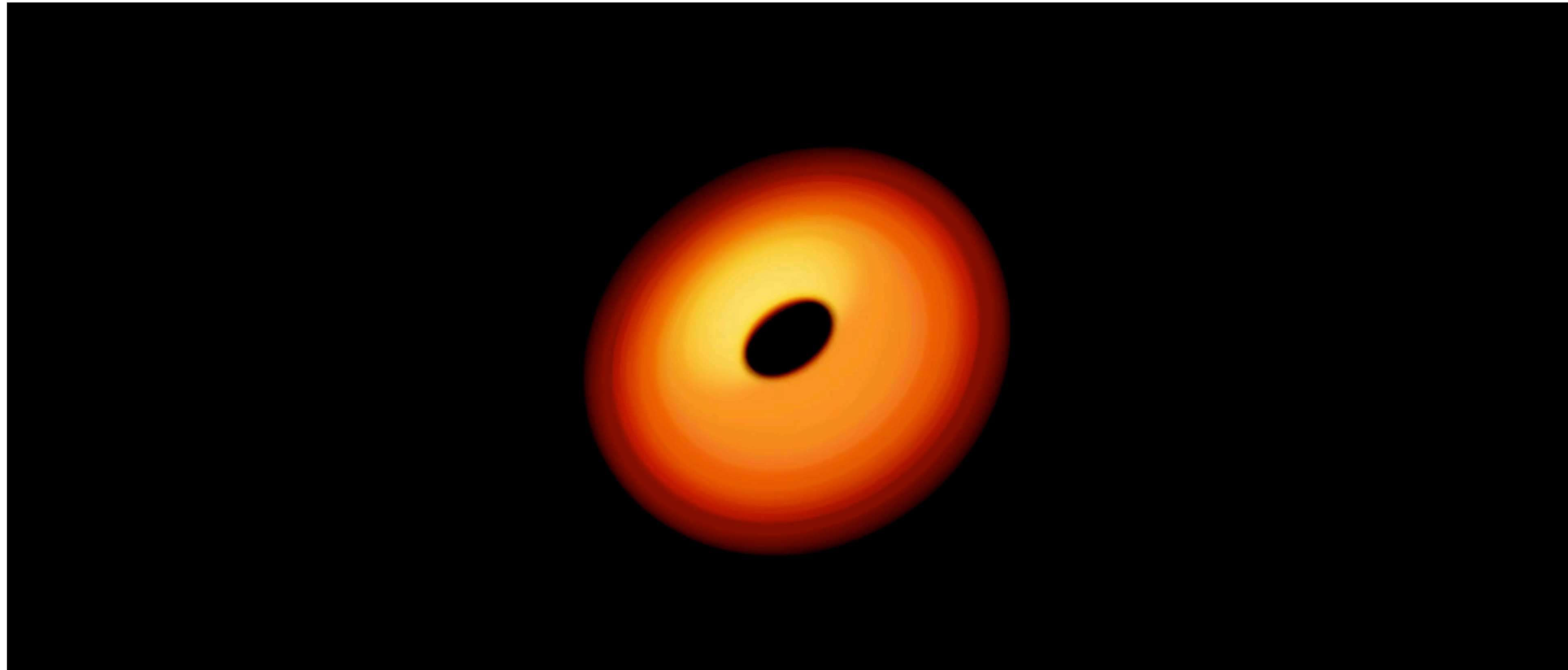
“mini-boson star”



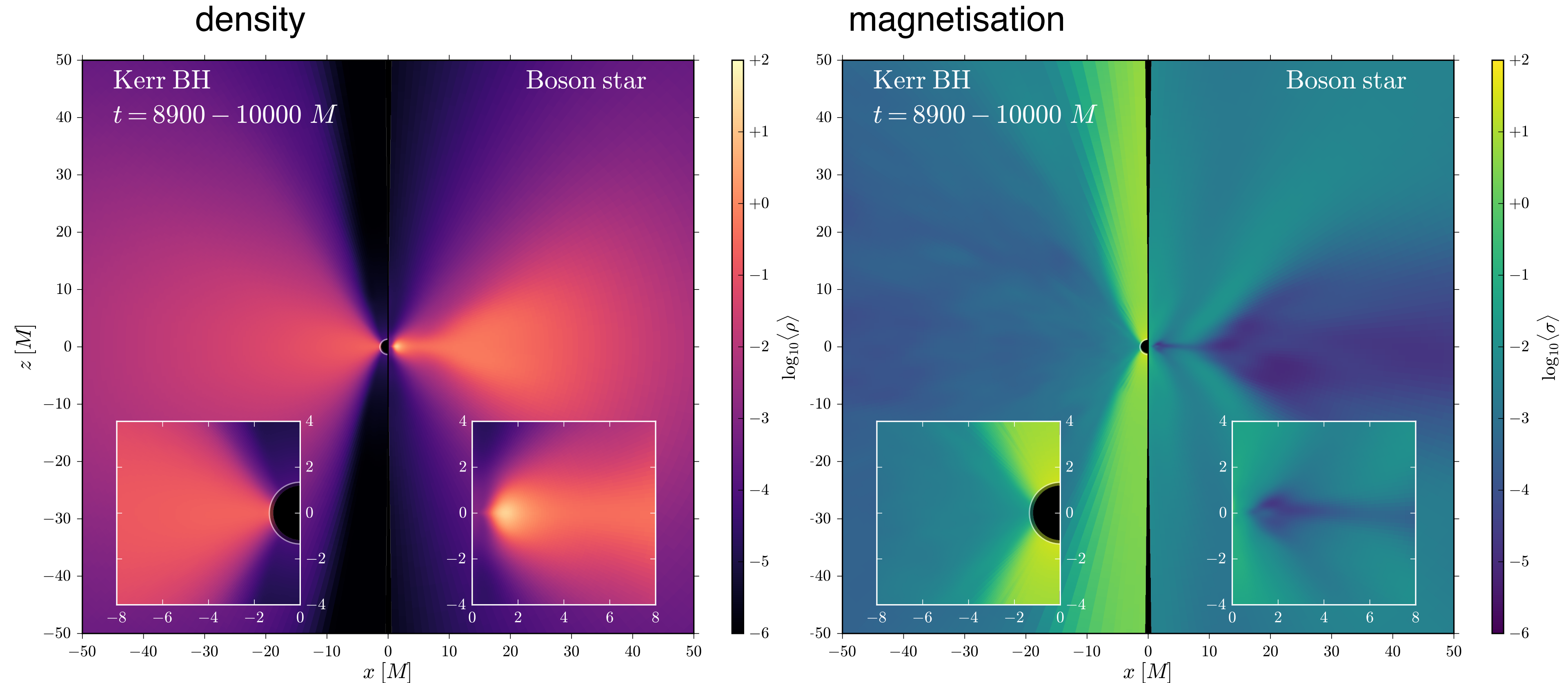
Boson Stars: GRMHD



Boson Stars: GRMHD



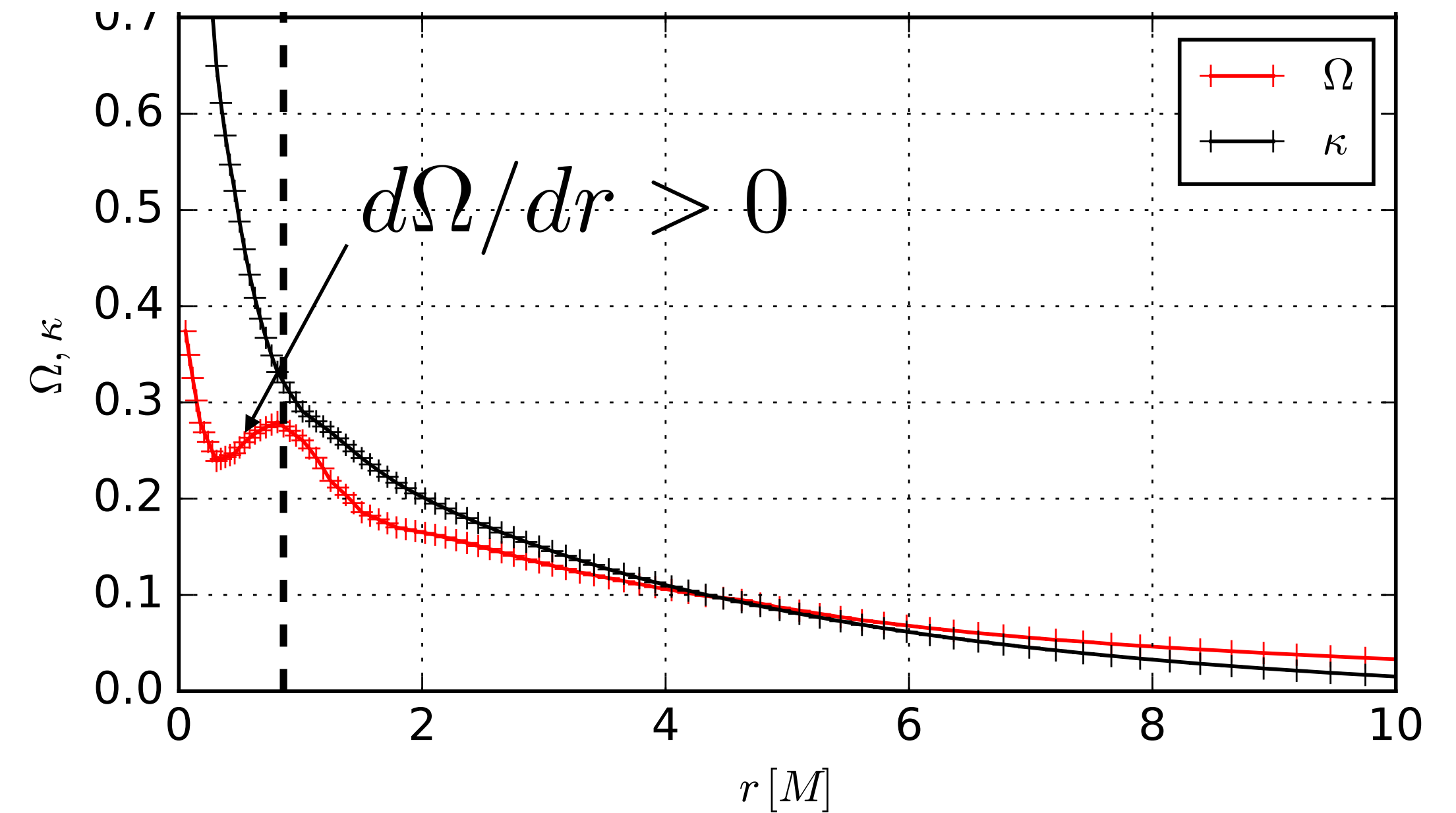
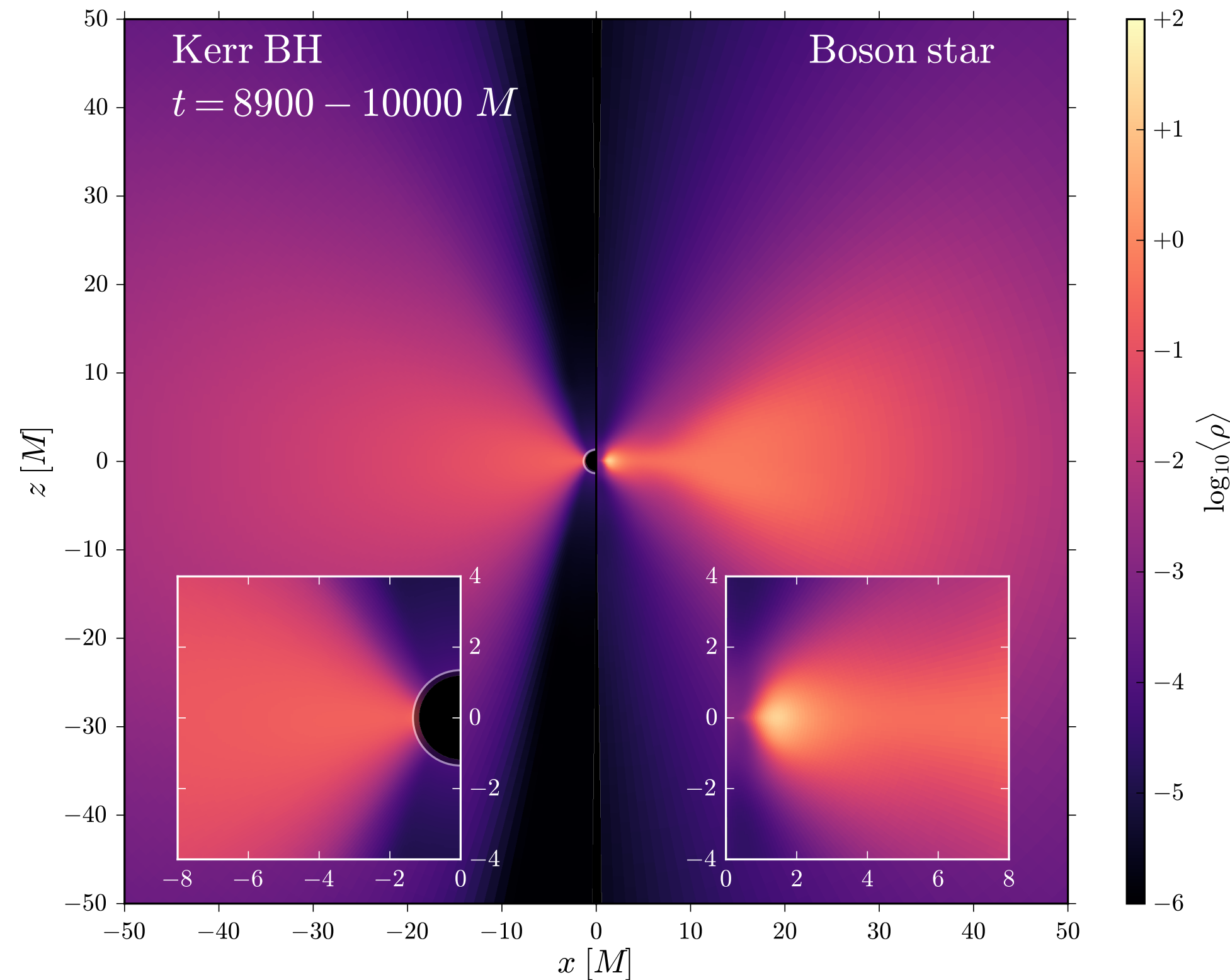
Boson Stars: GRMHD



- Formation of “mini-torus” inside of star due to centrifugal barrier
- No evacuated funnel in Boson star, slowly flowing out from the hotter and denser interior ($W < 1.05$) => **low magnetisation**



Boson Stars: GRMHD



- MRI stable in mini-torus interior: $d\Omega/dr > 0$
- QPO mini-torus oscillations with epicyclic frequency



Accretion onto strange objects

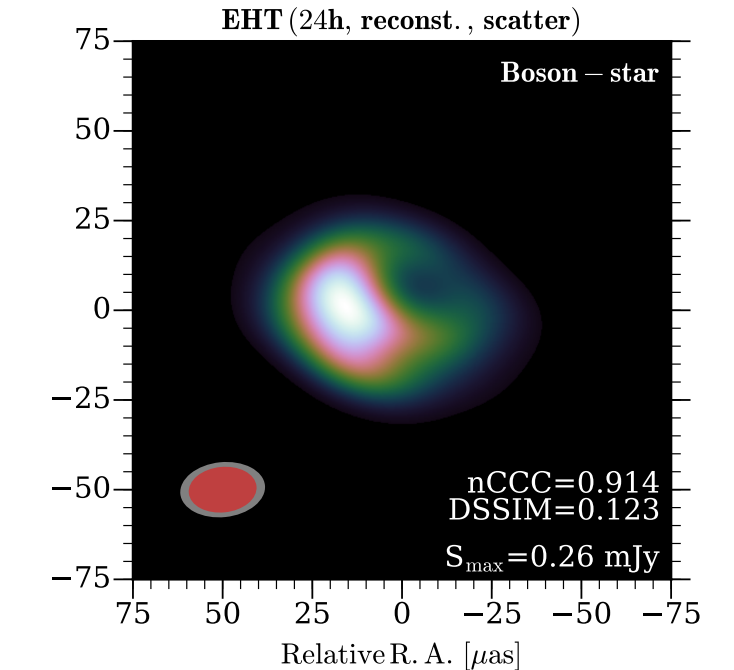
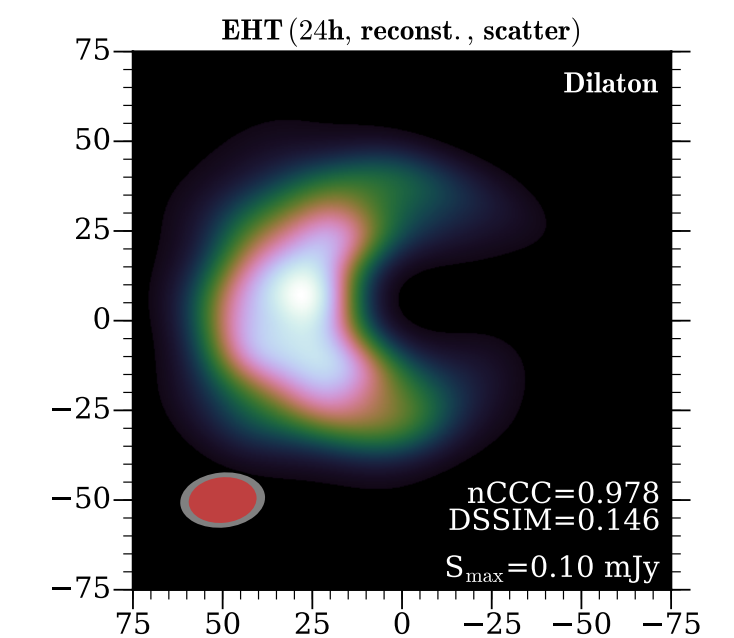
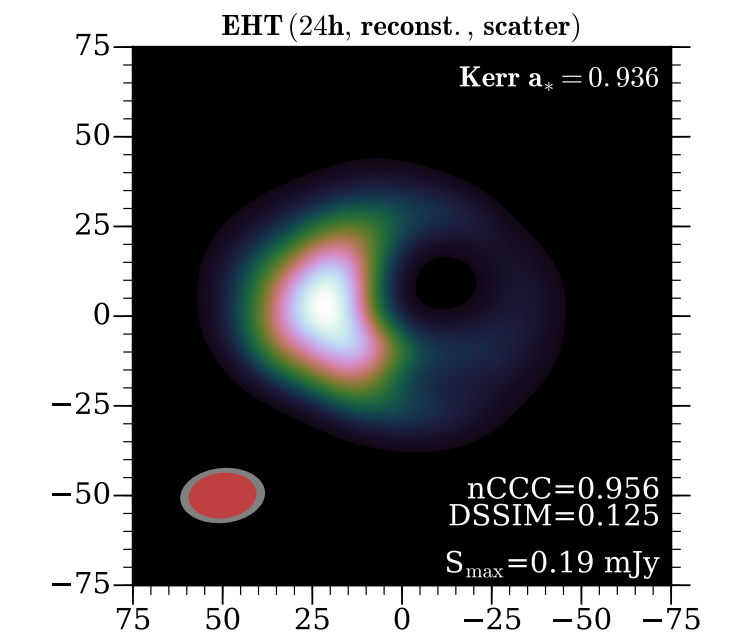
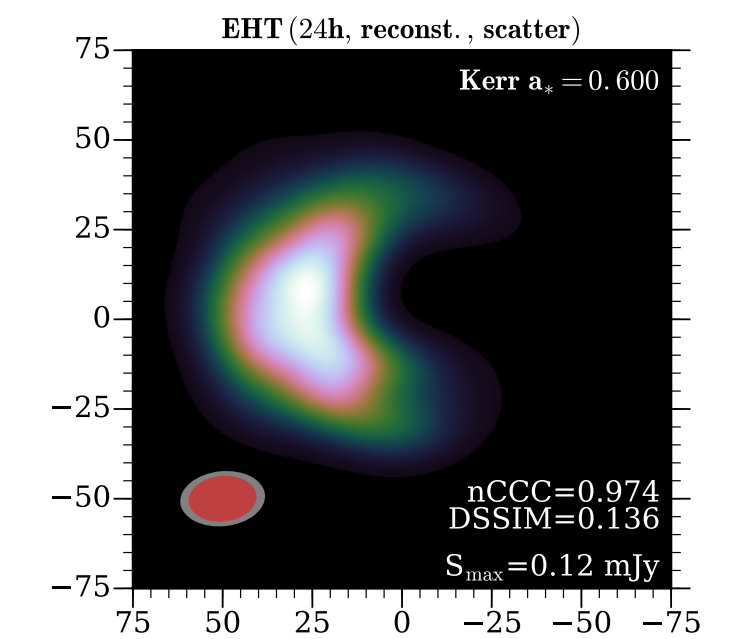
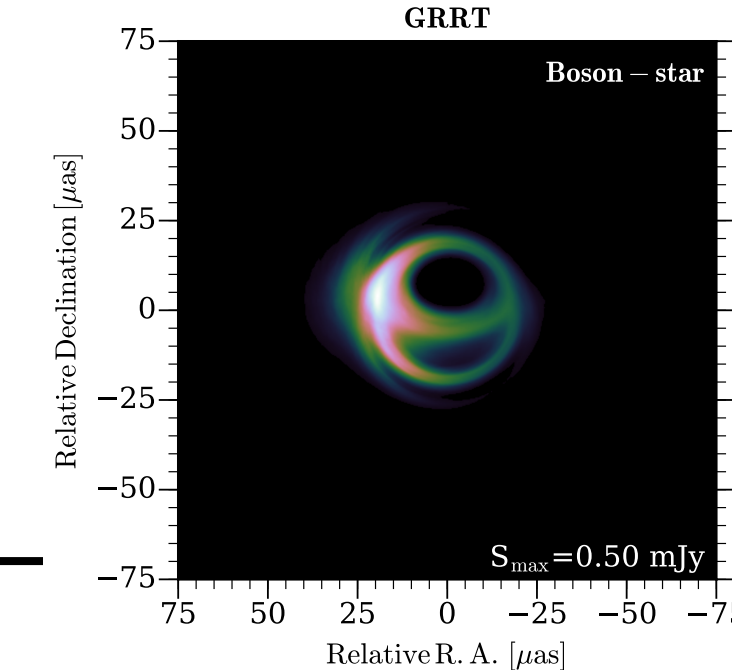
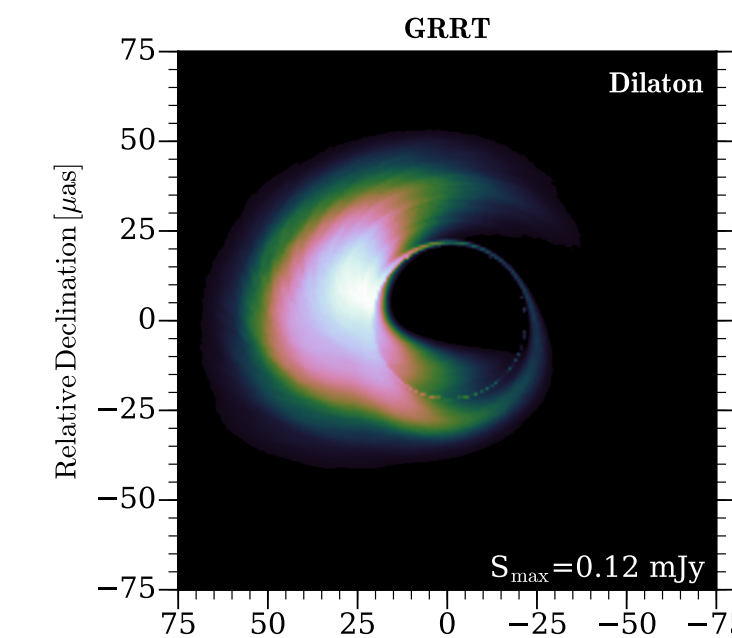
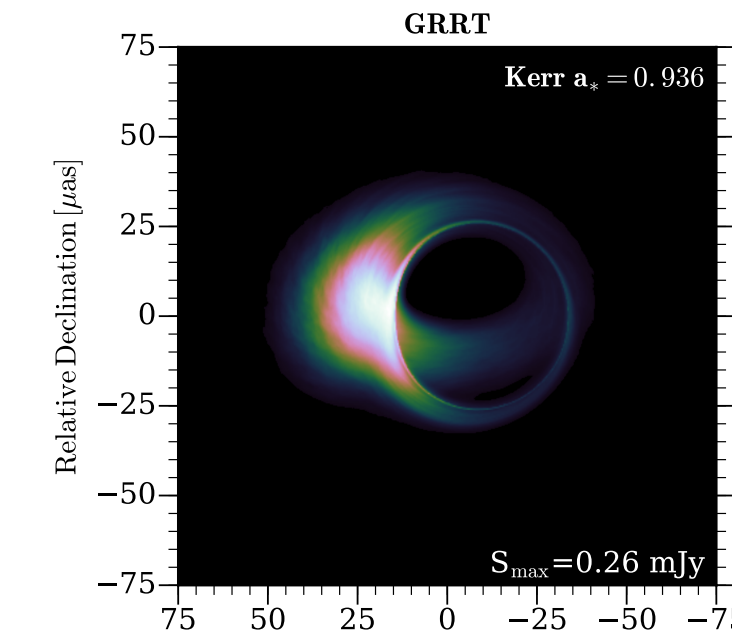
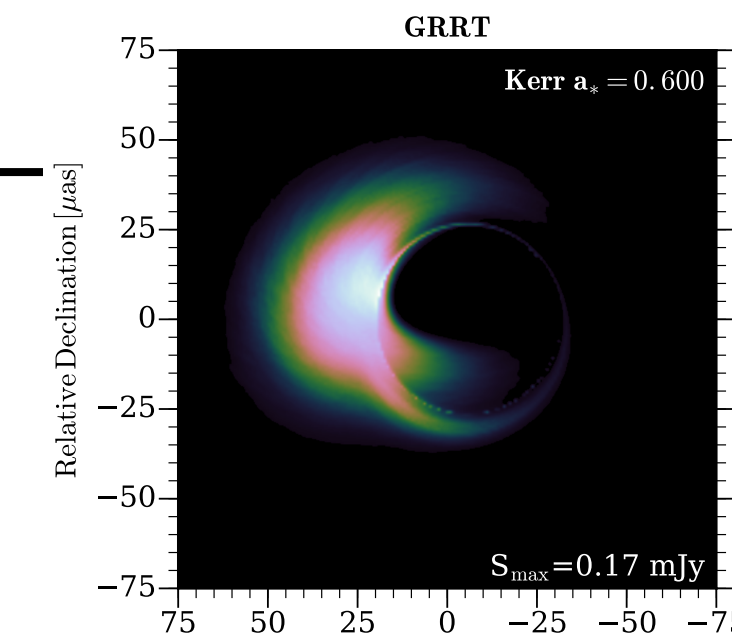
- It is presently **difficult to distinguish** between a **Kerr BH** and a **dilaton BH** on the basis of BH shadow images alone.
- **Dynamics matters:**
- Absence of an event horizon in a **Boson star** leads to **significant differences in the dynamics** of accretion
 - no magnetised funnel
 - development a dense mini-torus
- With SgrA* observations, we will **likely rule out** many non-BH objects:
 - Boson stars, naked singularities, Gravastars

Kerr BH
($a=0.6$)

Kerr BH
($a=0.9375$)

Dilation BH
($b=0.5$)

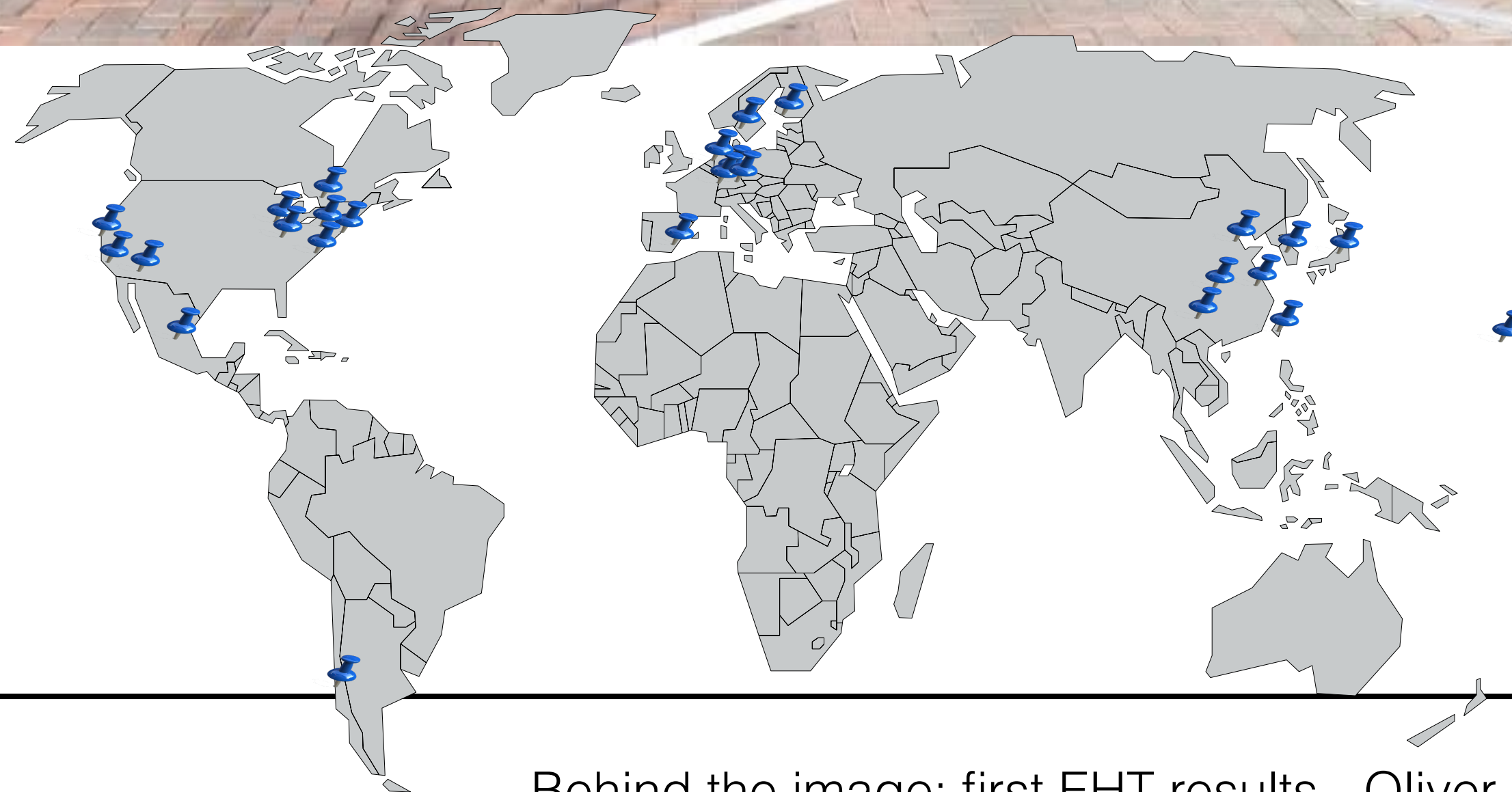
Boson star



Global Team at the EHT2016 Conference



11/2016; Cambridge, MA



Event Horizon Telescope

Behind the image: first EHT results - Oliver Porth. Saclay SAp seminar, May 21st 2019

Funding Support



Institutions on the EHT Board

Academia Sinica Institute of Astronomy and Astrophysics

University of Arizona

University of Chicago

East Asian Observatory

Goethe-Universität Frankfurt

Institut de Radioastronomie Millimétrique

Large Millimeter Telescope Alfonso Serrano

Max-Planck-Institute für Radioastronomie

MIT Haystack Observatory

National Astronomy Observatory of Japan

Perimeter Institute for Theoretical Physics

Radboud Universiteit Nijmegen

Smithsonian Astrophysical Observatory



Radboud Universiteit Nijmegen



SAO

Affiliated Institutions

Aalto University
Universiteit van Amsterdam
Arizona Radio Observatory
Instituto de Astrofísica de Andalucía
Instituto Nacional de Astrofísica, Óptica y Electrónica
Institute for Astrophysical Research
Boston University
Brandeis University
University of California, Berkeley
California Institute of Technology
Chinese Academy of Sciences
Cologne University
Universidad de Concepción
Cornell University
Institute of High Energy Physics
Huazhong University of Science & Technology
University of Illinois
Joint Institute for VLBI ERIC

Kavli Institute for Astronomy and Astrophysics
Korea Astronomy and Space Science Institute
Leiden University
University of Maryland
University of Massachusetts Amherst
Max Planck Institute for Extraterrestrial Physics
Nanjing University
National Astronomical Observatories of China
Onsala Space Observatory
Peking University
Purple Mountain Observatory
University of Science and Technology
University of Science and Technology of China
Seoul National University
Shanghai Astronomical Observatory
Institute of Statistical Mathematics
University of Waterloo
Yunnan Observatory



Follow updates online:



<https://eventhorizontelescope.org>



<https://twitter.com/ehtelelescope>



<https://www.facebook.com/ehtelelescope>